A SPECTROSCOPIC STUDY OF SQUARE PLANAR PLATINUM(II) COMPLEXES

A thesis submitted to the

UNIVERSITY OF CAPE TOWN

in fulfilment of the requirements for the degree of

MASTER OF SCIENCE

by

PHILIP SIMON HALL B.Sc.(Hons.)(U.C.T.)

Department of Inorganic Chemistry
University of Cape Town
Rondebosch 7700
South Africa

September 1983

ACKNOWLEDGEMENTS

My sincere thanks and appreciation are to be extended to

My supervisors, Professor D.A. Thornton and Dr. G.A. Foulds, for their interest, encouragement and discussions in directing this study.

Dr. G.E. Jackson, for his invaluable assistance and interest in the NMR/Computer research.

My colleagues in the School of Chemistry, especially Elizabeth Sutton for proof-reading this thesis.

Mrs. R. Karssen for the typing of this thesis.

The University of Cape Town and the South African Council for Scientific and Industrial Research for financial assistance.

SUMMARY

A number of spectroscopic techniques consisting of ultraviolet, ^{1}H-NMR and mass spectrometry have been used in the structural analysis of square planar Pt(II) complexes.

The complexes *trans*-[$PtBr_2$(Y)(R-an)] (Y = C_2H_4,CO; R-an = substituted aniline) were prepared and investigated by the spectrosopic techniques. Infrared assignments were aided by isotopic labelling studies. The discussion of the two series of complexes are based on their relation to one another.

The complexes *trans*-[PtX_2(CO)(L)] (X = Cl, Br; L = aniline, pyridine *N*-oxide, pyridine, ammonia, imidazole and pyrazole) were prepared from their corresponding ethylene analogues. Infrared assignments, with labelling studies, are given for the complexes. The bonding effects in these complexes were studied using ^{1}H-NMR and ultraviolet spectroscopy. The ^{1}H-NMR spectra reveal that there is a fluxional behaviour of the ligands in some of the complexes. Hence, cold temperature studies were required to "freeze out" this fluxional behaviour and observe the expected signals due to the ^{195}Pt-H coupling. The electronic effects are different when the ligand, L, was capable of forming σ-bonds with Pt^{2+}, compared to when

L was capable of forming both σ- and π-bonds with Pt^{2+}. The mass spectra show the M^+ peak and subsequent fragmentation in the complexes.

The fluxional behaviour of imidazole in *trans*-$[PtX_2(C_2H_4)(Him)]$ was monitored by cold temperature studies. Using band shape analysis (with the aid of a computer) the activation paramaters for the exchange processes were determined. The dependence of the imidazole proton signals on temperature, solvent and excess ligand, all indicate that an intermolecular exchange process is occurring. Studies on the complex *trans*-$[PtX_2(C_2H_4)(pyz)]$, and the effect of solvent on the complexes are being pursued, and it is hoped that an understanding of the role of the solvent in the exchange process will become apparent.

CONTENTS

CHAPTER FOUR

CHAPTER FIVE

CHAPTER SIX

CHAPTER 1

CHAPTER 1

1. INTRODUCTION

1.1. GENERAL

The platinum metals (Ru, Rh, Pd, Os, Ir, Pt) usugally occur together native or,less frequently, as arsenides, the main deposits being in Russia, Canada and South Africa. Small amounts are also present in cupronickel ores, and are obtained as by-products when such ores are worked for the base metals. The extraction of the metals from their ores (concentration in grams per ton) generally involves three major operations; concentration of the ore, extraction of the crude metal and finally, refining [1].

The ability of olefinic compounds to enter into complex formation with metallic salts has been known since Zeise obtained the complex $K[PtCl_3(C_2H_4)]$ from the products of reduction of platinic chloride with alcohol [2]. The number of such metal olefin complexes has since been considerably extended. The literature [3,4,5] indicates that, although the capability of combining with olefins is evenly distributed among the metals, it is most strongly exhibited by platinum. In addition to Zeise's salt, homologous complexes derived from other olefins [6,7] have been prepared, as well as the analogous ethylenetribromo

platinite, $K[PtBr_3(C_2H_4)]$ [8]. They have been extensively investigated and recently a number of their reactions have been shown to be of commercial interest. Hartley [9] has attributed three main factors which attracted interest to and sustained research on platinum complexes.

Firstly, in the divalent oxidation state,platinum readily forms complexes with ligands containing donor atoms from most groups of the periodic table. This has resulted in the characterization of many organo-platinum complexes.

Secondly, the recognition of the square-planar geometry of the divalent oxidation state opened up the possibility of *cis*- and *trans*- isomerization in such complexes. This led to the discovery of the *trans*-effect in Pt^{2+} complexes, which eventually resulted in the synthesis of all the three possible geometric isomers of $[Pt(py)(NH_3)BrCl]$ in the late 1920's.

Thirdly, the growth in interest in platinum was triggered by the sudden development in organometallic chemistry. This resulted from their great intrinsic value in the field of homogeneous catalysis.

Livingstone [10] has classified the principal uses of platinum as (i) chemical engineering, including catalytic applications, (ii) electrial engineering, (iii) jewellery, (iv) dental, medical and laboratory, (v) temperature measurements. The industrial applications of platinum and

its alloys is based on their high resistance to corrosion and high temperatures. The heaviest demand for platinum is as a catalyst, especially in petroleum reforming.

For some time coordination chemists have been aware of certain trends in the stability of metal complexes. One of the earliest correlations observed was the *Irving-Williams series of stability* [11]. Later, a further correlation noted was that certain ligands form their most complexes with specific metal ions. Chatt [12] showed that metal ions could be conveniently divided into two groups, which he labelled as class 'a' and class 'b'. Class 'a' metals are those which prefer to form complexes with elements of lower atomic number within a given group of the periodic table, whereas class 'b' metals prefer to form complexes with elements of higher atomic number in that group. Platinum was classified as a class 'b' metal and thus if allowed to react with the halides, the stability of the complexes would decrease in the order $I^- > Br^- > Cl^- >> F^-$.

Pearson [13] developed a similar theory and suggested the terms 'hard' and 'soft' to describe the members of class 'a' and class 'b' respectively. 'Hard' acids and bases tend to be slightly polarizable species while 'soft' acids and bases tend to be larger and more polarizable. Pearson suggested a simple principle for predicting the stability of complexes formed between acids and bases: *Hard acids*

prefer to bind to hard bases and soft acids prefer to bind to soft bases. Thus for example, platinum, a 'soft' acid would form a stronger complex with I^- than with Cl^- since I^- is a 'softer' base than Cl^-.

The principal oxidation states of Pt are +2 and +4, the only other important oxidation state is +1, where Pt-Pt bonds are involved. The +2 oxidation state is by far the commonest state and no compounds or complexes of these divalent metals with a coordination number of less than four are known, and indeed most of the divalent compounds are four-coordinate, with square-planar geometry. There are a number of quite stable, five-coordinate complexes of Pt^{2+}, all involving ligands that are considered to be π-acceptors. Octahedral complexes of Pt^{2+} are very few, and although they may be octahedral in the solid state, they probably dissociate in solution. Most octahedral complexes of platinum contain the metal in the +4 oxidation state.

To understand the preferential formation of square-planar platinum(II) complexes it is necessary to consider the crystal field splitting of the various geometries, see Figures 1.1 and 1.2. The essence of this crystal field theory [14] is that the five *d*-orbitals, which are degenerate and equal in energy in the gaseous metal ion, become differentiated in the presence of the electrostatic field due to the ligands. Those orbitals lying in the

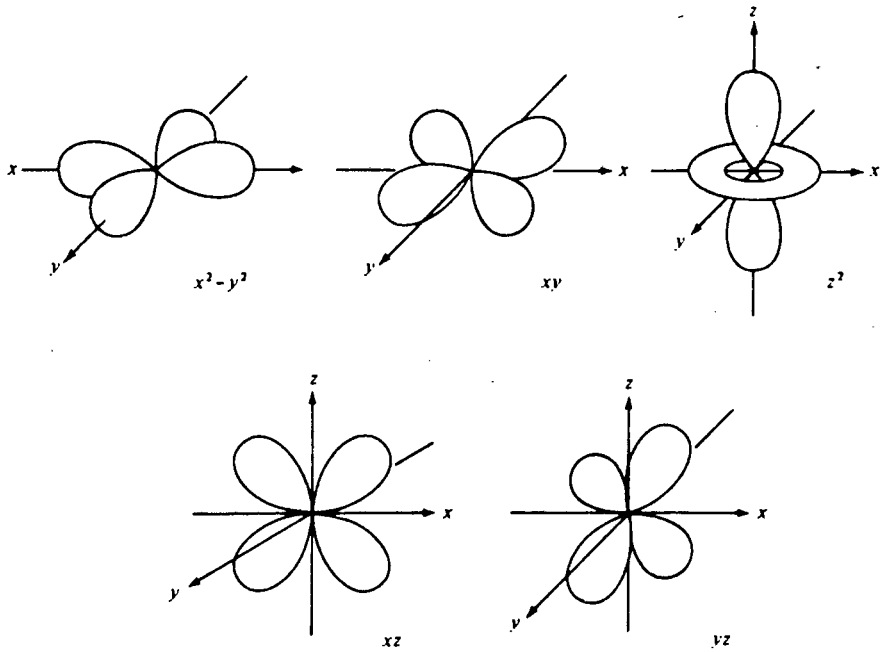

Fig.1.1. Spatial arrangement of the five *d* orbitals.(ref. 66)

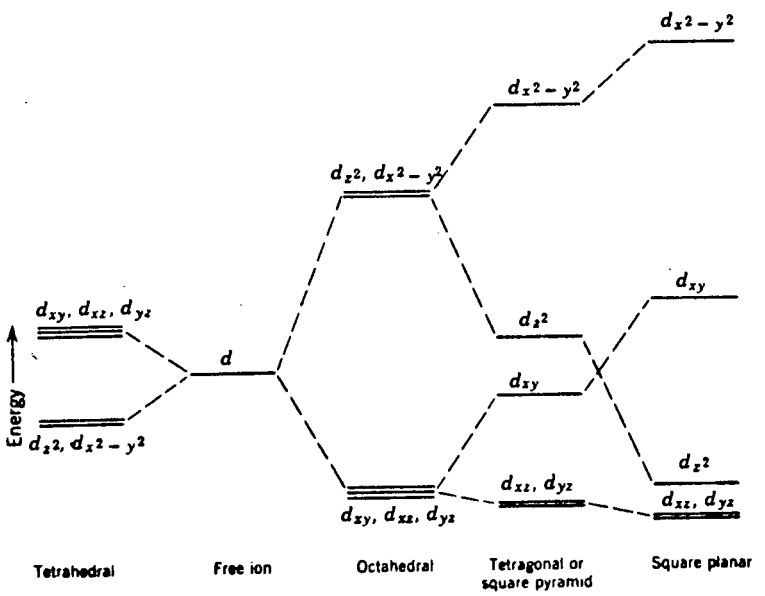

Fig.1.2. Crystal field splittings of the *d* orbitals of a central ion in regular complexes of various structures.(ref.70)

direction of the ligands are raised in energy with respect to those lying away from the ligands. By preferentially filling the low-lying levels, the *d*-electrons can stabilize the system, as compared to the case of random filling of the *d*-orbitals. The gain in bonding energy achieved in this way may be called the crystal field stabilization energy (CFSE).

With the above in mind and the fact that Pt^{2+} has eight *d*-electrons, it is quite apparent why square-planar geometry is most favoured, since it is possible to leave the $d_{x^2-y^2}$ orbital empty. The figure also shows that five-coordinate tetragonal structures are feasible, although to a lesser extent, since these also give rise to considerable ligand-field stabilization if the highest energy *d*-orbital is left empty. Furthermore, octahedral geometry would be expected to be rare, which is indeed the case.

1.2. STRUCTURE DETERMINATION: SPECTROSCOPIC METHODS

Structure determination is one of the fundamental operations in chemistry, and spectroscopy has proved to be a powerful tool for structure determination.

Streitwieser's [15] description of spectroscopy is as follows: Spectroscopy is an experimental process in which the energy differences between allowed states of a system are measured by detecting the frequencies of the corresponding light (energy) absorbed. The energy

difference between the different quantum states depends on the type of motion involved. That is, each type of motion corresponds to the absorption of light in a different region of the electromagnetic spectrum. Because the wavelengths required are so vastly different, different instrumentation is required for each spectral region.

Raman, microwave, infrared, visible and ultraviolet spectroscopy all use the above principle for their operation. Nuclear magnetic resonance spectroscopy differs slightly from the spectroscopic technique discussed above in that the differences in energy in the states being examined are created by a magnetic field. That is, the molecules are placed in a powerful magnetic field to create different energy states which are then detected by absorption of light of the appropriate energy.

Mass spectroscopy differs widely from the other forms of spectroscopy in that no absorption of energy is involved as described above. A mass spectrometer is an instrument that is designed to ionize gaseous molecules, separate the ions produced on the basis of their mass-to-charge ratio, and record the relative number of different ions produced.

The combination of information provided by each spectroscopic technique is often sufficient to elucidate even the most difficult structures.

1.3. METHODS OF ASSIGNING METAL-TO-LIGAND VIBRATIONS IN THE INFRARED SPECTRA OF TRANSITION METAL COMPLEXES

Among the many vibrations of coordination compounds, the metal-ligand vibrations are the most important since they provide direct information regarding the structure of the complex and the nature of the metal-ligand bonds. These vibrations appear below 600 cm^{-1} because of the high mass of the metal ion and the comparative weak nature of the M-L bond. These assignments are often difficult to interpret because the infrared spectrum is complicated by intermolecular interactions, lattice modes, lowering of symmetry, vibrational coupling and the appearance of ligand vibrations activated by complex formation [16,17].

The metal-ligand vibrations have been assigned by the following methods:

1.3.1. Since M-L vibrations are absent from the free ligands, a comparison of the spectra of the free ligand and its metal complex yield assignments of the metal-ligand modes. This method often fails to give unambiguous assignments because some ligand vibrations activated by complex formation may appear in the same region as the M-L vibrations [18].

1.3.2. The metal-ligand vibrations are expected to appear in the same region for complexes of identical metals with similar substituted ligands. This method has been used to assign

ν(Pt-N) in the complexes *trans*-[$PtBr_2$(Y)(L)] (where Y = CH_2CH_2 or CO, and L = substituted aniline) [19].

1.3.3. The M-L vibrations of a series of isostructural complexes are metal-sensitive and shift according to the properties of the metals. Hence, the infrared bands which follow the order of the CFSE's of the metals can be attributed to metal-ligand modes [20,21].

1.3.4. Theoretical calculations such as normal coordinate analysis using empirical metal-ligand and other bond lengths yield theoretical frequency values for the M-L and other vibrations of the complex [22].

1.3.5. The replacement of an atom by its isotope will result in a change of the frequency of any vibrations involving that particular isotopic species. Hence, if the isotopically substituted atom is the metal or the ligand donor atom, then the M-L vibration can be identified [23].
The expected isotopic shifts can be calculated [23], to a reasonable approximation, by assuming the labelled atom to be part of a simple harmonic diatomic molecule. The vibrational frequency of an harmonic diatomic molecule can be represented by the equation

$$\nu = \frac{1}{2\pi c}\left(\frac{f}{\mu}\right)^{\frac{1}{2}}$$

while the vibrational frequency of the corresponding

isotopically labelled system can be given by

$$\nu^i = \frac{1}{2\pi c}\left(\frac{f}{\mu^i}\right)^{\frac{1}{2}}$$

where ν = vibrational frequency,

f = harmonic force constant,

μ = reduced mass of the molecule,

c = velocity of light,

and the superscript, i, refers to the labelled system. If one then assumes that the force constants are unaltered by isotopic substitution, which to a good approximation is the case, the expected isotopic shifts may be calculated from

$$\frac{\nu^i}{\nu} = \left(\frac{\mu}{\mu^i}\right)^{\frac{1}{2}}$$

Thus, the greatest isotopic shifts can be expected for deuterated and tritiated molecules where the m^i/m ratios are largest (m^i = mass of heavier isotopomer and m = mass of the normal atom exchanged for it), and shifts of up to 1000 and 1300 cm^{-1}, respectively, have been observed. The isotope shifts in the case of lower m^i/m ratios, although appreciably smaller than the above compounds, are still considerable, and easily resolved with present-day commercial instruments. However, it should be noted that, the observed frequency shifts which result from labelling are subject to certain other factors, such as the extent to which the labelled atoms participate in the particular vibration, vibrational coupling, the number and nature of the atoms in the molecule that have been labelled and the

extent of hydrogen bonding. Thus the observed shift will be greatest if the molecule is simple with no vibrational coupling occurring, that is with each bond being as pure as possible.

The above account made reference only to isotopically labelled ligands, however, this can equally be applied to isotopically labelled metal ions [24]. This method is ideal for specifically assigning metal-to-ligand vibrations, but the shifts are generally small due to the relatively unfavourable m^i/m ratio, and may fall within the range of experimental error.

It has been extensively shown that the isotopic labelling method of assigning bands in infrared spectra is by far the most unambiguous and simple method [25]. The major limitation appears to be the availability and cost of the isotopes.

The isotopic labelling carried out in this research involved labelling of the ligand molecules as this method gives the most satisfactory results with regard to their subsequent assignments.

1.4. GROUP THEORY AND ITS APPLICATION TO MOLECULAR VIBRATIONS

The concept of symmetry is important to almost every aspect of life in our universe. For example, when molecules and

ions conglomerate into crystals they do so to give extensive structures with well-defined symmetry. The quantitative discussion of symmetry is called Group Theory [26,27]. By the application of Group Theory to molecules, useful information regarding the properties of the molecules can be obtained. In order to classify molecules according to their symmetry, all that is necessary is to list all their symmetry elements. Thus the name of the group to which a particular molecule belongs is determined by the symmetry elements that characterize it.

Consider a molecule composed of N atoms. All the movements (translational, rotational and vibrational) of the atoms in the molecule may be resolved into components along the x-, y- and z-axes. Thus, there are a total of $3 \cdot N$ possible movements in the molecule of which six are translational and rotational, while the remaining $3N-6$ ($3N-5$ for a linear molecule) are internal molecular vibrations. The symmetries of these vibrational modes are catagorized by labelleling each atom of the molecule with 3 Cartesian coordinates representing unit displacement vectors. The vectors now represent all the $3N$ degrees of freedom, and if we perform the symmetry operations we can relate new vector positions to old positions by [$3N$ x $3N$] matrices, whose character, forms a reducible representation, Γ_{total}. For example consider a molecule of square-planar geometry, *trans*-[$PrBr_2$(CO)(L)], as shown in Figure 1.3.

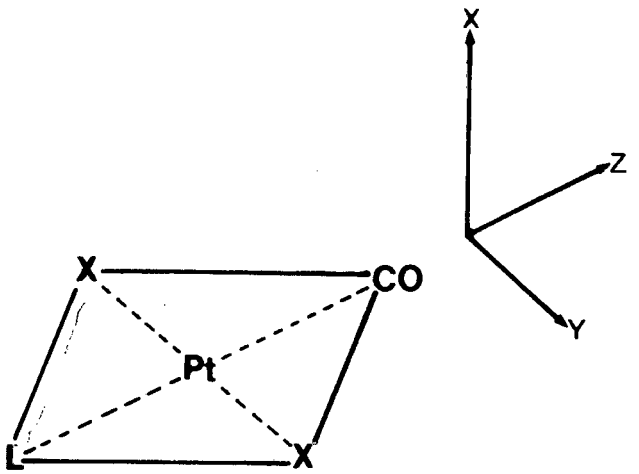

FIGURE 1.3 Square planar structure of *trans*-[$PtX_2(CO)(L)$]

Viewing the ligands as point masses, the molecule has an inherent C_{2v} symmetry for which Γ_{total} is:

C_{2v}	E	C_2	$\sigma_v(xz)$	$\sigma'_v(yz)$
Γ_{total}	15	-3	3	5

To determine the symmetry species of all the possible molecular motions, the following reduction formula is applied:

$$N_i = \frac{1}{h} \Sigma \chi_R \chi_I N$$

Where N_i = the number of times each irreducible representation appears in the reducible representation,

h = the order of the group

χ_R = character of the reducible representation

χ_I = character of the irreducible representation

N = number of symmetry operations in each class.

Thus the 15 possible molecular motions in *trans*-[$PtBr_2(CO)(L)$] are:

$$\Gamma_{3N} = 5A_1 + A_2 + 4B_1 + 5B_2$$

The molecular translations are obtained from the character table of the molecule. These are tables of the irreducible representations containing information regarding the nature of these representations and their properties. Thus for *trans*-[$PtBr_2(CO)(L)$] we have:

Symmetries for all molecular motions	$5A_1 + A_2 + 4B_1 + 5B_2$
Symmetries for translations	$A_1 + B_1 + B_2$
Symmetries for rotations	$A_2 + B_1 + B_2$
Symmetries for vibrations = Γ_{vib}	$4A_1 + 2B_1 + 3B_2$

To determine the number of stretches and bends constituting

Γ_{vib}, internal displacement vectors are chosen on a new basis for the point group representation. To determine the reducible representations for the stretches, vectors are drawn along the bonds. Any vector unshifted by a symmetry operation will contribute +1 to the corresponding matrix, while any vector shifted will contribute 0. For *trans*-[$PtBr_2$(CO)(L)] we have:

C_{2v}	E	C_2	$\sigma_v(xz)$	$\sigma'_v(yz)$
$\Gamma_{stretch}$	4	2	2	4

which reduces to

$$\Gamma_{stretch} = 3A_1 + B_2$$

and the bends are obtained by subtracting $\Gamma_{stretch}$ from Γ_{vib}, yielding

$$\Gamma_{bend} = A_1 + 2B_1 + 2B_2$$

Another aspect that can be determined from the symmetry elements is whether a fundamental, that is stretches and bends, is infrared or Raman active. A fundamental will be infrared active if, during vibration, there is a resultant change in dipole moment. The dipole moment changes in a similar manner as the x-, y- and z-coordinates and a vibration will be infrared active if it belongs to the same representation as any of the internal displacement vectors. This can be read directly from the character table.

Similarly, a fundamental will be Raman active, depending on the polarizability of the bond, if the mode involved belongs to the same representation as any of the operations in the last column of the character table. Thus for *trans*-$[PtBr_2(CO)(L)]$ which has C_{2v} symmetry there are four metal related stretches, all of which are infrared and Raman active. They are the symmetric and asymmetric Pt-Br stretches, the symmetric metal-to-ligand stretches, and the symmetric metal-to-carbonyl stretch. The full set of stretches and bends are shown in Figure 1.4.

In addition to the nine vibrational modes (4 stretches and 5 bends), there are three normal modes ($A_1+B_1+B_2$) principally associated with coordinated CO. These modes are also infrared and Raman active and are ascribed to the symmetric C-O stretch, and the in-plane and out-of-plane metal-to-carbonyl deformation.

The above discussion only applies when one considers the molecule to be an isolated unit [26], for instance, as in the gaseous phase where the vibrations of the molecule are restricted only by its own point symmetry. In the solid state the molecule can no longer be regarded as a separate entity and is subject to the symmetry restrictions of its solid environment. Hence, to perform a thorough vibrational analysis study one would need to consider the entire array of molecules, which is an impossible task. Fortunately, Site Group and Factor Group Analyses make

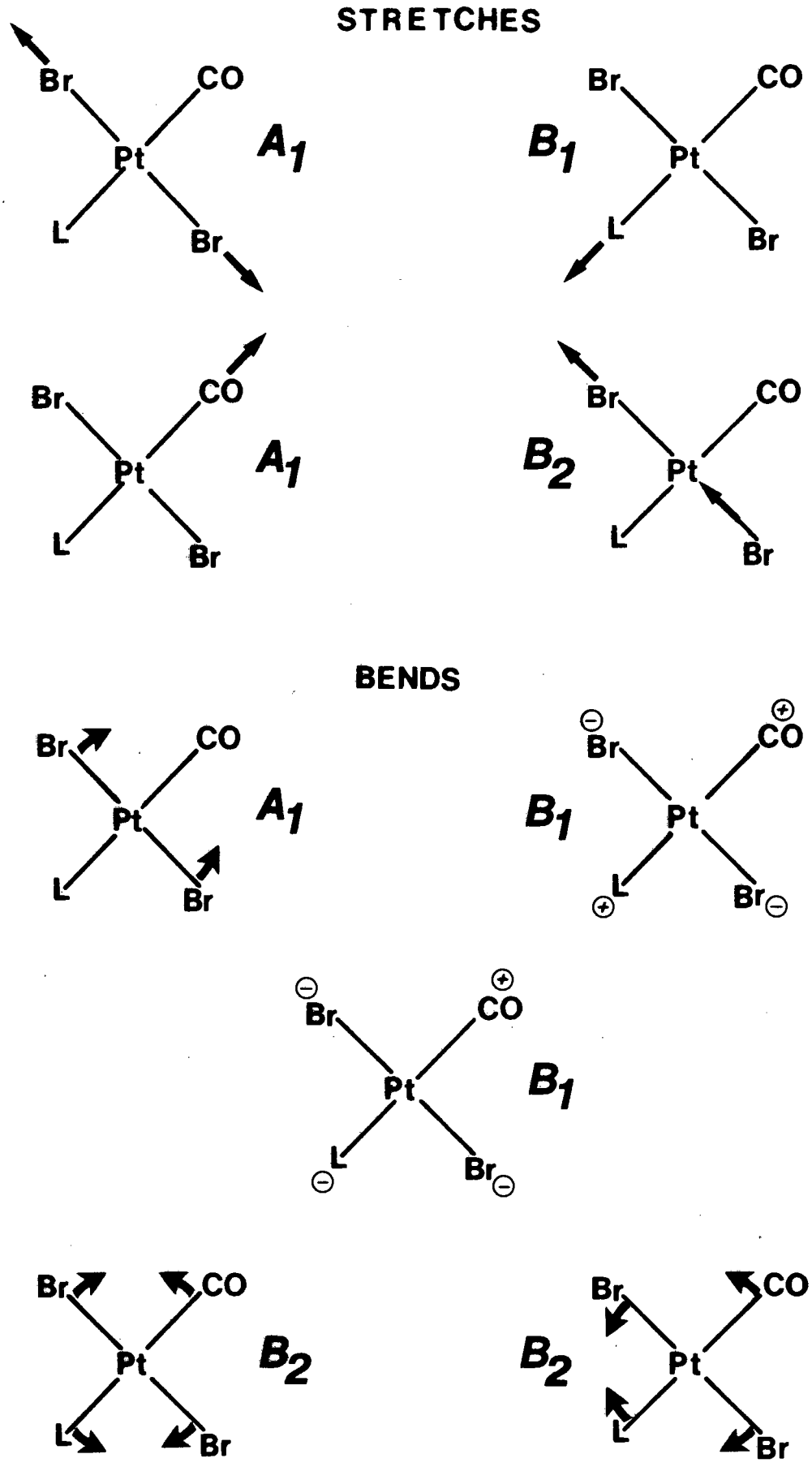

Fig. 1.4. Stretches and bends of trans-[$PtBr_2(CO)(L)$]

certain assumptions that give a valid approximation.

Factor Group Analysis is the more rigorous of the two approximations since it accounts for lattice modes and solid state splittings of nondegenerate vibrations of the free molecule. Halford [28], and Adams and Newton [29] list useful data for the use of these two analyses.

Hence, useful data can be obtained from Group Theory regarding the expected number and types of infrared bands in molecules. This data is helpful for the assignment of bands in infrared spectra.

1.5. THE RATIO ν^D/ν^H USED IN THE ASSIGNMENT OF THE C-H(D) AND RING VIBRATIONS IN METAL COMPLEXES

It has long been recognised that the majority of the infrared bands which originate in the internal vibrations of heterocyclic bases recur on an approximately band-for-band basis in the spectra of their metal complexes [30]. However, it was only recently that the ν^D/ν^H ratios of heterocyclic bases and their corresponding metal complexes have been fully exploited as a potential aid to assignment in their infrared spectra. The ratio (ν^D/ν^H) between the frequencies of corresponding bands in the infrared spectra of deuterated and normal molecules serves as an effective distinction between the C-H stretching (or bending) modes and the ring stretching (or bending) modes

in aromatic and heterocyclic compounds [23].

Thornton [31,32] and co-workers have studied the ν^D/ν^H ratio for a number of complexes of heterocyclic bases and the results of their findings may be summarized as follows:

1. The ratio ν^D/ν^H varies from 0.68 to 0.85 for the C-H modes.
2. The ratio ν^D/ν^H varies from 0.85 to 1.00 for the ring modes.

Distinction between the above modes and metal-ligand modes, or bands originating in the vibrations of other functional groups or other coordinated ligands is also possible since the latter generally yield ν^D/ν^H ratios very close to unity. Where apparent anomalous ratios are observed, the possibility of incorrect assignments or vibrational coupling must be taken into account.

1.6. BAND SHAPE ANALYSIS IN THE DETERMINATION OF NUCLEAR SPIN DYNAMICS

1.6.1. *Practical Band Shape Analysis*

Nuclear Magnetic Resonance (NMR) spectroscopy, in addition to providing valuable data in the form of chemical shifts and coupling constants, has been used extensively in the study of certain types of rapid equilibria. This has contributed much to the insight into the dynamic nature of molecular systems.

The line-widths and spectral shapes may change for various reasons, quite profoundly with temperature, and for this reason considerable effort [33-36] has been channelled into the determination of exchange rates from spectral shapes, so that activation parameters can be obtained from Arrhenius-type temperature-rate plots. Although it is sometimes possible to extract dynamic information from band shapes using simple formulae, the band shape formulae are generally too complicated for algebraic analysis and one must resort to numerical methods. Hence, it is quite normal to compute the band shapes using a digital computer and find a best fit to the experimental band shapes.

There are two basic types of computer programmes for calculating NMR spectra; non-iterative and iterative programmes, the latter being an expansion of the former. Both programmes take as their input a set of molecular paramaters (number of nuclei, chemical shift, coupling constants, etc.) and from these the computer calculates a trial spectrum - this is the non-iterative step. When the predicted spectrum bears an adequate resemblance to that observed, the programme may then be used in the iterative mode. The computer is now given additional data required for the experimental system from which the computer obtains optimum values of these paramaters by a least squares fit. The programme that we have used was developed by D.S. Stephenson and G. Binsch and is briefly described in the next paragraph.

DNMR5 [37,38] is an iterative programme that may simultaneously optimize up to 16 paramaters (chemical shifts, coupling constants, populations, effective transverse relaxation times, exchange rate constants, two baseline paramaters and the spectral origin) by a least-squares fitting of a theoretical band shape to experimentally digitized NMR signal intensities. The optimization is constrained by the total experimental band shape integral corrected for baseline increment and baseline tilt. The programme outputs information regarding the progress of the iteration, an error analysis of the final parameters and an agreement factor based on a calculated spectrum. It also, optionally, produces various forms of the original and computed spectra for comparison. See Appendix A for input/output information of program DNMR5.

1.6.2. *Calculation of Activation Parameters*

Once satisfactory relaxation times and exchange rate constants have been determined (by the computing process) as a function of temperature, we are now in a position to calculate the activation parameters for the chemical system investigated.

Nuclear exchange processes usually lend themselves to clearcut chemical interpretation and it is therefore standard practice to convert the corresponding rates to activation parameters. We can calculate the free energy of

activation from a single rate constant at a single temperature by means of the Eyring equation.

$$K = (k\,T/h)[\exp(-\Delta G^{\ddagger}/RT)]$$

where k, h, R = Boltzmann, Planck and Gas constant respectively

T = temperature

$\Delta G^{\ddagger}$ = free energy of activation difference between the initial and the transition state.

Rate constants measured over a range of temperatures may be converted into Arrhenius activation energies and frequency factors, or to enthalpies and entropies of activation by using the following equations:

$$K = A\exp(-E^{a}/RT)$$

$$K = (k\,T/h)[\exp(-\Delta H^{\ddagger}/RT)\exp(\Delta S^{\ddagger}/R)]$$

where A = Arrhenius pre-exponential factor

E^{a} = activation energy

$\Delta H^{\ddagger}$ = enthalpy of activation difference between the initial and the transition state

$\Delta S^{\ddagger}$ = entropy of activation difference between the initial and the transition state.

The generally used method for obtaining activation parameters is therefore to carry out a complete band shape study of the kinetics over as wide a temperature range as possible,

and then to obtain the Arrhenius activation parameters from a plot of $\log_{10}K$ (or LnK) against $1/T$, and to extract the parameters of interest from the slopes and intercepts. However, it is essential that error analysis be performed in order to test the validity of the calculated parameters, as explained below.

Various workers [39,40] have shown by statistical principles that dynamic parameters extracted from NMR band shapes are subject to systematic as well as statistical errors. From their findings it can be stated that $\Delta G^{\ddagger}$ is insensitive to errors in K and T, while E^{a} is very sensitive to errors in K and T. This is because although $\Delta H^{\ddagger}$ and $\Delta S^{\ddagger}$ are error-sensitive, the errors tend to cancel each other with the result that $\Delta G^{\ddagger}$ is insensitive to errors ($\Delta G^{\ddagger} = \Delta H^{\ddagger} - T\Delta S^{\ddagger}$). They also show that the best precision of the rate constant is obtained at the coalescence region where the band shape is most sensitive to the rate constant, K. As one diverges from the coalescence region the precision deteriorates, and it is for this reason that a least squares fit with error propagation is preferable to the normal graphical methods.

CHAPTER 2

CHAPTER 2

2. PHYSICAL METHODS

2.1. INFRARED SPECTRA

The mid-infrared spectra were determined on Nujol mulls (4000-400 cm^{-1}) and on hexachlorobutadiene (HCBD) mulls (3500-2500, 1500-1300 cm^{-1}) between potassium bromide plates on Perkin-Elmer 180 and Perkin-Elmer 983 spectrophotometers. The far-infrared spectra were obtained on Nujol mulls between polyethylene plates on a Digilab FTS 16 B/D interferometer (500-50cm^{-1}).

Solution spectra (2300-1900cm^{-1}) were determined between potassium bromide solution cells using spectroscopic chloroform on a Perkin-Elmer 983 spectrophotometer.

The quoted wavenumber accuracy of the Perkin-Elmer spectrophotometers is better than 1.00 cm^{-1}, and their repeatability better than 0.30 cm^{-1}. The Digilab interferometer behaves similarly, its added advantage is that it extends to a much lower wavenumber limit than the Perkin-Elmer systems and that it has the capability of storing the recorded spectra.

2.2. ELECTRONIC SPECTRA

The electronic spectra were recorded on a Varian Superscan 3 ultraviolet and visible spectrophotometer in the absorbance mode using spectroscopic methanol between 10mm cells.

2.3. ^{1}H-NUCLEAR MAGNETIC RESONANCE SPECTRA

The ^{1}H-NMR spectra were obtained at 90 MHz on a Bruker WH-90 D/S Fourier transform spectrometer and at 100 MHz on a Varian XL-100 continuous wave spectrometer. Deuterated chloroform and acetone were used as solvents and locks depending on the solubility of the complexes, while Tetramethylsilane (TMS) was used as the reference. Spectra were recorded at instrument operating temperature (ambient = 298 K) unless otherwise specified.

2.4. MASS SPECTRA

Mass spectra were measured on a V.G.Micromass 16F instrument operating in the electron impact mode, with electron beam energy 70eV and ion accelerating voltage 3kV, and with ion source temperatures in the range 100°-195°C.

2.5. MICROANALYSES

Microanalyses were performed by Mr. W.R.T. Hemsted, of

this University, on a Heraeus Universal Combustion Analyser Model CHN-MIKRO.

2.6 COMPUTATION

All computations were performed at the computer centre of the University of Cape Town on a Univac 1100/81 computer.

CHAPTER 3

CHAPTER 3

3. THE APPLICATION OF SPECTROSCOPIC TECHNIQUES TO THE COMPLEXES *trans*-[$PtBr_2(C_2H_4)$(R-an)] (R-an = substituted aniline)

3.1 INTRODUCTION

Platinum-olefinic complexes are the oldest class of organometallic complexes known; the first complex, $K[Pt(C_2H_4)Cl_3]$, known as Zeise's salt, was prepared in 1830 [2]. Initially, numerous electronic structures were proposed [41,42] to explain the structure and existence of the olefin-coordinated complex. This was partly due to the fact that its true structure, which was only solved in 1950, was plagued with more problems than almost any other X-ray investigation [43,44]. The main feature of this structure, as shown in Figure 3.1 is that the C-C axis of the coordinated ethylene is perpendicular to the $PtCl_3$ plane.

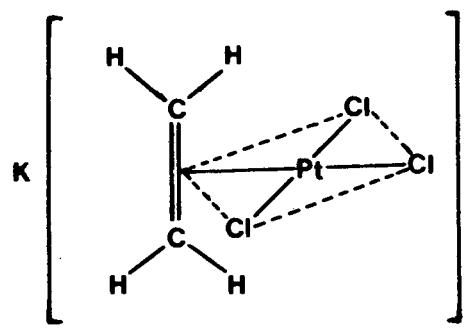

FIGURE 3.1 The Structure of $K[Pt(C_2H_4)Cl_3]$

The first successful treatment of the bonding in metal-olefin complexes was put forward by Dewar [45] for silver (I) olefin complexes. This was later extended by Chatt and Duncanson [46] to platinum(II) complexes. This theory involves a σ-bond from the full π-bonding orbital of the olefin to an empty hybrid orbital on the metal, complemented by π-back-donation of charge from a filled hybrid orbital on the metal to the empty π^* (antibonding) orbital on the olefin. This has generally become the accepted bonding mechanism in metal-olefin complexes and is shown diagramatically in Figure 3.2.

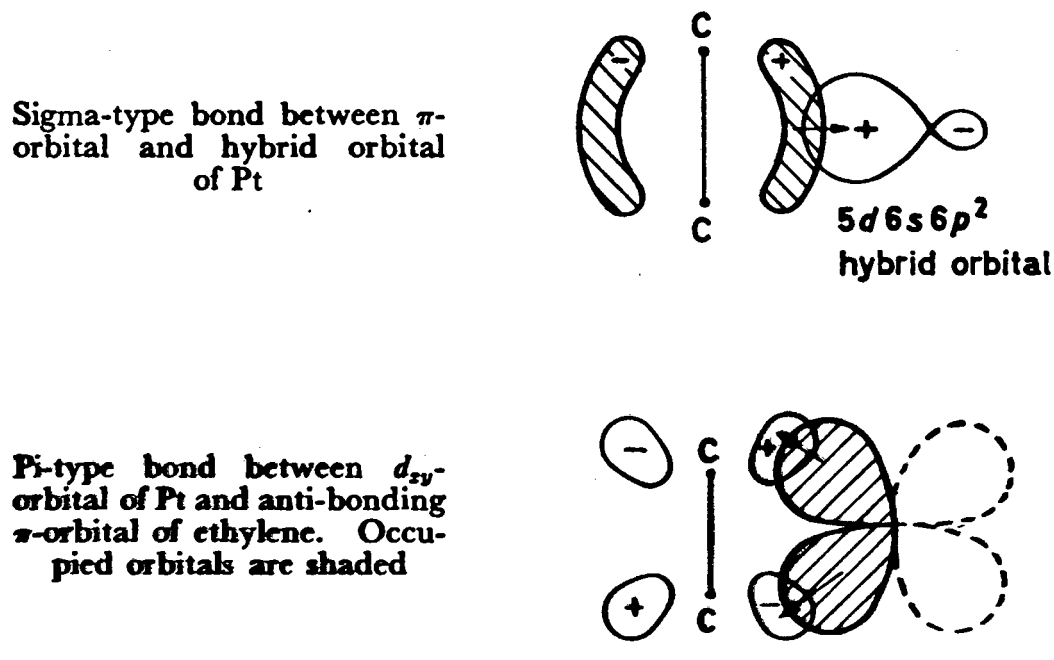

FIGURE 3.2 The bonding in $[PtCl_3(C_2H_4)]^-$

These platinum-olefinic complexes are formed when platinum(II) salts react with olefins in water. Since an excess of one olefin will displace another [47], ethylene complexes have been widely used as the starting material for the preparation of olefinic complexes. The volatility of ethylene aids the displacement reaction.

The platinum-olefinic complexes can react with a variety of ligands, those most commonly used being nitrogen donor ligands. To understand why many platinum-olefinic complexes can be formed, consider the following:
Amines bond to platinum(II) salts by donation of a pair of electrons in an sp^3 hybrid orital on the nitrogen to an empty orbital on the metal. Since there are no low energy empty orbitals on the nitrogen suitable for π-back-donation, the metal-nitrogen bond is a pure σ-bond. However, when amines are bonded to platinum which contains ligands capable of π-bonding, such as ethylene, the metal-to-nitrogen bond strengths are greatly enhanced.

It has been shown [9] that ligand substitution reactions of square-planar platinum(II) complexes occur as shown below:

$$[PtX_4]^{2-} + L \longrightarrow [PtX_3L]^- + X^-$$

normally follows a two-term rate law given by:

$$\text{rate} = \{K_1 + K_2[L]\}[PtX_4^{2-}]$$

where K_1 and K_2 are the first- and second-order rate constants corresponding to the solvent-dependent and solvent-independent step, respectively. However, when X=Cl and L=C_2H_4, then K_1 is zero [9] and hence the aquo-species $[PtCl_3(H_2O)]^-$ is not involved in the rate-determining step of the reaction. The possible mechanism for the formation of platinum(II) olefinic complexes is shown in Scheme 3.1.

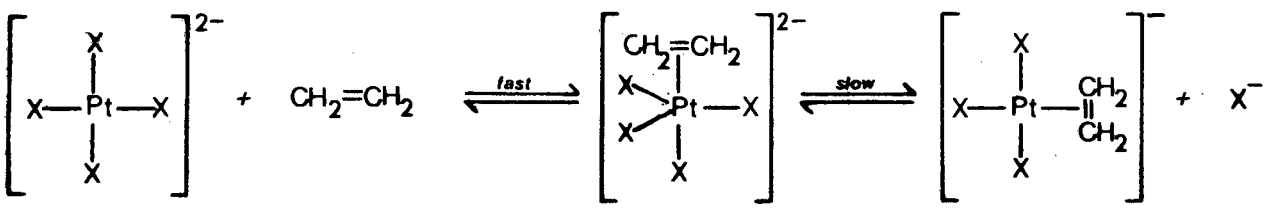

SCHEME 3.1

The incoming ligand will generally enter a position *trans* to the ethylene because of the latter's strong *trans*-effect [9,48]. The *trans*-effect has the result that in a substitution reaction where an incoming ligand might enter in two or more alternative positions with consequent displacement of the ligand occupying the position chosen, the position chosen is *trans* to that ligand present which ranks highest in the *trans*-effect series. This series is an empirical sequence of ligands commonly found bonded Pt(II), which is the ion that illustrates the effect most strikingly. In this series the ethylene ligand has

been placed as one of the ligands which offers the greatest *trans*-effect.

The *trans*-effect of ethylene is very pronouced as shown by the crystallographic data obtained from crystals of $K[PtX_3(C_2H_4)]$ where X=Cl or Br [43,49]. In both structures the Pt-X bond lengths for the halide *trans* to the ethylene were significantly longer than the other two Pt-X bond lengths where the halides are *trans* to each other.

Considering the above we may conclude that unless the incoming monodentate ligand, L, has a stronger *trans*-effect than ethylene, then the complex formed when L reacts with $K[PtX_3(C_2H_4)]$ will have the *trans*-configuration, as shown in Scheme 3.2.

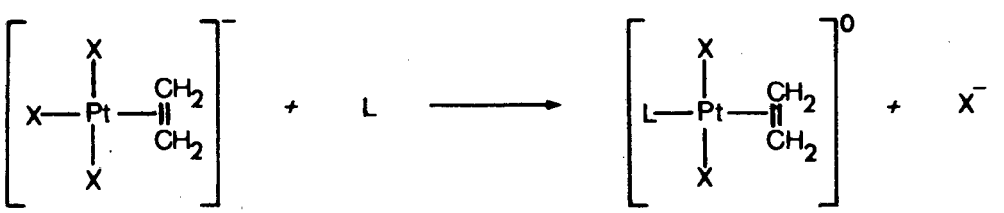

SCHEME 3.2

The vibrational spectra of metal-olefinic complexes are very difficult to interpret because the symmetry of these complexes are fairly low ($[Pt(C_2H_4)Cl_3]^-$ has C_{2v} symmetry) so that many of the fundamental modes have the same

symmetry properties and can therefore interact with each other [16]. Clearly there is no change of the C_{2v} symmetry when the platinum-olefinic complex reacts with a ligand as shown in Scheme 3.2. Hence, in order to simplify the interpretation of the vibrational spectra of these complexes with low symmetries it is necessary to consider Group Theory (See Chapter 1.4., Page 11). The $[PtX_3(C_2H_4)]^-$ ion has C_{2v} symmetry for which Group Theory predicts:

$$\Gamma_{vib} = 5A_1 + A_2 + 3B_1 + 3B_2$$

$$\Gamma_{stretch} = 3A_1 + B_1 + B_2$$

$$\Gamma_{bend} = 2A_1 + A_2 + 2B_1 + 2B_2$$

The stretches are assigned as follows:

A_1	$Pt-C_2$	symmetric stretching
	$Pt-X_2$	symmetric stretching
	$Pt-X_{trans}$	stretching
B_1	$Pt-C_2$	antisymmetric stretching
B_2	$Pt-X_2$	antisymmetric stretching

Fortunately these vibrations may be identified by means of the isotopic labelling technique. Briefly, this involves

labelling certain specific atoms of the complex and then recording the shifts of bands in their infrared spectra. Those bands which shift most are assigned to modes involving the labelled atom.

The "backbonding" mechanism for platinum-olefinic complexes mentioned earlier is further supported by the fact that in every case, except the case of the anion of Zeise's salt, $K[PtX_3(C_2H_4)]$, there is a lengthening of the C=C bond [50], and furthermore these complexes generally show intense metal-to-ligand charge- transfer (MLCT) bands in their electonic spectra [51,52]. These MLCT bands result from electronic excitation of the 5*d*-orbital of the metal to empty ligand-based orbitals. Apart from this excitation other metal-ligand interactions may occur [53], such as
$\pi \longrightarrow \pi^*$ (coordinated ethylene), and $X^- \rightarrow Pt^{2+}$ (charge transfer).

In this chapter a series of complexes *trans*-$[PtBr_2(C_2H_4)(R\text{-an})]$ (R-an = substituted aniline) have been prepared. The influence of the variation of R on the properties of the above complexes have been investigated by infrared, ^{1}H-NMR and ultraviolet spectroscopy.

3.2. PREPARATION OF COMPLEXES

3.2.1. *Preparation of $K[PtX_3(C_2H_4)]H_2O$ (X=Cl,Br)*

These compounds were prepared in a similar manner to that reported by Chatt and Searle [54]. A solution of $K_2[PtX_4]$ (9.28 mmol, 5.50 g for X=Br and 3.85 g for X=Cl) dissolved in water (30 ml) and HX (2.0 ml, sp.gr. 1.18 for HCl and 1.50 for HBr) was placed in a 250 ml round-bottom flask. The inlet of the flask was connected to a cylinder of ethylene gas. The flask was flushed with ethylene and then, with a positive pressure of ethylene being maintained, it was clamped in an automatic shaker and allowed to shake at ambient temperature. In the case where X=Cl the solution changed from dark red to golden yellow in five days, while the similar change for X=Br was affected in three days. These times can be substantially reduced by the catalytic activity of an added SnX_2 solution [55,56], or by substituting $K_2[PtX_4]$ with an ethanolic solution of $Na_2[PtX_4]$ [57]. The resultant golden yellow solutions were placed in evaporating dishes and the water was allowed to evaporate leaving a crystalline residue of $K[PtX_3(C_2H_4)]$ and KX and small traces of unreacted $K_2[PtX_4]$. This residue was then crushed and the $K[PtX_3(C_2H_4)]$ extracted with absolute ethanol (140 ml). The suspensions were filtered to remove KX and unreacted $K_2[PtX_4]$ and the yellow filtrates were divided, by volume, into seven equal (~1.20 mmol each) portions for immediate use in preparation

of the *trans*-$[PtX_2(C_2H_4)L]$ complexes.

Whenever aqueous rather than ethanolic solutions of $K[PtX_3(C_2H_4)]$ were required, the ethonol was evaporated under reduced pressure and water (10 ml) was added to the residue. The resulting solution was filtered to remove traces of fine platinum black which had precipitated.

The deuterated complexes, $K[PtX_3(C_2D_4)]$ were similarly prepared from ethylene-d_4 of 99% isotopic purity supplied by Merck, Sharp and Dohme (Canada) Ltd.

3.2.2. *Preparation of trans-$[PtBr_2(C_2H_4)(R\text{-}an)]$ (R-an = substituted aniline)*

Prior to formation of the complexes all liquid anilines were purified by vacuum distillation and solid anilines were purified by dissolution/reprecipitation or recrystallization. The complexes were prepared by essentially the same general method. This involved the slow addition of an ethanolic solution of the substituted aniline (1.00 mmol in 10 ml) to one portion of the freshly prepared $K[PtBr_3(C_2H_4)]$ (1.20 mmol in 20 ml) solution.

When the product precipitated immediately, the ethanol was allowed to partly evaporate and more ligand (0.15 mmol in 20 ml H_2O) was added. After stirring the reaction mixture

for a further period of time (5 min) to allow for the completion of the reaction, the product was isolated by vacuum filtration, washed well with water, and dried overnight over silica gel under reduced pressure.

When the product did not precipitate immediately, the solution was stirred overnight, ethanol being allowed to evaporate, until crystallization was essentially complete. More ligand (0.15 mmol in 20 ml cold H_2O) was then added and after stirring for a further period of time (20 min) the product was isolated and dried as described above.

The deuterated complex was similarly prepared from aniline-d_5 of 99% isotopic purity supplied by Merck, Sharp and Dohme (Canada) Ltd.

Yields were quantitative (>80%) and the composition and purity of all the yellow compounds were determined by microanalysis (C,H,N), Table 3.1.

3.3 ANALYSES OF COMPLEXES

Table 3.1

Analytical data for the complexes *trans*-[$PtBr_2(C_2H_4)$(R-an)]

R	Calculated			Found		
	%C	%H	%N	%C	%H	%N
H	20.2	2.3	2.9	20.3	2.3	3.0
m-CH_3	22.1	2.7	2.9	21.9	2.6	2.9
m-OCH_3	21.4	2.6	2.8	21.4	2.6	2.8
m-F	19.0	2.0	2.8	19.5	2.0	3.1
m-Cl	18.8	1.8	2.7	18.8	1.9	2.7
m-NO_2	18.4	1.9	5.4	18.6	2.0	5.4
m-Br	17.3	1.8	2.5	17.4	1.8	2.5
m-I	16.0	1.7	2.3	16.0	1.7	2.3
p-*n*-C_4H_9	27.1	3.6	2.6	27.3	3.6	2.8
p-C_2H_5	23.8	3.0	2.8	23.9	3.0	3.0
p-CH_3	22.1	2.7	2.9	22.1	2.7	2.9
p-OCH_3	21.4	2.6	2.8	21.4	2.6	2.8
p-Cl	18.8	1.8	2.7	18.9	1.9	2.8
p-Br	17.3	1.8	2.5	17.4	1.8	2.5
p-I	16.0	1.7	2.3	16.7	1.7	2.2
3,5-di-CH_3	23.9	3.0	2.8	23.8	3.0	2.8

3.4 RESULTS

Table 3.2

Principal infrared band frequencies (cm^{-1}) for the complexes *trans*-[$PrBr_2(C_2H_4)$(R-an)][a]

R	σ	ν_{as}(Pt-C_2)	ν_s(Pt-C_2)	ν(Pt-N)	ν(C=C)
m-NO_2	0.71	420	353	374	1250
m-Br	0.39	459	377	393	1250
m-Cl	0.37	426	377	397	1251
m-I	0.35	462	373	421	1248
m-F	0.33	450	380	424	masked
p-I	0.28	454	353	404	1227
p-Br	0.23	461	360	408	1234
p-Cl	0.23	458	378	410	1249
m-OH_3	0.11	457	386	427	1250
H	0	477	384	434	1252
(C_2D_4)		(42)	(9)	(0)	
(an-d_5)		(0)	(2)	(31)	
m-CH_3	-0.07	480	378	431	1249
p-C_2H_5	-0.15	486	391	453	1249
3,5-di-CH_3	-0.16	483	384	443	1251
p-*n*-C_4H_9	-0.16	484	390	440	masked
p-CH_3	-0.17	487	390	451	1254
p-OCH_3	-0.27	496	386	485	masked

[a] In all the complexes ν(Pt-Br) occur at 244 $\pm$ 6cm^{-1} and is unshifted by deuteration.
Values in parentheses are the shifts (cm^{-1}) induced by deuteration.

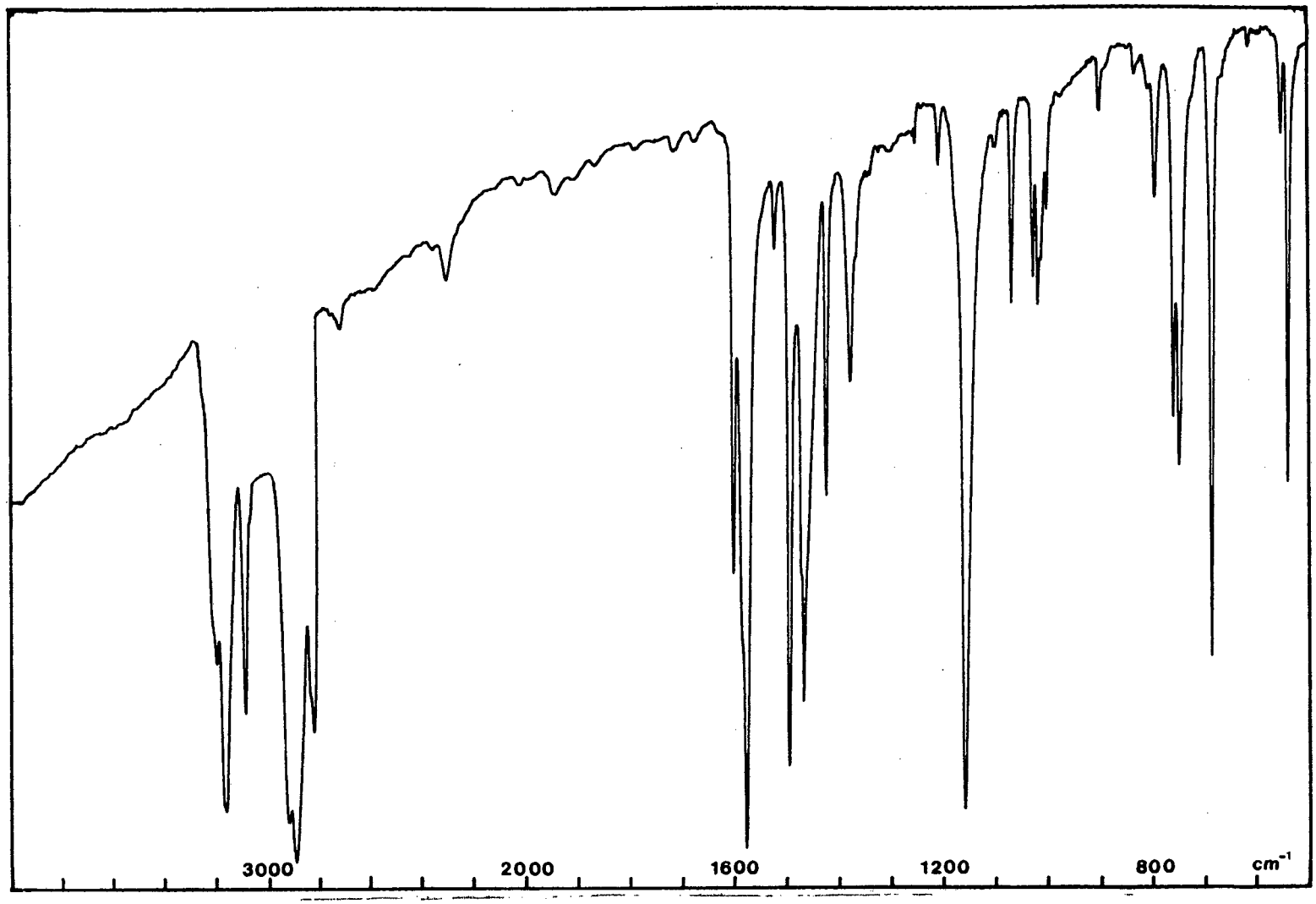

Fig. 3.3. Infrared spectrum of trans-[PtBr$_2$(C_2H_4)(an)]

Table 3.3

^{1}H-NMR data for *trans*-[$PtBr_2(C_2H_4)$(*p*-R-an)] (*p*-R-an = para substituted aniline)[a]

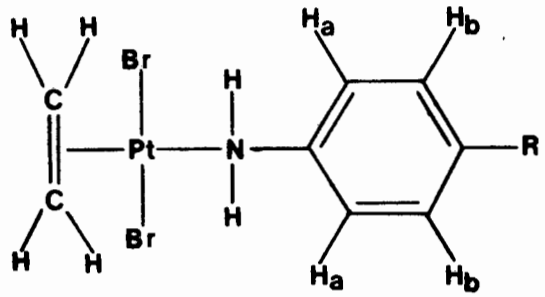

R	Olefin protons		Aniline protons		Other protons
	J_{Pt-H}		δ_{H_a}	δ_{H_b}	δ
p-I	66.0	4.83	7.72	7.27	
p-Br	66.0	4.82	7.53	7.30	
p-Cl	66.0	4.82	7.48	7.30	
p-C_2H_5	65.0	4.80	7.45	7.18	1.24 triplet (CH_3)
					2.66 quartet (CH_2)
p-*n*-C_4H_9	65.0	4.80	7.40	7.19	0.95 triplet (CH_3)
					1.45 multiplet (CH_2-CH_2)
					2.61 triplet (CH_2)
p-CH_3	65.0	4.81	7.41	7.16	2.34 (CH_3)
p-OCH_3	65.0	4.80	7.44	6.87	3.81 (OCH_3)

[a] The ^{1}H-NMR spectra were run on a Bruker WH-90 spectrometer using $CDCl_3$ as the solvent and lock and TMS as reference. All the chemical shifts are reported in ppm and the chemical coupling in Hz.

Table 3.4

^{1}H-NMR data for *trans*-[$PtBr_2(C_2H_4)$(*m*-R-an)] (*m*-R-an=meta substituted aniline)[a]

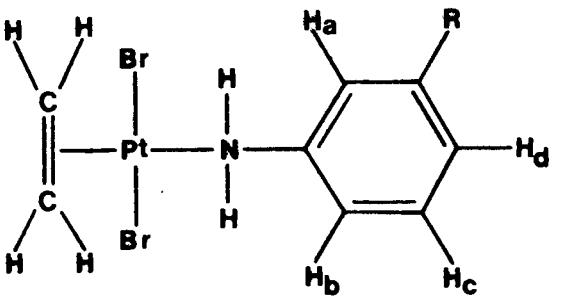

R	Olefin protons J_{Pt-H}		Aniline protons δ_{H_a} δ_{H_b} δ_{H_c} δ_{H_d}	Other protons δ
m-NO_2	61.0	4.84	(7.40)	
m-Br	66.0	4.84	(7.40)	
m-Cl	66.0	4.83	(7.40)	
m-I	66.0	4.82	(7.26)	
m-F	66.0	4.84	(7.28)	3.82(OCH_3)
m-OCH_3	65.0	4.81	(7.10)	
H	65.0	4.79	(7.36)	
m-CH_3	65.0	4.82	(7.31)	2.39(CH_3)

a The ^{1}H-NMR spectra were run on a Bruker WH-90 spectrometer, using $CDCl_3$ as the solvent and lock and TMS as reference. All the chemical shifts are reported in ppm and the chemical coupling in Hz.
Values in parentheses indicate mean of the multiplet.

Table 3.5

^{1}H-NMR data for *trans*-[$PtBr_2(C_2H_4)$(3,5-di-CH_3-aniline)][a]

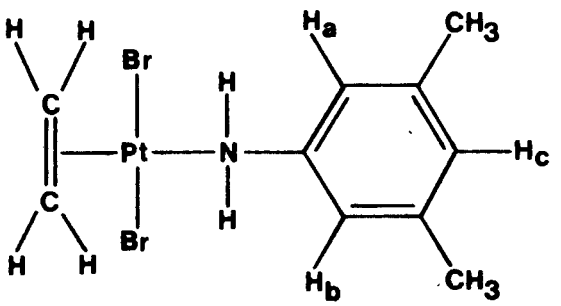

Olefinic protons		Aniline protons			Other protons
J_{Pt-H}		δ_{H_a}	δ_{H_b}	δ_{H_c}	δ
65.0	4.80	7.12	7.12	6.9	2.34(2 x CH_3)

a The ^{1}H-NMR spectra were run on a Bruker WH-90 spectrometer, using $CDCl_3$ as the solvent and lock and TMS as reference. All the chemical shifts are reported in ppm and the chemical coupling in Hz.

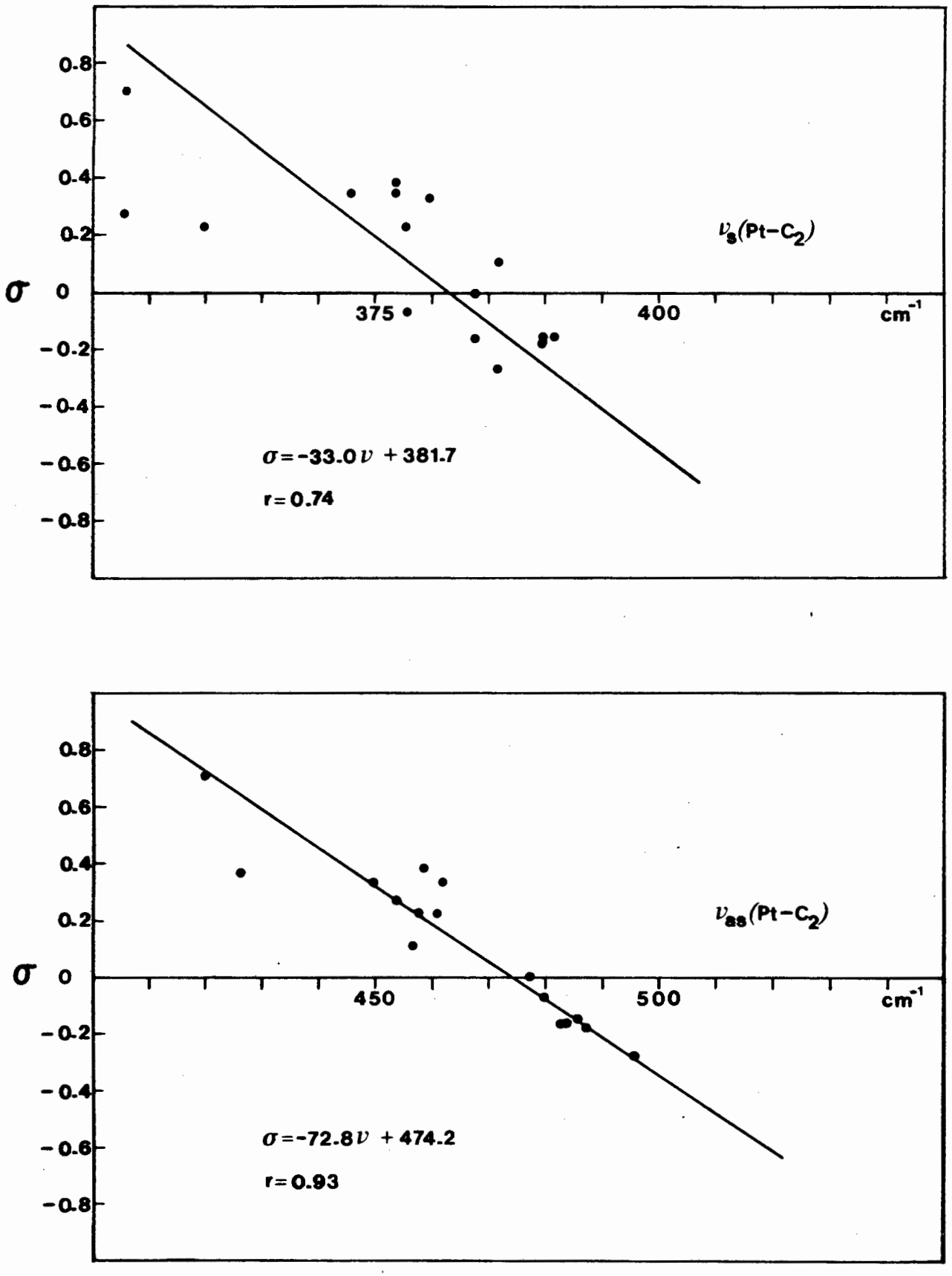

Fig. 3.4. Relationship between Hammett σ- values of R and $\nu_s(Pt-C_2)$ (top) and $\nu_{as}(Pt-C_2)$ (bottom)

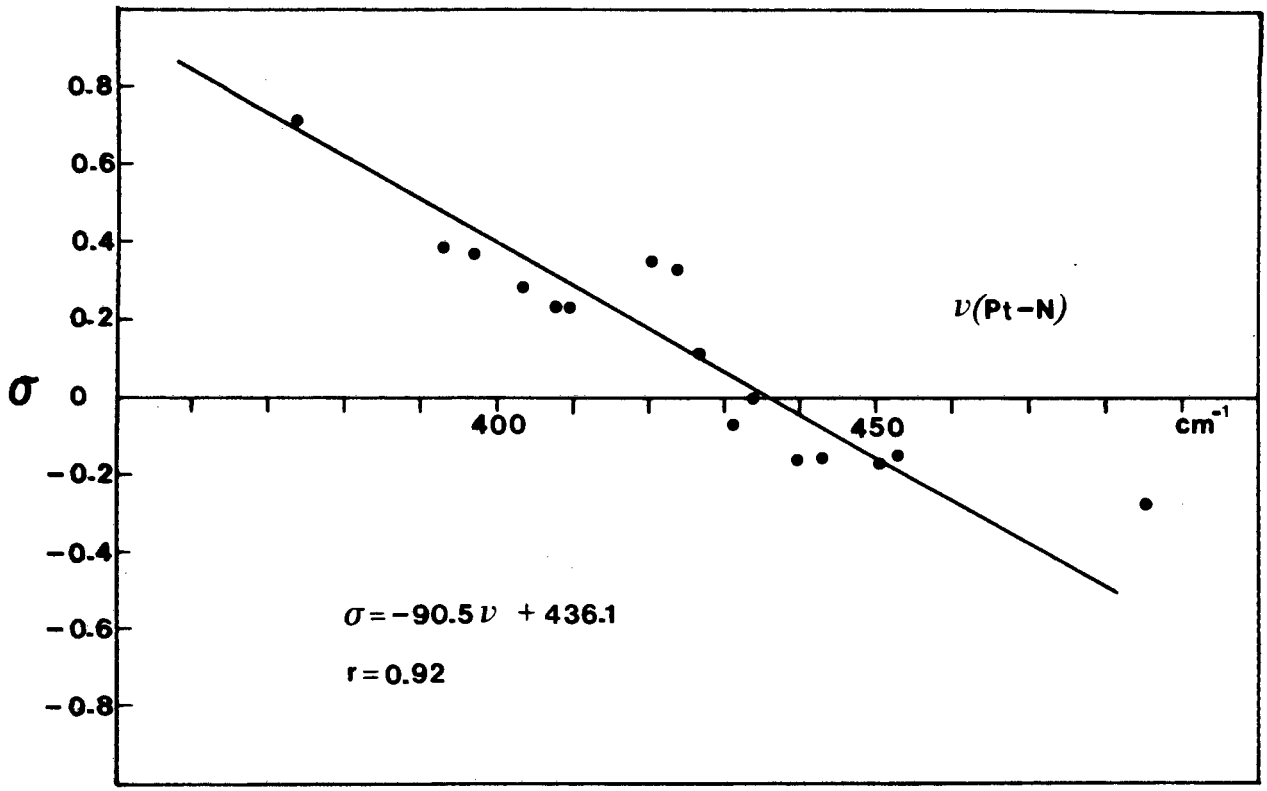

Fig. 3.5. Relationship between Hammett σ-value of R and ν(Pt-N)

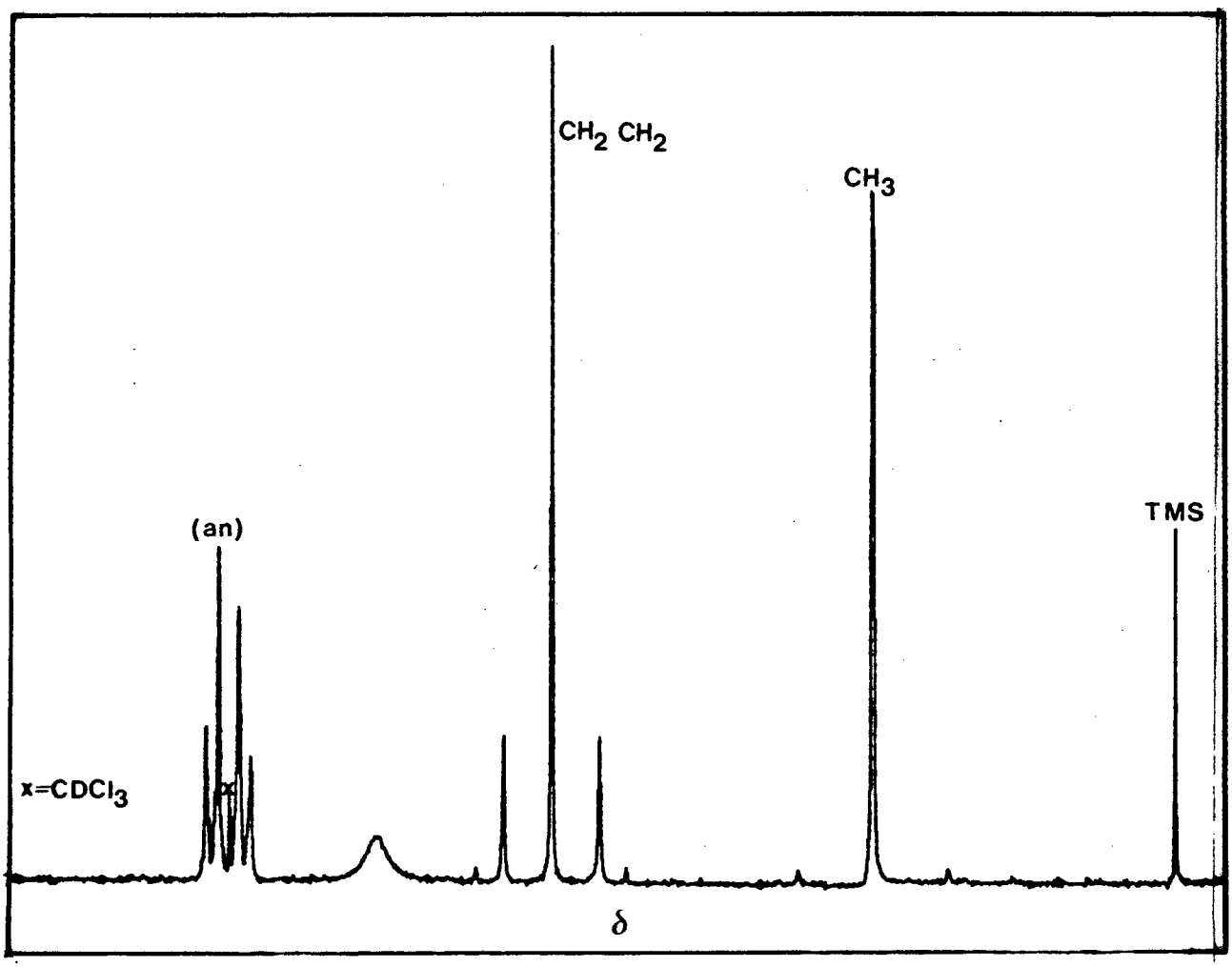

Fig. 3.6. ^{1}H-NMR spectrum of trans-[PtBr$_2$(C$_2$H$_4$)(p-CH$_3$-an)]

Table 3.6

UV data for the complexes *trans*-$[PtBr_2(C_2H_2)(R\text{-an})]$

R	σ	λ_{max}(nm)		Assignment
m-NO_2	0.71	210(br)	32 434	$Br^- \rightarrow Pt^{2+}$ + $\pi \rightarrow \pi^*(C_2H_4)$
		250(br)	92 136	$5d(Pt) \rightarrow \pi^*(C_2H_4)$ + $\pi \rightarrow \pi^*$(an)
m-Br	0.39	204	47 030	$Br^- \rightarrow Pt^{2+}$
		245	9 321	$\pi \rightarrow \pi^*$(an) + $\pi \rightarrow \pi^*(C_2H_4)$
		291	2 966	$5d(Pt) \rightarrow \pi^*(C_2H_4)$
m-Cl	0.37	204	48 713	$Br^- \rightarrow Pt^{2+}$
		239	12 430	$\pi \rightarrow \pi^*$(an) + $\pi \rightarrow \pi^*(C_2H_4)$
		265	5 375	$5d(Pt) \rightarrow \pi^*(C_2H_4)$
m-I	0.35	211	52 034	$Br^- \rightarrow Pt^{2+}$ + $\pi \rightarrow \pi^*(C_2H_4)$
		245	9 158	$\pi \rightarrow \pi^*$(an) + $5d(Pt) \rightarrow \pi^*(C_2H_4)$
m-F	0.33	203	33 390	$Br^- \rightarrow Pt^{2+}$
		209	32 560	$\pi \rightarrow \pi^*(C_2H_4)$
		268	3 733	$5d(Pt) \rightarrow \pi^*(C_2H_4)$ + $\pi \rightarrow \pi$(an)
p-I	0.28	201	55 410	$Br^- \rightarrow Pt^{2+}$
		211	42 681	$\pi \rightarrow \pi^*(C_2H_4)$
		245	20 592	$\pi \rightarrow \pi^*$(an) + $5d(Pt) \rightarrow \pi^*(C_2H_4)$
p-Br	0.23	201	38 015	$Br^- \rightarrow Pt^{2+}$
		213	27 749	$\pi \rightarrow \pi^*(C_2H_4)$
		241	13 597	$\pi \rightarrow \pi^*$(an)
		304	694	$5d(Pt) \rightarrow \pi^*(C_2H_4)$
p-Cl	0.23	201	31 403	$Br^- \rightarrow Pt^{2+}$
		211	29 813	$\pi \rightarrow \pi^*(C_2H_4)$
		242	10 335	$\pi \rightarrow \pi^*$(an)
		300	994	$5d(Pt) \rightarrow \pi^*(C_2H_4)$

Table 3.6 Continued/

R	σ	λ_{max}(nm)		Assignment
m-OCH_3	0.11	205	58 129	$Br^- \rightarrow Pt^{2+}$
		245	7 403	$\pi \rightarrow \pi^*$(an) + $\pi \rightarrow \pi^*(C_2H_4)$
		275	5 065	$5d$(Pt) $\rightarrow \pi^*(C_2H_4)$
H	0	202	24 945	$Br^- \rightarrow Pt^{2+}$
		210	31 265	$\pi \rightarrow \pi^*(C_2H_4)$
		264	4 158	$\pi \rightarrow \pi^*$(an) + $5d$(Pt) $\rightarrow \pi^*(C_2H_4)$
m-CH_3	-0.07	202	36 915	$Br^- \rightarrow Pt^{2+}$ + $\pi \rightarrow \pi^*(C_2H_4)$
		266	4 537	$\pi \rightarrow \pi^*$(an) + $5d$(Pt) $\pi^*(C_2H_4)$
p-C_2H_5	-0.15	202	36 722	$Br^- \rightarrow Pt^{2+}$
		208	35 273	$\pi \rightarrow \pi^*(C_2H_4)$
		271	4 831	$\pi \rightarrow \pi^*$(an) + $5d$(Pt) $\rightarrow \pi^*(C_2H_4)$
3,5-di-CH_3	-0.16	206	62 377	$Br^- \rightarrow Pt^{2+}$ + $\pi \rightarrow \pi^*(C_2H_4)$
		271	6 019	$\pi \rightarrow \pi^*$(an) + $5d$(Pt) $\rightarrow \pi^*(C_2H_4)$
p-*n*-C_4H_9	-0.16	201	32 880	$Br^- \rightarrow Pt^{2+}$
		210	29 110	$\pi \rightarrow \pi^*(C_2H_4)$
		265	5 026	$\pi \rightarrow \pi^*$(an) + $5d$(Pt) $\rightarrow \pi^*(C_2H_4)$
p-CH_3	-0.17	202	34 832	$Br^- \rightarrow Pt^{2+}$
		209	35 888	$\pi \rightarrow \pi^*(C_2H_4)$
		265	5 067	$\pi \rightarrow \pi^*$(an) + $5d$(Pt) $\rightarrow \pi^*(C_2H_4)$
p-OCH_3	-0.27	201	34 697	$Br^- \rightarrow Pt^{2+}$ + π $\pi^*(C_2H_4)$
		265	5 924	$\pi \rightarrow \pi^*$(an) + $5d$(Pt) $\rightarrow \pi^*(C_2H_4)$

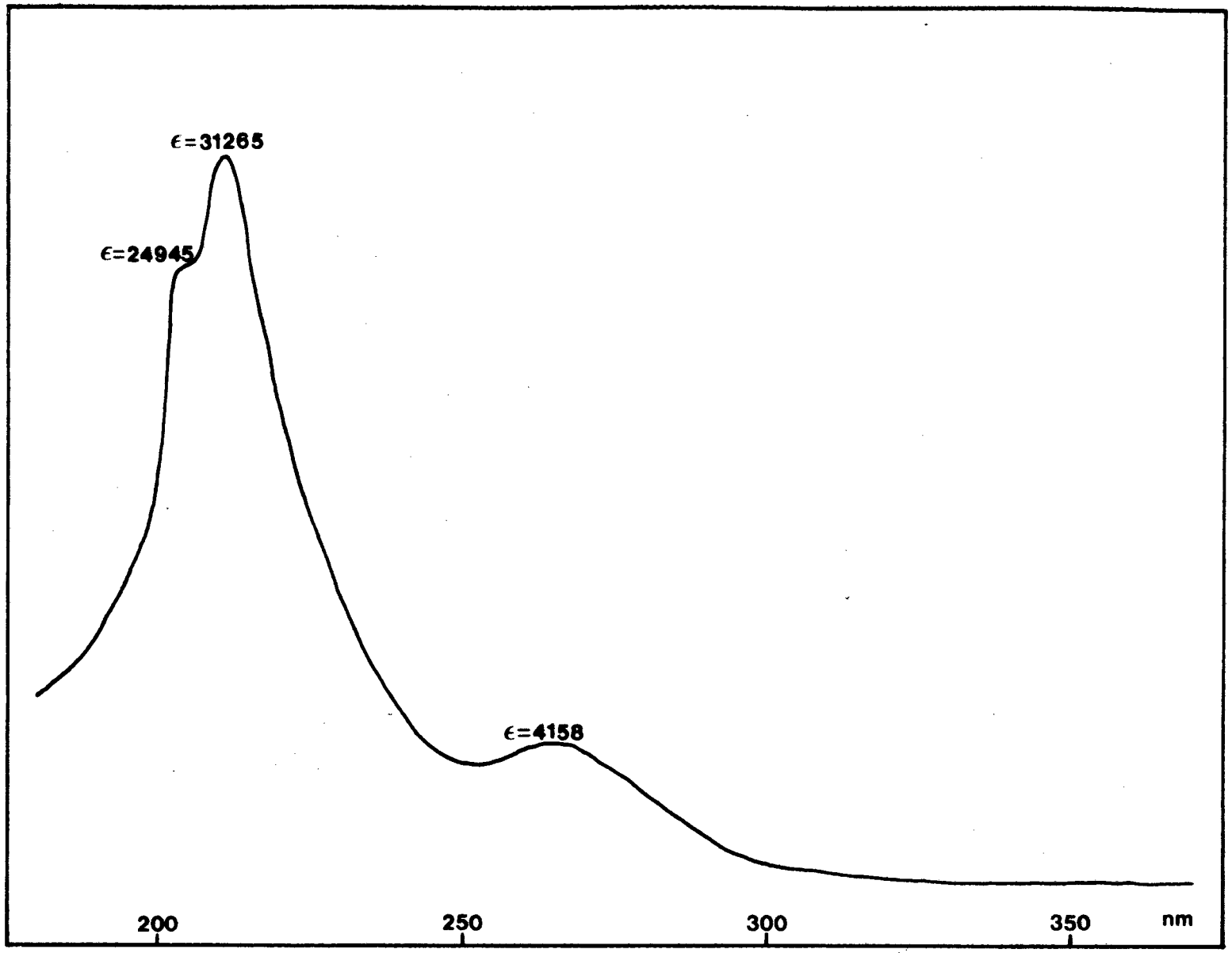

Fig. 3.7. The UV spectrum of trans-[$PtBr_2(C_2H_4)(an)$]

3.5 DISCUSSION

3.5.1 *Infrared Spectra*

The bromo- rather than the chloro-complexes were chosen for this study because ν(Pt-Cl) and ν(Pt-N) are practically coincident whereas ν(Pt-Br) and ν(Pt-N) are well separated. The bands of major interest which are most likely to be influenced by the substituent effects are ν(Pt-C_2) (antisymmetric and symmetric), ν(Pt-N), ν(C=C) and ν(Pt-Br). Assignments for these bands were determined by (separately) deuterating ethylene (C_2D_4) and aniline (aniline-d_5) in the complexes. Bands below 600 cm^{-1} which shift to lower frequency on ethylene deuteration but not on aniline deuteration are assigned to ν(Pt-C_2) and those shifted by aniline deuteration but not by ethylene labelling are assigned to ν(Pt-N). Bands unshifted by both types of labelling are assigned to ν(Pt-Br). In this way, clear distinction between the three types of metal-ligand stretching frequencies is possible. The details of the assignment technique have been given elsewhere [58].

The infrared data are reported in Table 3.2, and a plot of the frequencies of these bands against σ are shown in

Figures 3.4 and 3.5. This Hammett constant, σ, is an indication of the ability of the substituent to either withdraw electrons from an aromatic ring or donate them into it. It is clear that both $\nu(Pt-C_2)$ and $\nu(Pt-N)$ increase as the electron-releasing capacities of the substituents increase (negative σ-values), indicating that the electronic effects of the substituents are transmitted through the molecule. It would be anticipated that the $\nu(Pt-N)$ band would be particularly sensitive to the substituent effect and this is reflected by the considerable shift in $\nu(Pt-N)$ over the range of σ-values of the substituent studied. No regular effect on $\nu(C=C)$ is observable. It is interesting to note that the mass effects of substituents do not appear to influence the frequency to any noticeable extent. Evidently the large mass of the platinum atom insulates the coordinated anilines so that their high frequency modes of vibration are independent of the masses of the various substituents.

3.5.2 *^{1}H-NMR Spectra*

The ^{1}H-NMR data for the substituted anilines are recorded in Tables 3.3, 3.4 and 3.5 and a typical spectrum shown in Figure 3.6. J_{Pt-H} is relatively constant and is consistent with the NMR data for analogous complexes in which the aniline is replaced by pyridine, pyrazine, imidazole, ammonia and pyridine *N*-oxide [60]. There is also little variation in the chemical shift of the olefinic protons

which are too far removed from the substituent for its shielding effect to be felt. A similar observation was made for the complexes *trans*-$[PtCl_2(C_2H_4)(R\text{-}py)]$ [60] and *trans*-$[PtCl_2(C_2H_4)(R\text{-}an)]$ [59]. The chemical shifts of the aromatic protons tend to be higher for electron-withdrawing substituents which clearly increase the electron density within the aromatic ring and hence the shielding of the aromatic protons.

3.5.3 *Electronic Spectra*

The UV data are reported in Table 3.6 and a typical spectrum shown in Figure 3.7. By analogy with similar complexes previously studied [53,59,60], we expect the $\pi \longrightarrow \pi^*$ transitions of coordinated aniline and the ethylene as well as the $5d \longrightarrow \pi^*$(ethylene) inverse charge transfer and the $Br^- \longrightarrow Pt^{2+}$ charge transfer bands to be present. As observed in earlier work [59], the $\pi \longrightarrow \pi^*$(aniline) transition exhibits maximum sensitivity to the nature of R, but no linear correlation exists due to the broad nature of the electronic bands.

CHAPTER 4

CHAPTER 4

4. THE APPLICATION OF SPECTROSCOPIC TECHNIQUES TO THE COMPLEXES *trans*-$[PtBr_2(CO)(R\text{-an})]$ (R-an = substituted aniline)

4.1 INTRODUCTION

One of the most active areas of research is the structure of transition metal complexes wherein carbon monoxide groups are ligands. Schutzenberger [61] first recognised carbon monoxide as a ligand in his preparation and characterization of $Pt(CO)_2Cl_2$, although the first binary metal carbonyl, tetracarbonylnickel was discovered in 1890 [62].

Forerunners in this field [42,47,63] realized the analogous roles of carbon monoxide and ethylene in coordination compounds and suggested this for their early interpretations of the bonding in both carbonyl- and olefinic-metal complexes. In agreement with their views were the results of reactions of $K[PtCl_3(C_2H_4)]$ and their formally similar counterparts, carbonyl trichloro platinite, $K[PtCl_3(CO)]$.

As in metal-olefinic complexes, metal carbonyls are formed because in addition to the metal-carbon σ-bond, another

type of bond exists. The accepted view [64,65] of bonding in metal carbonyl complexes is one in which charge is donated from the ligand to the metal by a σ-bond and withdrawn from the metal atom into the π^* (antibonding) orbitals of the ligand by π-bonding. This is diagramatically represented in Figure 4.1. The electron density in the π^* orbitals is dependent, amongst other things, on the charge donation from ligand to metal and hence the σ-and π-bonding is synergic.

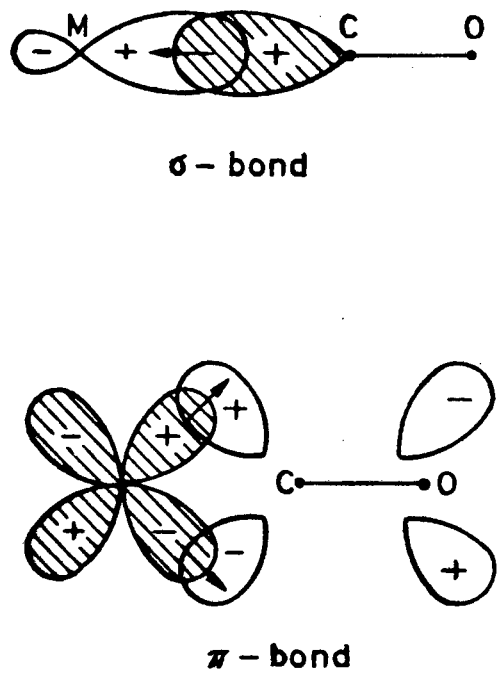

FIGURE 4.1 The bonding in metal carbonyls

According to the preceding description of the bonding, as the extent of back donation from the metal to the ligand

increases, the M-C bond becomes stronger and the C≡O bond becomes weaker. The infrared spectra of these systems provide a most convenient and useful estimate of this. Thus the characteristic stretching frequency of the C-O bond in carbon monoxide itself is 2155 cm^{-1} but in metal carbonyls it is around 2000 cm^{-1}. The lowered frequency shows that the bonding between carbon and oxygen is weakened. Furthermore, the synergic effect could lead to the prediction that as negative charge is added to the metal the ν(CO) would decrease, as it does in the isoelectronic series [66]:

$Ni(CO)_4$	$Co(CO)_4^-$	$Fe(CO)_4^{2-}$
2060	1890	1790 cm^{-1}

Hence for metal-carbonyl complexes, weakening of the C-O bond, insofar as electronic factors are concerned is due entirely to back-donation from metal $d\pi$-orbitals to CO π^* orbitals, with the σ-donation slightly cancelling some of this effect.

In the inital work [67] on metal carbonyl complexes, the complexes were synthesized *via* the $[PtCl_3(CO)]^-$ ion. This unfavourable route was soon curtailed when it was realised than an excess of one olefin would displace another. The new and simpler route [68] as depicted in Scheme 4.1, involved the displacement of ethylene by carbon monoxide, with retention of configuration [69,70] in platinum-

ethylene complexes. This discovery made available a large number of platinum(II) carbonyl complexes.

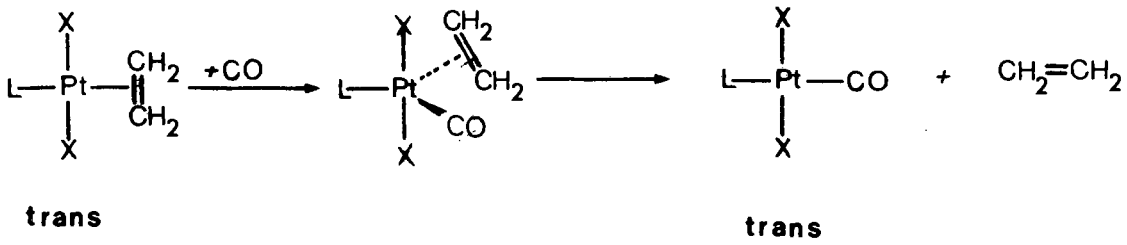

trans **trans**

SCHEME 4.1

The *trans*-effect of carbon monoxide is very pronounced as shown by its "high" position in the *trans*-effect series. Unfortunately, to date no X-ray crystallographic data is available for $Z[PtX_3(CO)]$ (X=halogen, Z=counterion) thus the Pt-X bond lengths cannot be compared to evaluate the *trans*-effect of the carbon monoxide ligand. Nevertheless, by analogy with the ethylene complexes for which the X-ray structures have been determined, it is expected that due to the *trans*-effect of the carbon monoxide ligand, the Pt-X bond *trans* to the carbon monoxide ligand will be longer than the other two Pt-X bonds.

The carbonyl complexes have the same C_{2v} symmetry as their ethylene counterparts, thus similar infrared spectral bands are expected whenever the vibrations do not involve the ligand (carbon monoxide or ethylene). The metal-carbonyl

stretching frequencies which appear, normally in a restricted frequency range of the infrared spectrum, are particularly amenable to experimental study since ordinarily only one intense, easily identifiable band is present. As previously mentioned, the ethylene and carbonyl complexes have similar bonding schemes, hence it is not surprising that their electronic spectra are similar. They show the expected strong metal-to-ligand charge transfer band as well as the other ligand-metal interactions.

In this chapter a series of complexes *trans*-[$PtBr_2$(CO)(R-an)] (R-an = substituted aniline) have been prepared. The influence of the variation of R on the properties of the above complexes have been investigated by infrared, ^{1}H-NMR and ultraviolet spectroscopy.

4.2 PREPARATION OF COMPLEXES

4.2.1 *Preparation of trans-[$PtBr_2$(CO)(R-an)] (R-an = substituted aniline)*

Prior to formation of the complexes the chloroform and *n*-hexane solvents required were dried and distilled over phosphorus pentoxide and sodium, respectively. This is essential to prevent the rapid decomposition of the carbonyl complexes and the precipitation of elemental platinum [71].

The carbonyl complexes were all prepared from their corresponding ethylene analogues. The ethylene complex (1 mmol) was dissolved in dry chloroform (30 ml), and carbon monoxide was bubbled through the solution, the temperature of the solution being maintained just above ($\sim 5^{o}$) room temperature. After several minutes (3-60 min), depending on the substituent on the aniline ring, the colour of the solution changed from an initial bright yellow to a final pale, greenish-yellow. At this point the solution was concentrated by blowing off chloroform in a stream of warm air, and, on addition of dry *n*-hexane (20 ml) to the cloud point the product precipitated. The product was isolated by vacuum filtration, washed with *n*-hexane and stored over silica gel in a vacuum dessicator (< 0.1 mm Hg).

Yields were quantitative (> 90%) and the composition and purity of all the greenish-yellow compounds were determined by microanalysis (C,H,N), Table 4.1.

4.3 ANALYSES OF COMPLEXES

Table 4.1

Analytical data for the complexes *trans*-$[PtBr_2(CO)(R\text{-an})]$

R	Calculated			Found		
	%C	%H	%N	%C	%H	%N
H	17.7	1.5	2.9	17.7	1.5	2.9
m -CH_3	19.6	1.9	2.9	19.6	1.9	2.9
m -OCH_3	19.0	1.8	2.8	19.3	1.8	2.7
m -F	16.6	1.2	2.8	17.4	1.3	3.0
m -Cl	16.5	1.2	2.8	16.5	1.2	2.8
m -NO_2	16.1	1.2	5.4	16.5	1.3	5.5
m -Br	15.2	1.1	2.5	15.3	1.1	2.5
m -I	14.0	1.0	2.3	14.1	1.0	2.3
p -*n*-C_4H_9	24.8	2.8	2.6	24.8	2.8	2.7
p -C_2H_5	21.4	2.2	2.8	22.0	2.3	2.8
p -CH_3	19.6	1.9	2.9	19.6	1.9	2.9
p -OCH_3	19.0	1.8	2.8	19.0	1.8	2.8
p -Cl	16.5	1.2	2.7	16.6	1.2	2.9
p -Br	15.2	1.1	2.5	15.3	1.1	2.5
p -I	14.0	1.0	2.3	13.9	1.0	2.3
3,5-di-CH_3	21.5	2.2	2.8	21.5	2.2	2.8

4.4 RESULTS

Table 4.2

Principal infrared band frequencies (cm^{-1}) for the complexes *trans*-[$PtBr_2$(CO)(R-an)][a]

R	σ	δ(PtC≡O)	ν_s(Pt-C)	ν(Pt-N)	ν(C≡O)[b]
m-NO_2	0.71	495	473	355	2127.8
m-Br	0.39	502	475	368	2126.5
m-Cl	0.37	511	477	377	2126.4
m-I	0.35	504	491	359	2126.3
m-F	0.33	515	486	422	2126.5
p-I	0.28	518	483	363	2126.1
p-Br	0.23	512	486	369	2126.3
p-Cl	0.23	527	483	388	2126.6
m-OH_3	0.11	526	490	428	2125.5
H	0	530	493	434	2125.5
(an-d_5)		(3)	(2)	(20)	
m-CH_3	-0.07	532	506	460	2124.8
p-C_2H_5	-0.15	533	501	465	2124.5
3,5-di-CH_3	-0.16	533	505	469	2124.9
p-*n*-C_4H_9	-0.16	539	513	468	2124.7
p-CH_3	-0.17	530	506	476	2124.9
p-OCH_3	-0.27	542	508	477	2124.6

[a] In all the complexes ν(Pt-Br) occur at 253 ± 4cm^{-1} and is unshifted by deuteration.

[b] ν(C≡O) determined in chloroform solution: Precision = ±0.5cm^{-1} over three determinations.
Number in parentheses are the shifts (cm^{-1}) induced by deuteration.

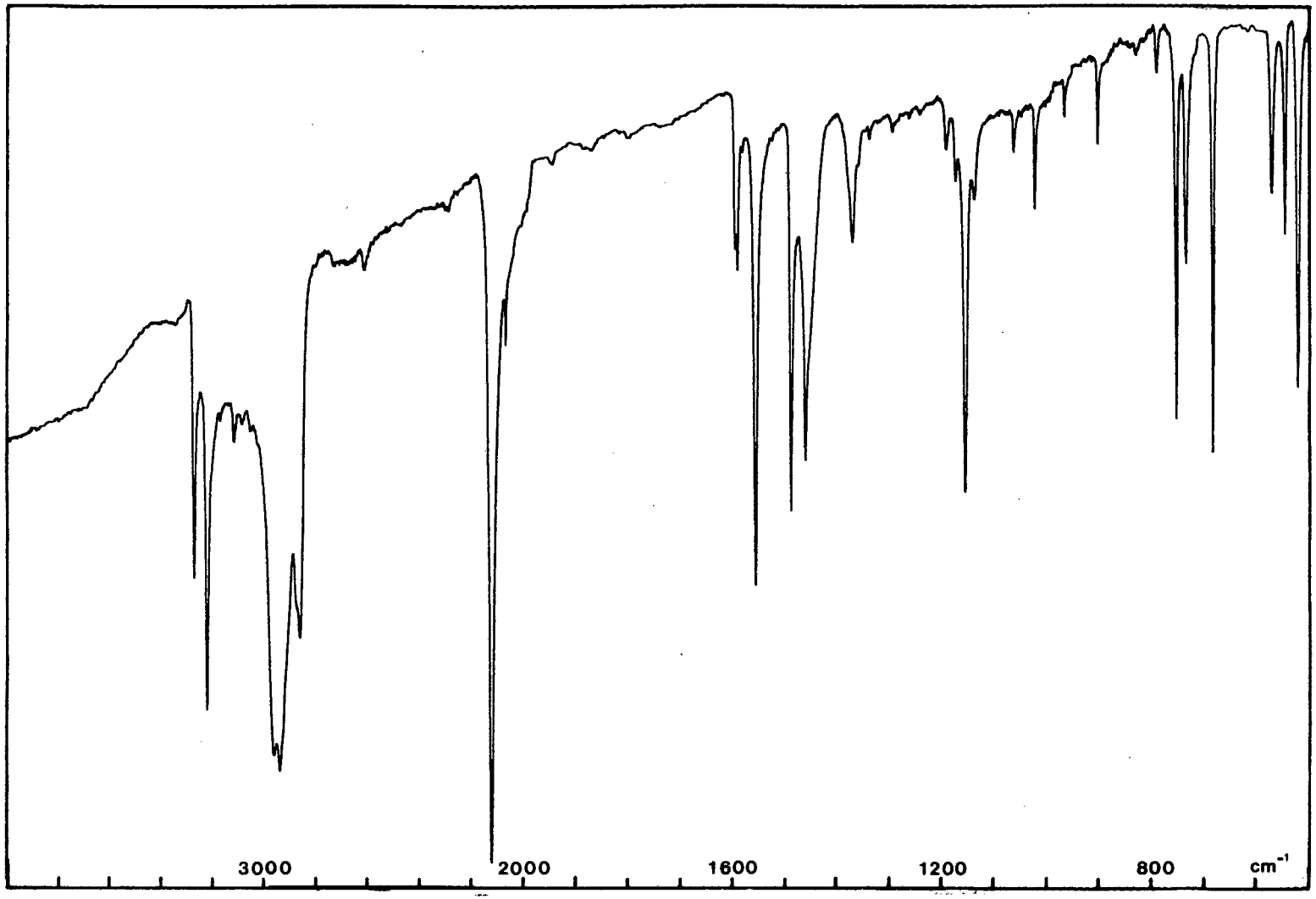

Fig. 4.2. Infrared spectrum of trans-[$PtBr_2(CO)(an)$]

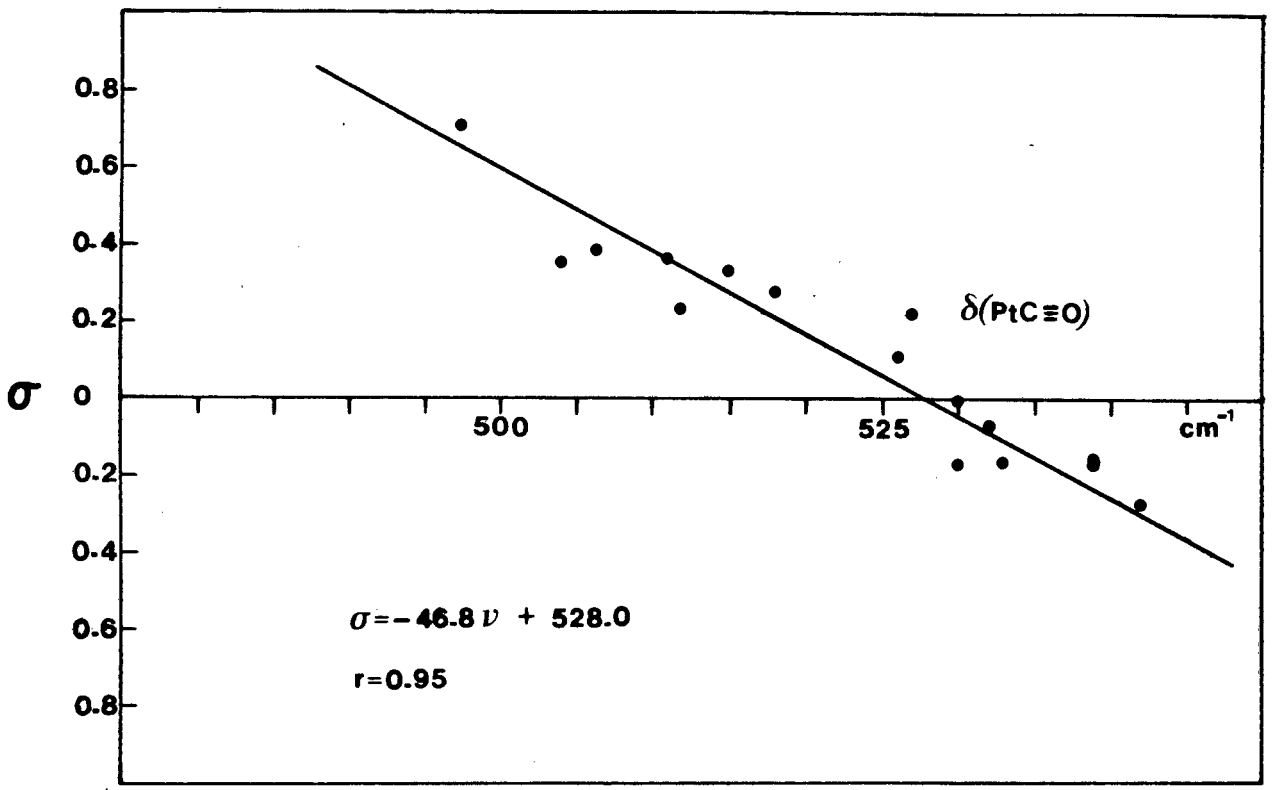

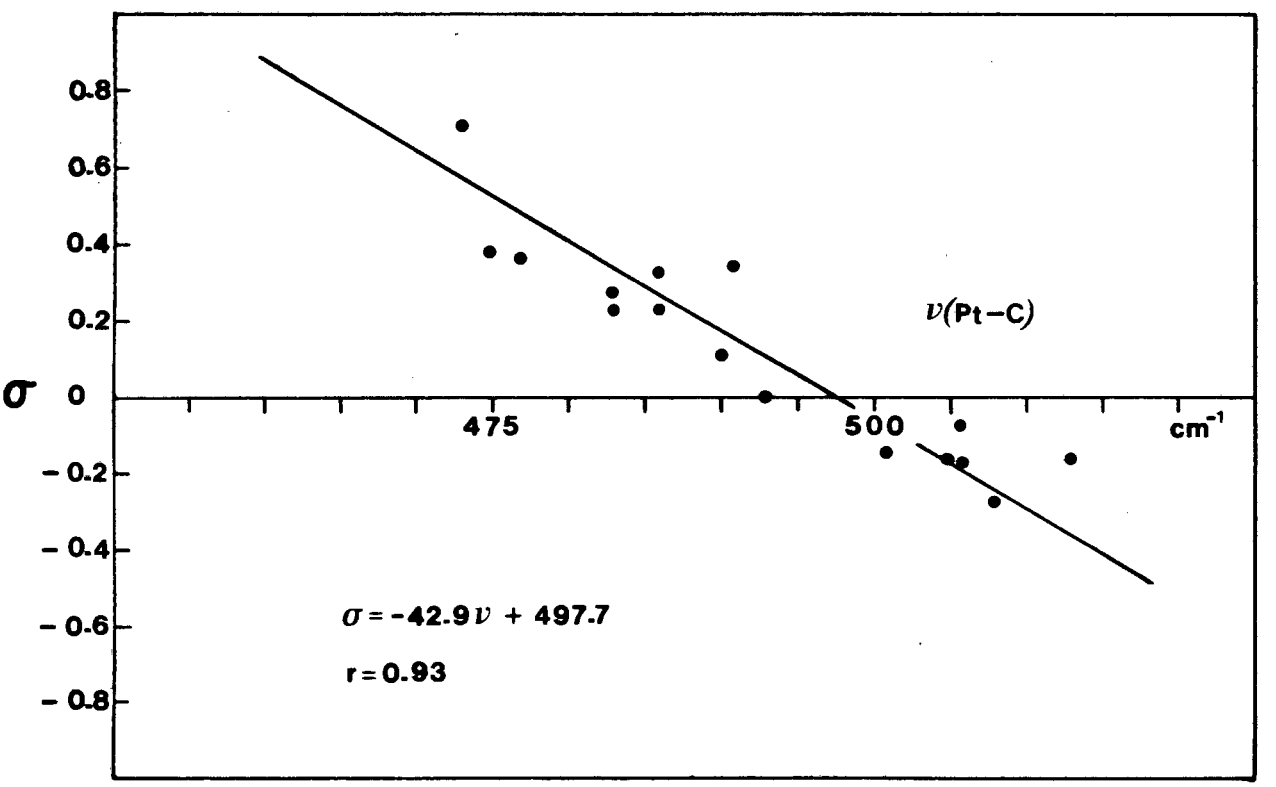

Fig. 4.3. Relationship between Hammett σ-value of R and infrared frequencies

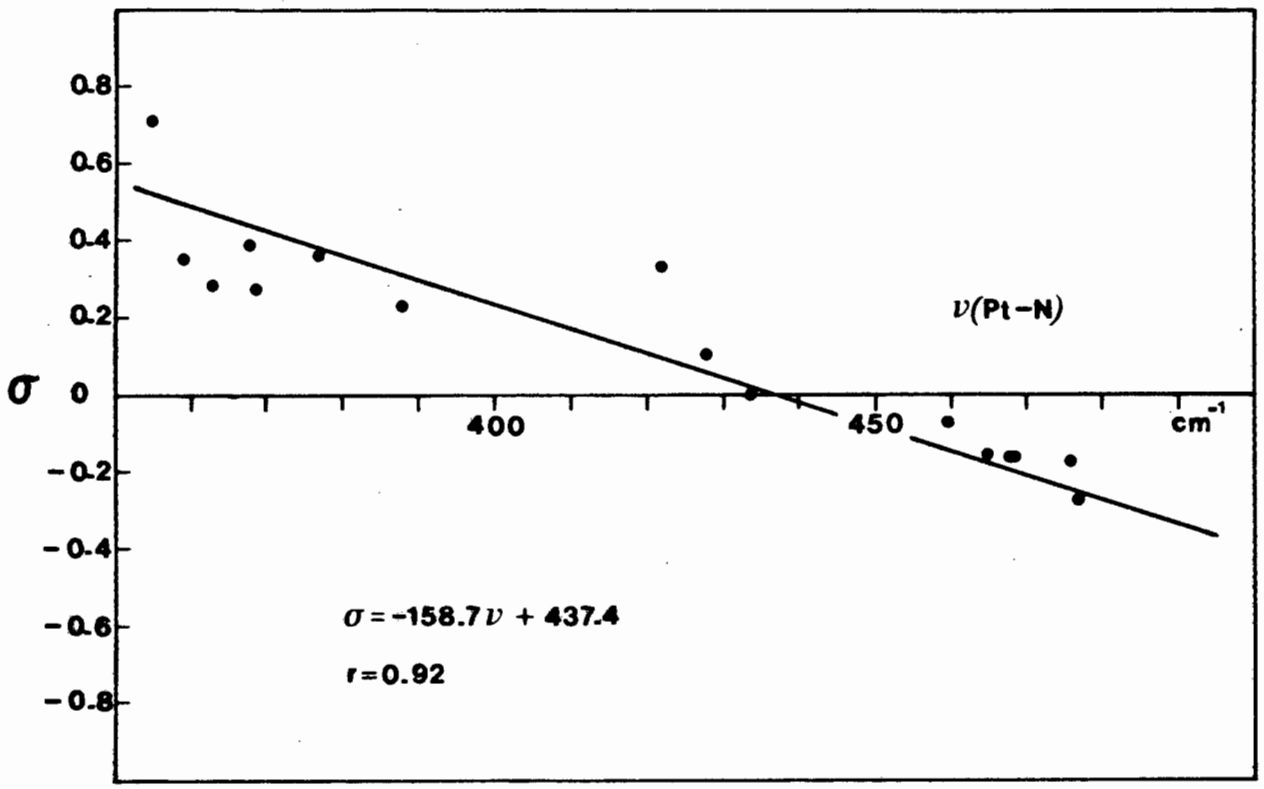

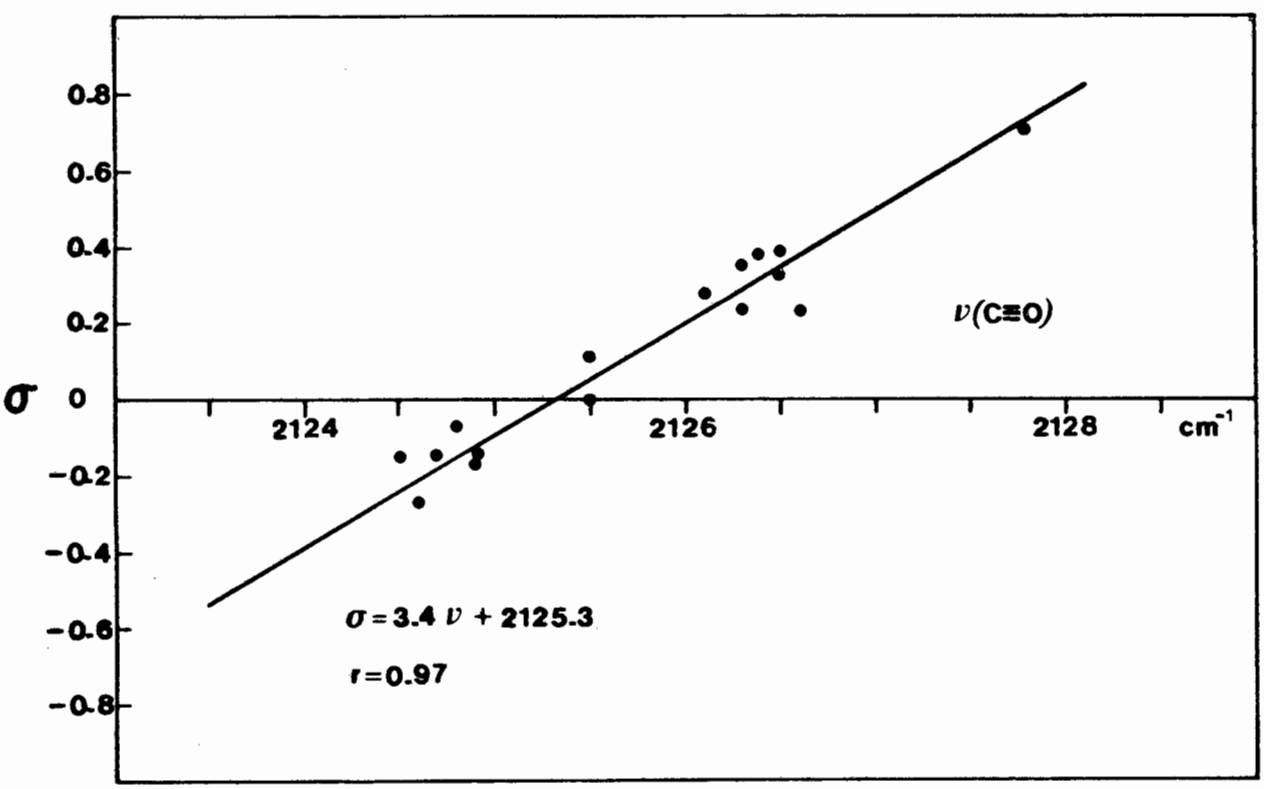

Fig. 4.4. Relationship between Hammett σ- value of R and infrared frequencies

TABLE 4.3

^{1}H-NMR data for the complexes *trans*-[$PtBr_2$(CO)(R-an)][a]

R	σ	δ_{H_a}	δ_{H_b}	δ_{H_c}	δ_{H_d}	Other protons
m-NO_2	0.71		(8.08)			
m-Br	0.39		(7.45 & 7.72)			
m-Cl	0.37		(7.48)			
m-I	0.35		(7.58)			
m-F	0.33		(6,90 & 7.20)			
p-I	0.28	7.84	7.13			
p-Br	0.23	7.60	7.40			
p-Cl	0.23	7.55	7.35			
m-OCH_3	0.11		(7.00 & 7.20)			3.11 (OCH_3)
H	0		(7.42)			
m-CH_3	-0.07		(7.20)			2.39 (CH_3)
p-C_2H_5	-0.15	7.40	7.15			1.18 triplet (CH_3)
						2.60 quartet (CH_2)
p-*n*-C_4H_9	-0.16	7.43	7.22			0.95 triplet (CH_3)
						1.5 multiplet (CH_2-CH_2)
						2.6 triplet (CH_2)
3,5-di-CH_3	-0.16		(7.0)			2.30 (2 x CH_3)
p-CH_3	-0.17	7.45	7.20			2.33 (CH_3)
p-OCH_3	-0.27	7.48	6.92			3.80 (OCH_3)

a The ^{1}H-NMR spectra were run on a Bruker WH-90 spectrometer using CD_3COCD_3 as a solvent and lock and TMS as reference. All the chemical shifts are reported in ppm and the chemical coupling in Hz.
Values in parentheses indicate mean of the multiplet(s).

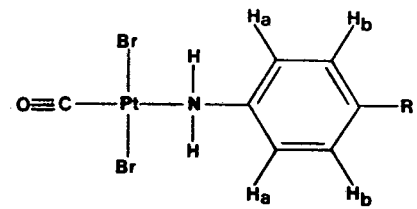

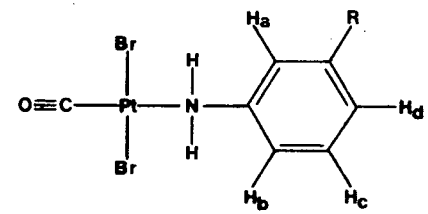

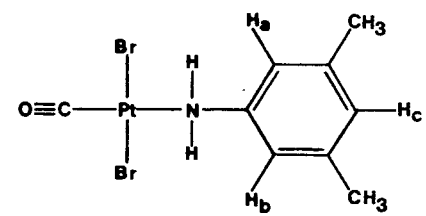

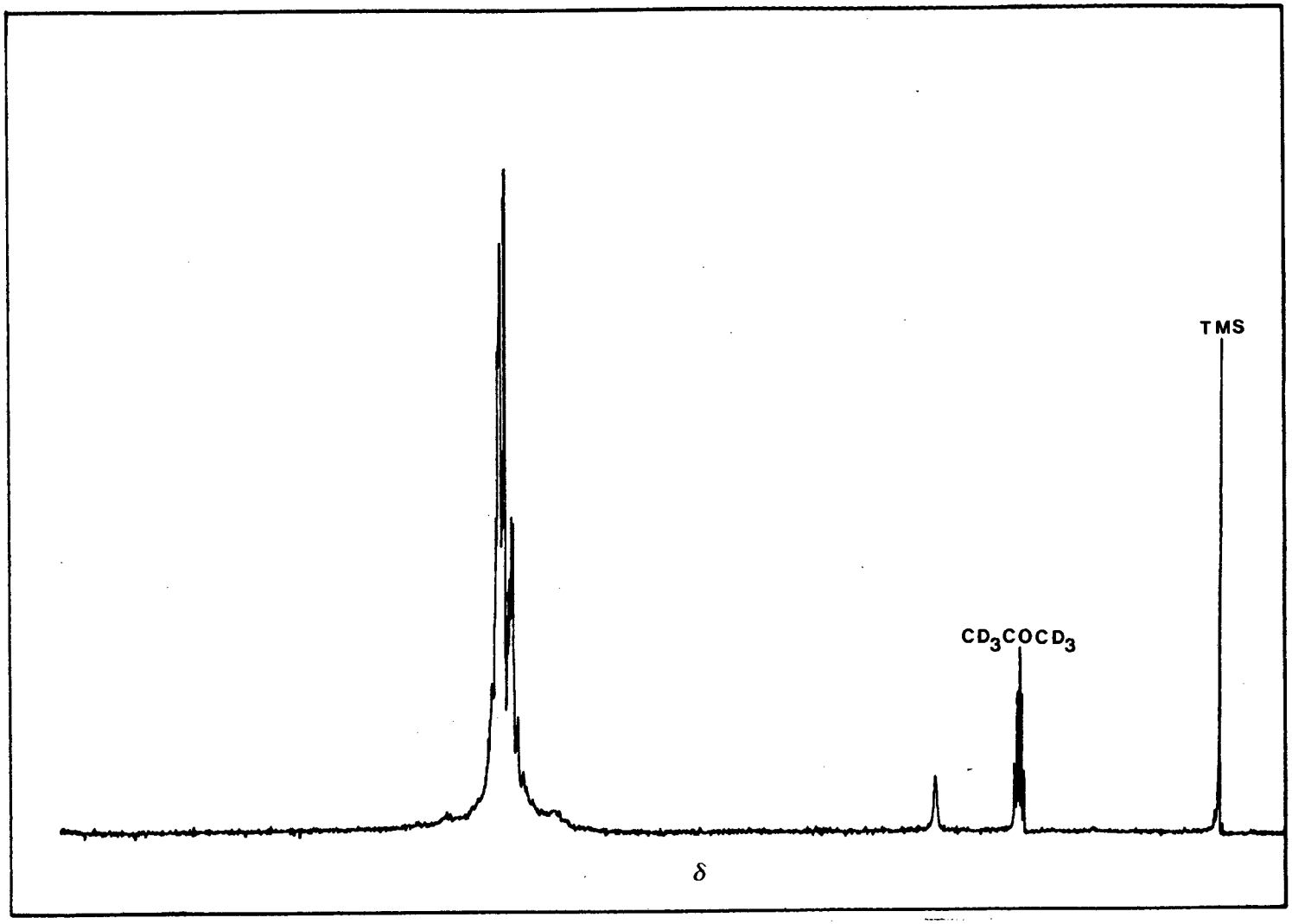

Fig. 4.5. ^{1}H-NMR *spectrum of trans-*$[PtBr_2(CO)(an)]$

Table 4.4

UV data for the complexes *trans*-$[PtBr_2(CO)(R\text{-an})]$

R	σ	λ_{max}(nm)		Assignment
m-NO_2	0.71	205	28 182	$Br^- \rightarrow Pt^{2+}$
		227	20 936	$\pi \rightarrow \pi^*$ (an)
		250	12 883	$\pi \rightarrow \pi^*$ (CO)
		283	4 026	5*d* (Pt) $\rightarrow \pi^*$ (CO)
m-Br	0.39	203	58 062	$Br^- \rightarrow Pt^{2+}$
		237	11 105	$\pi \rightarrow \pi^*$ (an) + $\pi \rightarrow \pi^*$ (CO)
		287	2 538	5*d* (Pt) $\rightarrow \pi^*$ (CO)
m-Cl	0.37	204	56 183	$Br^- \rightarrow Pt^{2+}$
		240	11 360	$\pi \rightarrow \pi^*$ (an) + $\pi \rightarrow \pi^*$ (CO)
		288	2 763	5*d* (Pt) $\rightarrow \pi^*$ (CO)
m-I	0.35	202	39 013	$Br^- \rightarrow Pt^{2+}$
		211	47 646	$\pi \rightarrow \pi^*$ (an)
		242	10 232	$\pi \rightarrow \pi^*$ (CO)
		290	2 558	5*d* (Pt) $\rightarrow \pi^*$ (CO)
m-F	0.33	202	38 141	$Br^- \rightarrow Pt^{2+}$
		232	12 323	$\pi \rightarrow \pi^*$ (an) + $\pi \rightarrow \pi^*$ (CO)
		280	2 347	5*d* (Pt) $\rightarrow \pi^*$ (CO)
p-I	0.28	202	46 368	$Br^- \rightarrow Pt^{2+}$
		246	18 547	$\pi \rightarrow \pi^*$ (an) + $\pi \rightarrow \pi^*$ (CO)
		214	2 558	5*d* (Pt) $\rightarrow \pi^*$ (CO)
p-Br	0.23	202	38 015	$Br^- \rightarrow Pt^{2+}$
		241	14 434	$\pi \rightarrow \pi^*$ (an) + $\pi \rightarrow \pi^*$ (CO)
		290	1 981	5*d* (Pt) $\rightarrow \pi^*$ (CO)

Table 4.4 Continued/

R	σ	λ_{max}(nm)		Assignment
p -Cl	0.23	202	43 602	$Br^- \rightarrow Pt^{2+}$
		241	13 902	$\pi \rightarrow \pi^*$(an) + $\pi \rightarrow \pi^*$(CO)
		288	2 527	5*d*(Pt)$\rightarrow \pi^*$(CO)
m -OCH_3	0.11	204	54 316	$Br^- \rightarrow Pt^{2+}$
		239	7 242	$\pi \rightarrow \pi^*$(an) + $\pi \rightarrow \pi^*$(CO)
		283	2 304	5*d*(Pt)$\rightarrow \pi^*$(CO)
H	0	202	34 273	$Br^- \rightarrow Pt^{2+}$
		238	8 047	$\pi \rightarrow \pi^*$(an) + $\pi \rightarrow \pi^*$(CO)
		282	2 077	5*d*(Pt)$\rightarrow \pi^*$(CO)
m -CH_3	-0.07	202	45 164	$Br^- \rightarrow Pt^{2+}$
		236	9 971	$\pi \rightarrow \pi^*$(an) + $\pi \rightarrow \pi^*$(CO)
		279	2 932	5*d*(Pt)$\rightarrow \pi^*$(CO)
p -C_2H_5	-0.15	202	38 097	$Br^- \rightarrow Pt^{2+}$
		233	10 179	$\pi \rightarrow \pi^*$(an) + $\pi \rightarrow \pi^*$(CO)
		280	2 327	5*d*(Pt)$\rightarrow \pi^*$(CO)
3,5-di-CH_3	-0.16	204	52 010	$Br^- \rightarrow Pt^{2+}$
		238	8 309	$\pi \rightarrow \pi^*$(an) + $\pi \rightarrow \pi^*$(CO)
		285	2 462	5*d*(Pt)$\rightarrow \pi^*$(CO)
p -*n*-C_4H_9	-0.16	201	46 586	$Br^- \rightarrow Pt^{2+}$
		234	11 568	$\pi \rightarrow \pi^*$(an) + $\pi \rightarrow \pi^*$(CO)
		281	3 439	5*d*(Pt) π^*(CO)
p -CH_3	-0.17	202	38 463	$Br^- \rightarrow Pt^{2+}$
		236	8 221	$\pi \rightarrow \pi^*$(an) + $\pi \rightarrow \pi^*$(CO)
		279	2 741	5*d*(Pt)$\rightarrow \pi^*$(CO)
p -OCH_3	-0.27	202	34 337	$Br^- \rightarrow Pt^{2+}$
		237	7 754	$\pi \rightarrow \pi^*$(an) + $\pi \rightarrow \pi^*$(CO)
		283	3 600	5*d*(Pt)$\rightarrow \pi^*$(CO)

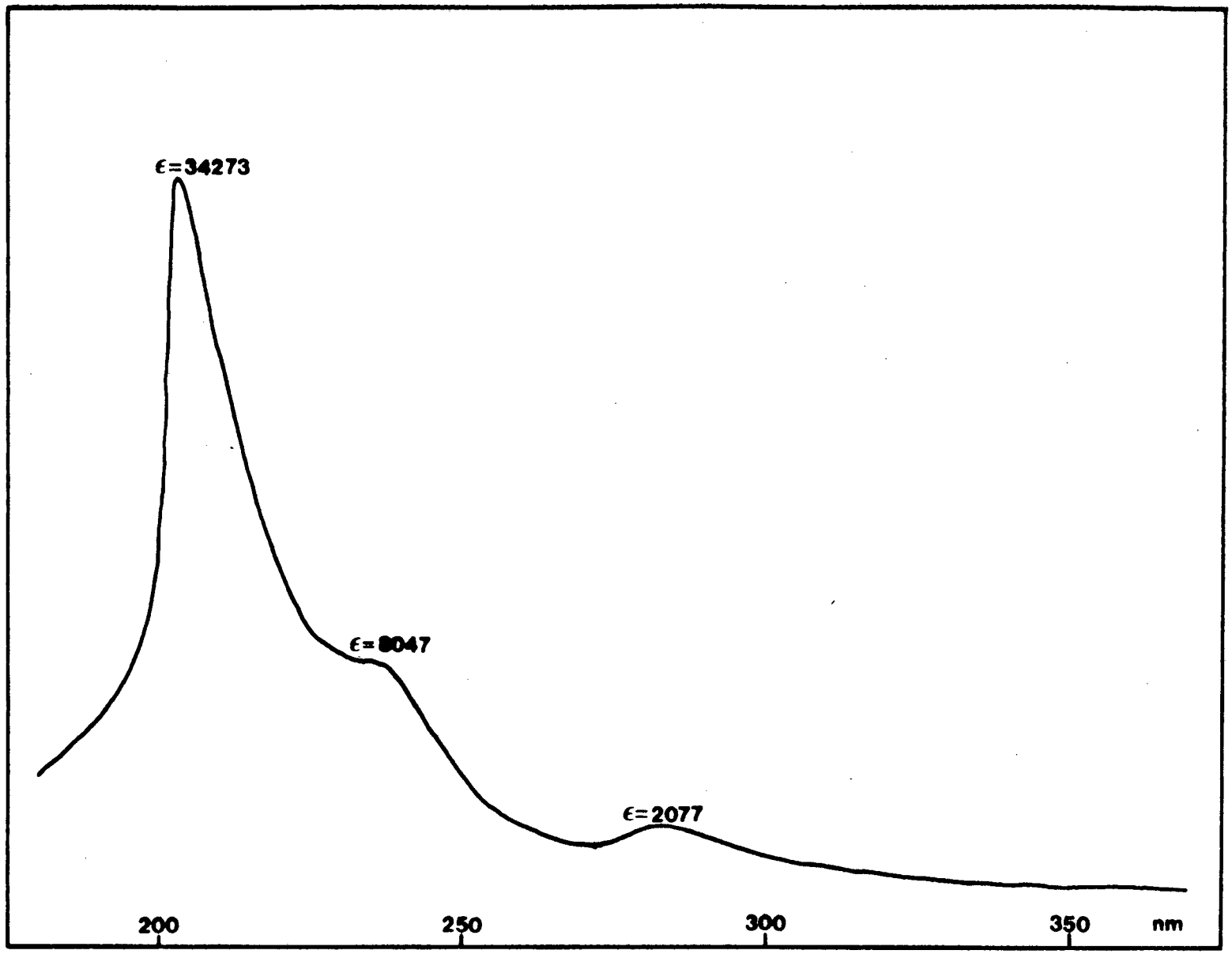

Fig. 4.6. The UV spectrum of trans-[$PtBr_2(CO)(an)$]

4.5 DISCUSSION

4.5.1 *Infrared Spectra*

The bands of major interest which are most likely to be influenced by the substituents are ν(Pt-C), δ(PtC≡O), ν(Pt-N) and ν(C≡O). Assignments for the ν(Pt-N) bands were determined by deuterating aniline (aniline-d_5), while the metal-carbonyl bands were assigned empirically.

A plot of the frequencies of these bands against σ are shown in Figures 4.3 and 4.4 and the frequency data are given in Table 4.2. As observed in the ethylene complexes, these carbonyl complexes show similar substituent effects. There is a large increase in ν(Pt-N) and a smaller increase in ν(Pt-C) as the electron-releasing capacities of the substituent increase (negative σ-values). ν(C≡O) exhibits, as expected from bonding considerations, a well defined trend towards lower frequency as the electron-releasing capacity of the substituents increases. The internal similarity of the infrared spectra of the various substituents suggests that they all have the same *trans*-configuration.

4.5.2 ^{1}*H-NMR Spectra*

The ^{1}H-NMR data for the substituted anilines are recorded in Table 4.3, and a typical spectrum is shown in Figure 4.5.

The complete disappearance of the olefinic proton peaks shows that there was total displacement of ethylene by carbon monoxide in the preparation of the complexes. As observed in the ethylene analogues, there is a tendency for the chemical shifts of the aromatic protons to be higher for electron-withdrawing substituents which clearly increase the electron density within the aromatic ring and hence the shielding of the aromatic protons.

4.5.3 *Electronic Spectra*

The UV data are reported in Table 4.4 and a typical spectrum shown in Figure 4.6. By analogy with the ethylene complexes, we expect to observe the $\pi \longrightarrow \pi^*$ transitions of the coordinated aniline and the carbon monoxide as well as the $5d \longrightarrow \pi^*(CO)$ inverse charge transfer band and the $Br^- \longrightarrow Pt^{2+}$ charge transfer bands. As observed in earlier work [59], the $\pi \longrightarrow \pi^*(CO)$ transition exhibits maximum sensitivity to the nature of R.

CHAPTER 5

CHAPTER 5

5. THE STRUCTURAL ANALYSIS OF VARIOUS DERIVATIVES OF *trans*-[$PtX_2(CO)(L)$] and [$Pt_2X_4(CO)_2(pz)$] (X=Cl,Br; L = aniline(an), pyridine *N*-oxide (pyO), pyridine (py), ammonia (NH_3), imidazole (Him), pyrazole (pyz) and pyrazine (pz)).

5.1 INTRODUCTION

The facile displacement of ethylene from platinum-ethylene complexes [68,70] has made available a large number of platinum carbonyl complexes, as shown in Scheme 5.1. The complexes are particularly amenable to study because they are readily prepared and usually stable crystalline compounds.

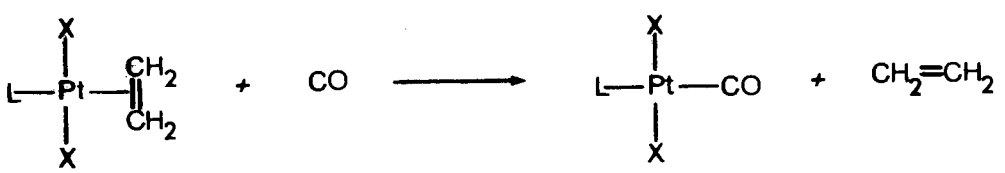

SCHEME 5.1

It is now generally agreed that the *trans*-effect in platinum(II) complexes is largely determined by the character

of the bond between the ligand and the platinum atom. Thus, with a ligand such as CO, π-bonding (back bonding between the filled *d*-orbitals of the metal and the unfilled *p*-orbitals of the coordinating ligand atom) accounts for much of the bond strength.

In the previous chapter we studied the affect of varying the substituent on a particular ligand in the complexes *trans*-$[PtBr_2(CO)(L)]$. In this chapter, we will examine the effect of substituting the entire ligand in the complexes *trans*-$[PtX_2(CO)(L)]$. As may be expected, the complexes formed by the various ligands should differ substantially from each other. For instance, ammonia does not only differ structurally from pyridine, but also it has no π-bonding.

In this chapter, ^{1}H-NMR, infrared, ultraviolet and mass spectroscopy, have been used to examine the nature of the complexes.

5.2 PREPARATION OF COMPLEXES

5.2.1 *Preparation of the complexes trans-*$[PtX_2(C_2H_4)(L)]$ *(X=Cl, Br; L = aniline (an), pyridine N-oxide (pyO), pyridine (py), ammonia* (NH_3)*, imidazole (Him) and pyrazole (pyz))*

Refer to Chapter 3.2.1 for the preparation of $K[PtX_3(C_2H_4)]$.

The complexes *trans*-$[PtX_2(C_2H_4)(L)]$ (X = Cl, Br; L = py, NH_3, Him, pyz) were prepared by the slow addition of an aqueous solution of ligand (1.30 mmol in 10 ml) to one portion of aqueous $K[PtX_3(C_2H_4)]$ (1.20 mmol in 10 ml). The product precipitated immediately and after stirring for 5 min., the product was isolated by vacuum filtration, washed well with water, and dried overnight over silica gel under reduced pressure.

The complexes *trans*-$[PtX_2(C_2H_4)(L)]$ (X = Cl, Br; L = an, pyO) were prepared by the slow addition of an ethanolic solution of ligand (1.00 mmol in 10 ml) to one portion of ethanolic $K[PtX_3(C_2H_4)]$ (1.20 mmol in 20 ml). The solution was stirred overnight, ethanol being allowed to evaporate until crystallization was essentially complete. More ligand (0.15 mmol in 20 ml cold H_2O) was then added and after stirring (5 min), the product was isolated and dried as described above.

The deuterated complexes were similarly prepared using the following labelled ligands supplied by Merck, Sharp and Dohme (Canada) Ltd. (isotopic purity in parentheses): aniline-d_5 (99%), Imidazole-d_4 (98%), ammonium-d_4 hydroxide-*d* (26% W/W in D_2O, 99%), pyridine-d_5 *N*-oxide (98%) and the following labelled ligand supplied by Prochem B.O.C. Ltd.: pyridine-d_5 (99%).

The deuteroimine (ND) groups of 1,2,4,5 - tetradeuteroimidazole (Him-d_4) undergo rapid exchange in aqueous or

ethanolic solutions to yield complexes containing 2,4,5 - trideuteroimidazole (Him-d_3). Similarly, the ammonium-d_4 hydroxide (ND_4OD) undergoes rapid exchange to form ammonium hydroxide (NH_4OH). Hence D_2O must substitute H_2O in the preparation of the complex containing ammonia.

Composition and purity of all the compounds were determined by microanalysis (C,H,N) before converting them into their carbonyl analogues.

5.2.2 *Preparation of the complexes trans-[$PtX_2(CO)(L)$] (X = Cl, Br; L = aniline (an), pyridine N-oxide (pyO), pyridine (py), ammonia (NH_3), imidazole (Him) and pyrazole (pyz)).*

These were all prepared from their corresponding ethylene analogues using the same method as described previously (See Chapter 4.2.1),except for the following modifications.

For L = py, *n*-hexane (10 ml) was added before the cloud point occurred and the resulting solution was placed over silica gel in a large partly evacuated dessicator and stored at -5^oC overnight. The solvent evaporated and long, thin needle-like crystals extending the width of the beaker appeared. These were collected and washed as described previously.

For L = pyO and NH_3,the *n*-hexane was also added (just sufficient volume to prevent reprecipitation) to the chloroform before carbon monoxide was bubbled through the

solution. Then, the original procedure was continued.

All the complexes were stored over silica gel in a vacuum dessicator (< 0.1 mm Hg) at -5°C after their composition and purity were determined by microanalysis (C,H,N), Table 5.1.

5.2.3 *Preparation of the complexes trans-*$[PtX_2(C_2H_4)(pz)]$ *and* $[Pt_2X_4(C_2H_4)_2(pz)]$ *(X = Cl, Br; pz = pyrazine).*

The complexes *trans*-$[PtX_2(C_2H_4)(pz)]$ were prepared by the dropwise addition of an aqueous solution of $K[PtX_3(C_2H_4)]$ (1.2 mmol in 50 ml) to an aqueous solution of pyrazine (12.0) mmol in 20 ml) with constant stirring. After stirring the solution for 5 min., the product was isolated by vacuum filtration, washed well with water and dried overnight over silica gel under reduced pressure.

The complexes *trans*-$[Pt_2X_4(C_2H_4)_2(pz)]$ were prepared by the dropwise addition of an aqueous solution of pyrazine (1.5 mmol in 30 ml) to an aqueous solution of $K[PtX_3(C_2H_4)]$ (3.6 mmol in 20 ml) with constant stirring. The product, which precipitated immediately, was isolated and dried as described above.

The deuterated complexes were similarly prepared from pyrazine-d_4 of 99.04% isotopic purity supplied by Merck, Sharp and Dohme (Canada) Ltd.

Composition and purity of all the compounds were determined by microanalysis (C,H,N) before converting them into their carbonyl complexes.

5.2.4 *Preparation of the complexes trans-*$[Pt_2X_4(CO)_2(pz)]$ *and* $[PtX_2(CO)(pz)]$ *(X = Cl, Br; pz = pyrazine)*

The complexes *trans*-$[Pt_2X_4(CO)_2(pz)]$ were prepared from their corresponding ethylene complexes using the same method described previously (See Chapter 4.2.1), except that larger volumes (~70 ml) of chloroform were required to dissolve the ethylene complexes.

Attempted preparation of trans-$[PtX_2(CO)(pz)]$

1) Several attempts to prepare these complexes from their corresponding ethylene complexes by the usual method always resulted in the formation of the bridging complex, *trans*-$[Pt_2X_4(CO)_2(pz)]$.
2) A solution of $H[Pt(CO)X_3]$ was prepared [72] by the treatment of carbon monoxide on an aqueous solution of $K_2[PtX_4]$ acidified with HX. Reaction of this solution with pyrazine, in various molar ratios, always resulted in the formation of the bridging dimer, *trans*-$[Pt_2X_4(CO)_2(pz)]$. When a large excess (>10 x moles) of pyrazine was added, the complex *trans*-$[PtX_2(pz)_2]$ was formed as verified by its infrared spectrum [73] and microanalysis.

3) Crystals of $[PtCl_2(CO)_2]_2$ were prepared [74,75] by the action of dry chlorine and carbon monoxide over finely divided platinum black at about 260°C. Reaction of the crystals with pyrazine, in various molar ratios, either resulted in the formation of the bridging dimer *trans*-$[Pt_2Cl_4(CO)_2(pz)]$, or *trans*-$[PtX_2(pz)_2]$, or no reaction occurred.

4) The salts $NR_4[PtX_3(CO)]$ (R = Pr^n_4,Bu^n_4) were prepared [76] by the action of carbon monoxide on a suspension of $[NR_4]_2[Pt_2X_6]$. Reaction of the product with pyrazine, in various molar ratios, resulted in either the formation of *trans*-$[PtX_2(pz)_2]$, or no reaction occurred.

5.3 ANALYSES OF COMPLEXES

TABLE 5.1

Analytical data for the complexes *trans*-$[PtX_2(CO)(L)]$ (X = Cl, Br; L = aniline, pyridine *N*-oxide, pyridine, ammonia, imidazole and pyrazole) and the complexes *trans*-$[Pt_2X_4(CO)_2(pz)]$ (X = Cl, Br; pz = pyrazine).

Complex	Calculated			Found		
	%C	%H	%N	%C	%H	%N
trans-$[PtCl_2(CO)(L)]$						
L = aniline	21.7	1.8	3.6	21.8	1.9	3.7
pyridine *N*-oxide	18.5	1.3	3.6	18.6	1.3	3.5
pyridine	19.3	1.4	3.8	19.2	1.4	3.8
ammonia	3.9	1.0	4.5	4.0	1.0	4.5
imidazole	13.3	1.1	7.7	13.3	1.1	7.7
pyrazole	13.3	1.1	7.7	13.0	1.1	7.5
trans-$[PtBr_2(CO)(L)]$						
L = aniline	17.7	1.5	2.9	17.6	1.5	2.9
pyridine *N*-oxide	15.1	1.1	2.9	15.1	1.1	2.9
pyridine	15.6	1.1	3.0	15.7	1.1	3.1
ammonia	3.0	0.8	3.5	3.0	0.8	3.5
imidazole	10.7	0.9	6.2	10.7	0.9	6.2
pyrazole	10.7	0.9	6.2	10.8	0.9	6.2
trans-$[Pt_2Cl_4(CO)_2(pz)]$	10.8	0.6	4.2	10.9	0.6	4.2
trans-$[Pt_2Br_4(CO)_2(pz)]$	8.5	0.5	3.3	8.7	0.6	3.3

5.4 INFRARED RESULTS

TABLE 5.2

Internal ligand frequencies (cm^{-1}) and assignments for the complexes *trans*-$[PtCl_2(CO)(L)]$

L	Unlabelled	L-deuterated		Assignment[a]
NH_3	3292	2459		
	3200	2427		ν(N-H)
		2377		
	2145 (2129)[b]	2145 (2130)		ν(C≡O)
	2139	2138		
	1636	1296		NH_2 scissor
	1535	1210		
	1294	1073		NH_2 twist
	784	505		NH_2 wag
py	3122	2603		
	3110	2479		ν(C-H)
	3059	2359		
	2123 (2133)	2121 (2133)		ν(C≡O)
	1612	1571	8a	ν(ring)
		1536	8b	
	1483	1327	19a	
	1451	1238	19b	
	1354	894	14	δ(C-H)
	1242	845	3	
	1218	839	9a	
	1213	835		
	1157	830	15	
	1072	983	18b	
	1022	1030	12	δ(ring)
	941	804		γ(C-H)
	760	778	11	δ(ring)
	688	638	4	
	685			
	660	631	6a	

TABLE 5.2 continued/

L	Unlabelled	L-deuterated		Assignment[a]
py	507	503		
	503	498		γ(ring)
	433	397		
pyO	3134	2335		
	3109	2315		ν(C-H)
	3083	2308		
	3055	2284		
	2108 (2117)	2108 (2117)		ν(C≡O)
	1615	1571		
		1549	4	ν(ring) + ν(N-O)
	1473	1353	5	ν(ring)
	1259	1141	6	ν(N-O)
	1245	1248		ν(ring)
	1197	1196		
	1186	875	7	
	1173	859	18	
	1156	844		δ(C-H)
	1153	830		
	1094	817	19	
	1068	782		
	1053	1040		
	1027	1009	9	δ(ring)
	1004	989		
	935	765	26	
	831	567	23	γ(C-H)
	776	531	27	
	669	657	28	γ(ring)
	598	567	11	
an	3229	3229		
	3182	3184		ν(N-H)
	3123	3118		
	3051	2390		
		2366		ν(C-H)
	3025	2331		

TABLE 5.2 continued/

L	Unlabelled	L-deuterated	Assignment[a]
an	2121 (2130)	2144 2120 (2130)	ν(C≡O)
	1599	1581	ν(ring)
	1575	1573 1563	NH_2 scissor
	1493	1424	ν(ring)
	1471	1380	
	1216	1206	
	1191	1137	
	1178	1173	NH_2 twist
	1073	842	δ(C-H)
	1028	822	
	767	769	NH_2 wag
	756	757	γ(C-H)
	691	657	γ(ring)
	643	617	
	580	574	
	530	531	NH_2 rock
Him	3550	3348	ν(N-H)
	3179	2597	ν(C-H)
	3157	2369	
	3136	2338	
	2965	2883	ν(N-H)·····Cl
	2847	2597	
	2129 2116 (2127)	2129 2116 (2127)	ν(C≡O)
	1545	1493	ν(ring)
	1516	1471	
	1510	1452	
	1483	1429	
	1428	1400	
	1328	1193	
	1272	1283	δ(N-H)

TABLE 5.2 continued/

L	Unlabelled	L-deuterated	Assignment[a]
Him	1261	945	
	1225	978	
	1183	896	
	1131	876	δ(C-H)
	1096	867	
	1073	828	
	1067	820	
	853	772	
	837	739	δ(ring)
	753	729	
	744		
	708	707	
	653	589	
	646	582	γ(C-H)
	613	521	
	504	497	γ(ring)

trans-[$PtCl_2$(Y)(pyz)] Y = C_2H_4	C_2D_4	*trans*-[$PtCl_2$(CO)(pyz)]		
3315	3316	3325,3305		ν(N-H)
3156	3156			
3139	3139	3138		ν(C-H)Him
3113	3114			
3089	2328			ν(C-H)ethylene
		2120		
		2107	(2132)	ν(C≡O)
		2062		
		1997		
1566	1566	1551		
1512	1512	1518		ν(ring)
1480	1480	1490		
1437	1438	1442		
1422	809			CH_2 scissor

TABLE 5.2 continued/

trans-[$PtCl_2(Y)(pyz)$] Y = C_2H_4	C_2D_4	*trans*-[$PtCl_2(CO)(pyz)$]	Assignment
1411	1407	1415	ν(ring)
1375	1375		
1351	1353	1357	
1281	1281	1276	δ(C-H)Him
1271	1270		δ(C-H)Him
1257	961		δ(C-C)ethylene
1247			δ(C-H)ethylene
1187	1187	1192	δ(C-H)Him
1167	1167	1179	δ(N-H)
1121	1120	1129	δ(C-H)Him
1064	1064	1076	
1052	1051	1057	
1019	755		CH_2 wag
950	950	977	δ(ring)
910	911	913	
875	875	871	
784	785		γ(C-H)Him
772	773	767	
723			CH_2 rock
677	676	662	γ(ring)
654	654		
619	620	626	
589	588	569	
571	571		

[a] Band numbers refer to those given in references [77] (L = pyO) and [78] (L = py).
Values in parentheses are those obtained in chloroform solution.

TABLE 5.3

Internal ligand frequencies (cm^{-1}) and assignments for the complexes *trans*-$[PtBr_2(CO)(L)]$

L	Unlabelled	L-deuterated		Assignment[a]
NH_3	3280	2420		ν(N-H)
		2369		
	3201	2331		
	2128 (2126)	2126 (2125)		ν(C≡O)
	1626	1287		NH_2 scissor
	1529	1202		
	1289	1067		NH_2 twist
	782	772		NH_2 wag
py	3098	2599		ν(C-H)
	3075	2476		
	3048	2359		
	3041	2331		
	2126 (2128)	2126 (2128)		ν(C≡O)
	2111	2111		
	1609	1568	8a	ν(ring)
	1599	1534	8b	
	1483	1325	19a	
	1451	1238	19b	
	1352	789	14	δ(C-H)
	1243	739	3	
	1213	641	9a	
	1160	678	15	
	1092	1042	18b	δ(ring)
	1076	982		
	1020	1033	12	
	870		10b	γ(C-H)
	762	739	11	δ(ring)
	758	733		
	692	532		γ(C-H)
	689	529	4	
	660	559	6a	δ(ring)

TABLE 5.3 continued/

L	Unlabelled	L-deuterated		Assignment[a]
py	507	504		
	440	403	16b	γ(ring)
	437			
pyO	3113	2395		
	3078	2331		ν(C-H)
	3063	2307		
	3036	2284		
	2097 (2113)	2101 (2113)		ν(C≡O)
	2052	2049		
	1612	1569		
		1547	4	ν(ring) + ν(N-O)
	1473	1351	5	ν(ring)
	1262	1145	6	ν(N-O)
	1194	1195		ν(ring)
	1171	875	7	
	1159	858	18	
	1156	843		δ(C-H)
	1095	829	19	
	1070	787	8	
	1056	1040		
	1033	1017	9	δ(ring)
	1026	994		
	1004	988		
	967	778		
	933	764	26	
	830	573		
	814	564		γ(C-H)
	804	545		
	773	531	27	
	673	655	28	
	637	636		γ(ring)
	591	573	11	

TABLE 5.3 continued/

L	Unlabelled	L-deuerated	Assignment[a]
an	3262	3263	ν(N-H)
	3213	3214	
	3108	3102	
	3045	2359	ν(C-H)
	3007	2331	
	2119 (2125)	2122 (2125)	ν(C≡O)
	1599		
	1595	1579	ν(ring)
	1569		
	1561	1559	NH_2 scissor
	1493	1377	ν(ring)
	1466	1299	
	1198	1166	
	1180	1135	
	1162	1158	NH_2 twist
	1145	1022	δ(C-H)
	1069	842	
	1029	822	
	973	790	
	909	765	
	798	749	ν(ring)
	760	764	NH_2 wag
	742	738	
	691	534	ν(C-H)
	578	529	δ(ring)
	554		NH_2 rock
	483	465	γ(ring)
Him	3345	3343	ν(N-H)
	3173	2597	ν(C-H)
	3153	2366	
	3131	2336	
	2964		
	2849		

TABLE 5.3 continued/

L	Unlabelled	L-deuterated	Assignment[a]
	2123 2109 (2121)	2122 2109 (2121)	ν(C≡O)
	1545	1491	ν(ring)
	1515 1510	1473	
	1495	1417	
	1479	1404	
	1429	1373	
	1328	1291	
	1271	1278	
	1265	945	δ(C-H)
	1221	977	δ(N-H)
	1191	894	
	1131	875	
	1102	867	δ(C-H)
	1072	828	
	1068	821	
	852	774	δ(ring)
	835	738	
	751	564	δ(C-H)
	742	727	δ(ring)
	695	695	
	653	587	γ(ring)
	645	581	
	611	564	
	504	502	

trans-[PtBr$_2$(Y)(pyz)] Y = C_2H_4	C_2D_4	*trans*-[PtBr$_2$(CO)(pyz)]	
3304	3302	3308	ν(N-H)
3155	3154	3154	ν(C-H)Him
3316	3135	3137	
3113	3112		

TABLE 5.3 continued/

trans-[PtBr$_2$(Y)(pyz)] Y = C_2H_4	C_2D_4	*trans*-[PtBr$_2$(CO)(pyz)]	Assignment
3084	2324		
3006	2217		ν(C-H) ethylene
		2109 (2127)	ν(C≡O)
		2061	
1511	1512	1535,1517	ν(ring)
1480	1479	1488	
1423	807		CH_2 scissor
1408	1408	1411	ν(ring)
1348	1347	1354	δ(C-H)Him
1268	1268	1274	
1243	959		ν(C-C) ethylene
1167	1166	1174	(N-H)
1124	1124	1129	
1063	1063	1070	δ(C-H)Him
1052	1052	1056	
1015			CH_2 wag
949	948	999	
910	910	913	δ(ring)
904	903	903	
872	872	868	
787	789		γ(C-H)Him
781	781	761	
721			CH_2 rock
666	666	661	
651	651		γ(ring)
619	619	620	
579	580		
562	564		

a Band numbers refer to those given in references [77] (L = pyO) and [78] (L = py).

b Values in parentheses are those obtained in chloroform solution.

TABLE 5.4

Metal-ligand frequencies and ligand isotopically-induced shifts (cm^{-1}) in the infrared spectra of the complexes *trans*-$[PtX_2(CO)(L)]$

L,X	δ(PtC≡O)	ν(Pt-C)	ν(Pt-N)	ν(Pt-Cl)	Other
NH_3,Cl	531 (0)	465 (6)	479 (7)	349 (1)	208 (3)
					168 (3)
					152 (1)
					123 (0)
py,Cl	541 (3)	479 (0)	226 (13)	353 (0)	215 (2)
					159 (1)
					124 (1)
pyO,Cl	580 (5)	508 (1)	440 (23)	352 (1)	216 (2)
			413 (20)		158 (1)
					129 (1)
an,Cl	557 (0)	484 (4)	477 (17)	345 (0)	215 (-)
			369 (11)		172 (5)
					132 (0)
					104 (-)
Him,Cl	543 (3)	538 (2)	252 (13)	350 (0)	162 (0)
	485 (2)				128 (0)
					99 (1)
					84 (1)
pyz[a],Cl	599	545	248	355	225
	495				183
					166
					126
trans-$[PtCl_2(C_2H_4)(pyz)]$[b]					
		492 (41)	266 (3)	349 (0)	186 (1)
		398 (18)			146 (1)
					130 (0)
					90 (5)

TABLE 5.4 continued/

L,X	δ(PtC≡O)	ν(Pt-C)	ν(Pt-N)	ν(Pt-Br)	Other
NH_3,Br	528 (0)	481 (3)	466 (8)	254 (0)	205 (4) 174 (2) 99 (1) 90 (1)
py,Br	544 (4) 507 (3)	488 (0)	230 (19)	261 (1)	185 (10) 102 (0) 80 (2)
pyO,Br	576 (6) 490 (8)	511 (1)	436 (19) 402 (14)	258 (1)	222 (6) 180 (-) 134 (3)
an,Br	530 (3)	493 (2)	434 (20)	254 (0)	219 (-) 207 (6) 165 (-) 149 (5)
Him,Br	538 (0)	479 (0)	229 (8)	271 (6)	196 (6) 97 (2) 85 (-)
pyz[a],Br	587 537	500	280	222	186 150 125
trans-$[PtBr_2(C_2H_4)(pyz)]$[b]					
		489 (39) 396 (17)	282 (1)	223 (1)	203 (2) 182 (3) 130 (0) 82 (-)

[a] Assignments made empirically by comparison with ethylene analogue due to unavailability of labelled pyrazole.

[b] Numbers in parentheses are the shifts (cm^{-1}) induced by C_2D_4 labelling.

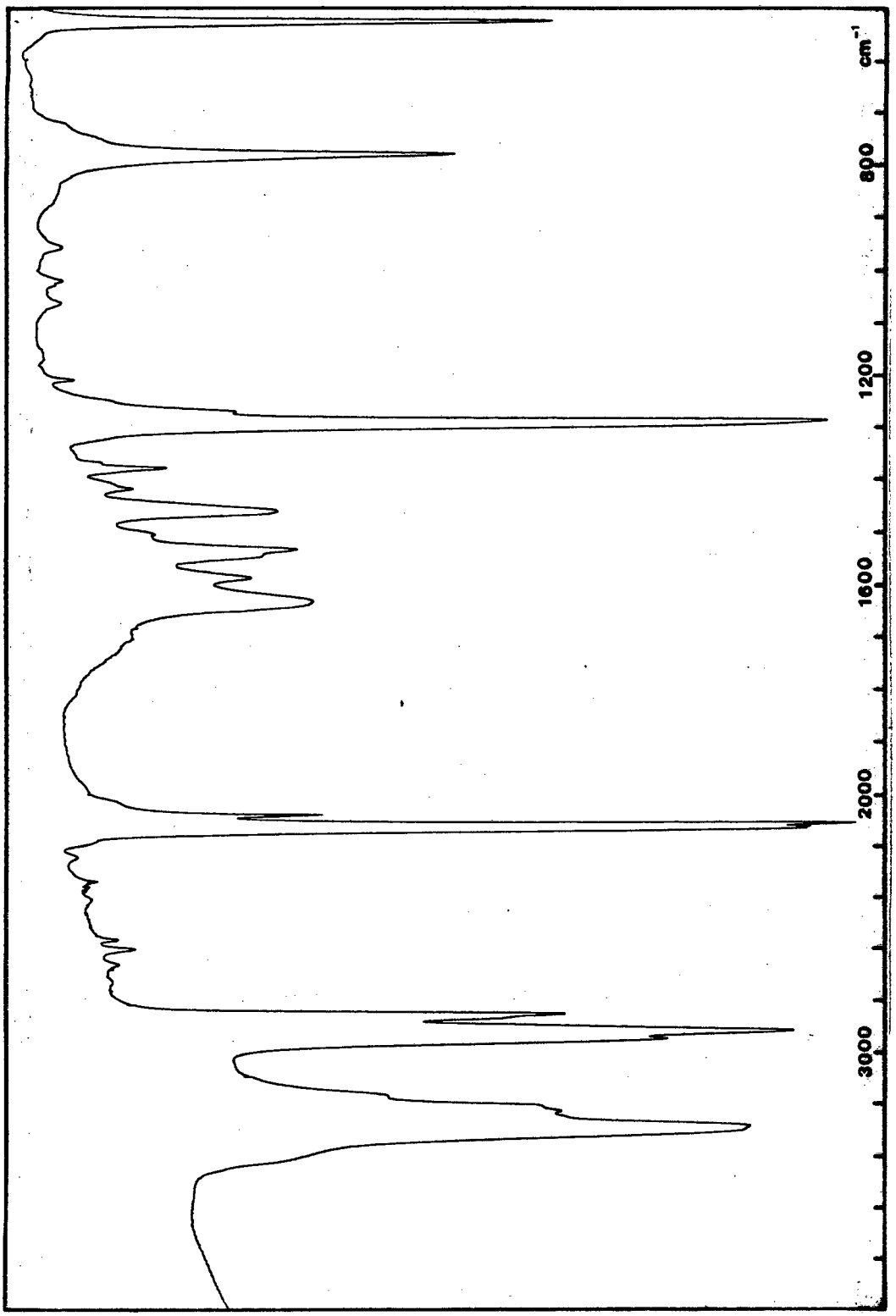

Fig. 5.1. Infrared spectrum of trans-[$PtCl_2(CO)(NH_3)$]

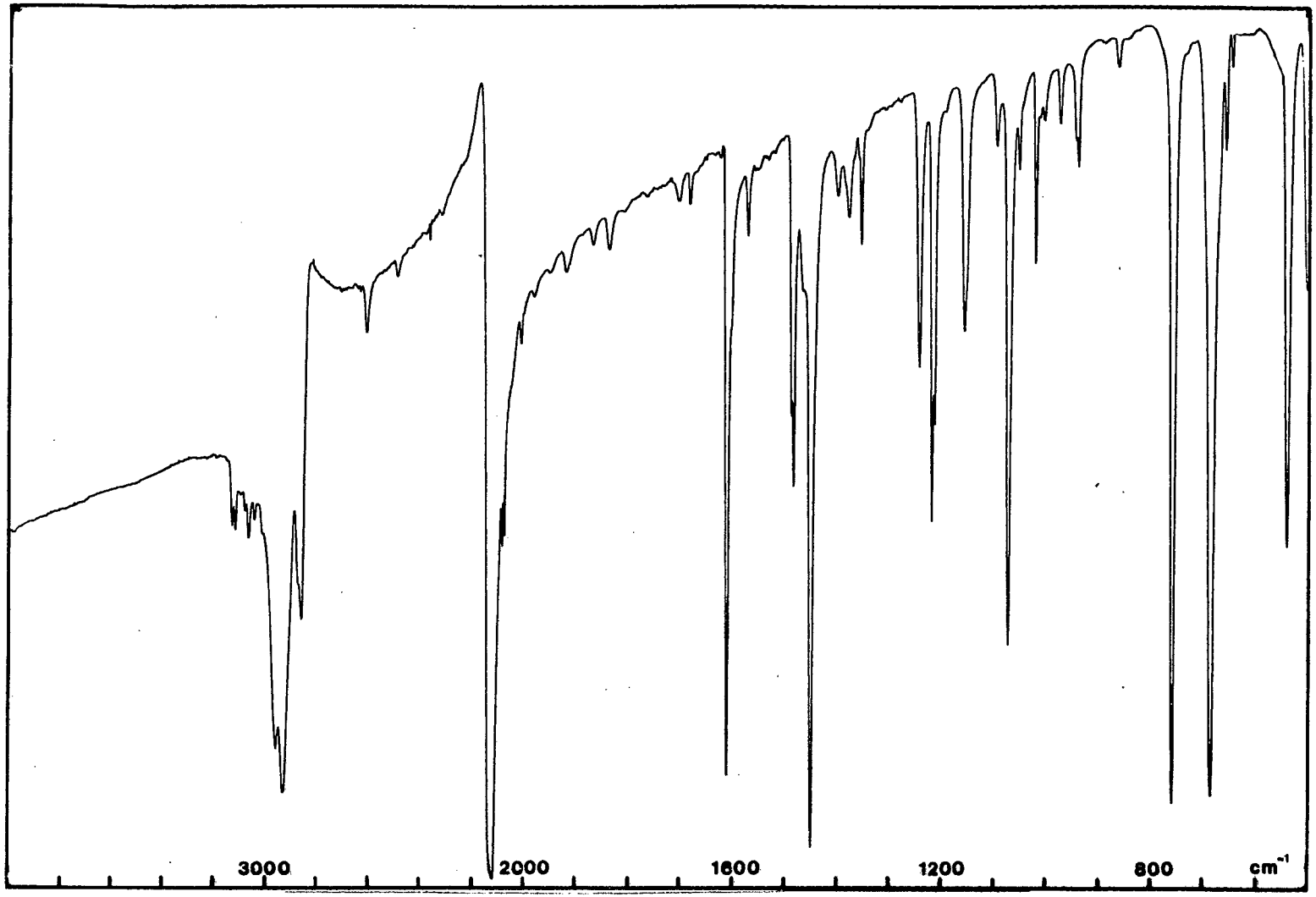

Fig. 5.2. Infrared spectrum of trans-[$PtCl_2(CO)(py)$]

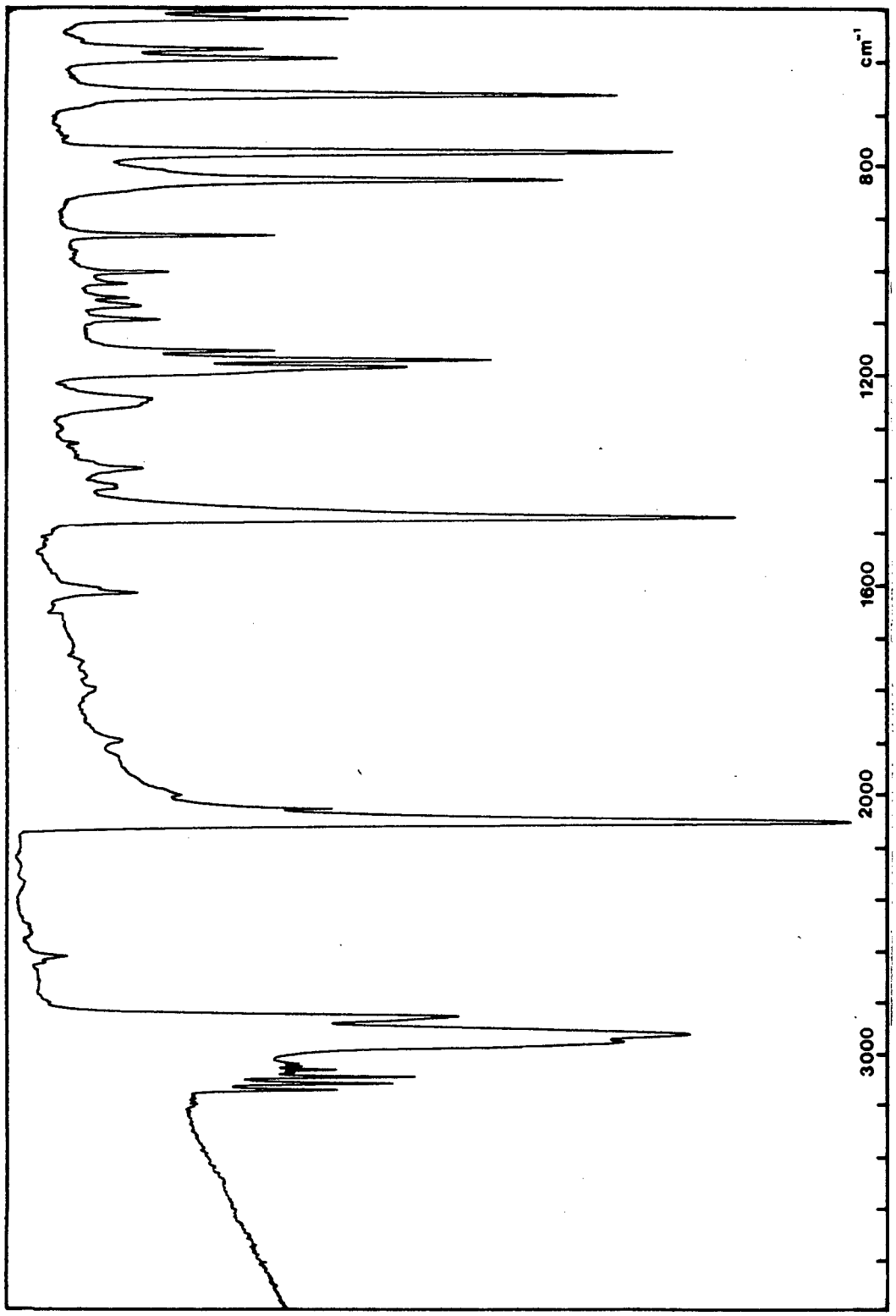

Fig. 5.3. Infrared spectrum of trans-[$PtCl_2$(CO)(pyO)]

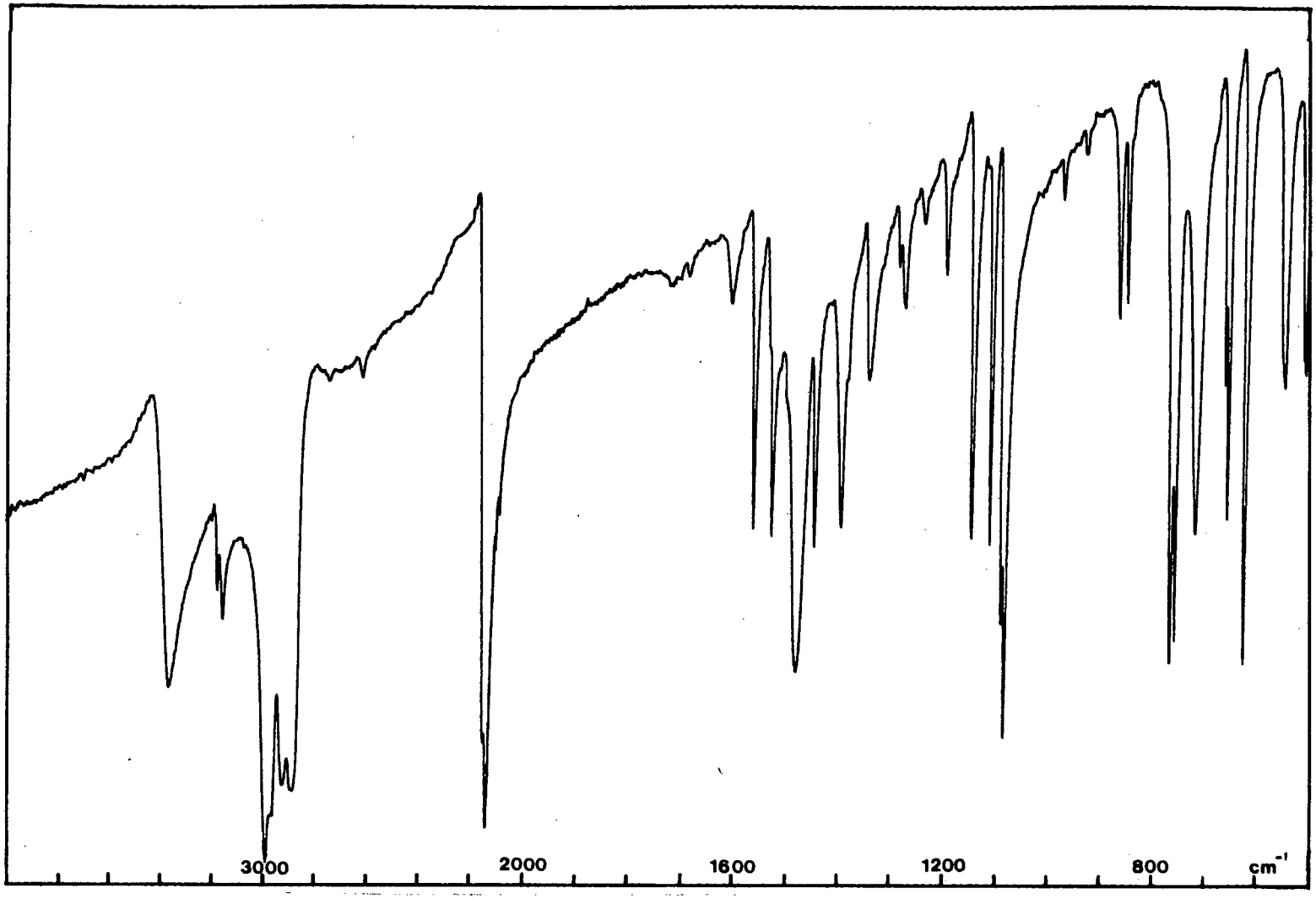

Fig. 5.4. Infrared spectrum of trans-[$PtCl_2(CO)(Him)$]

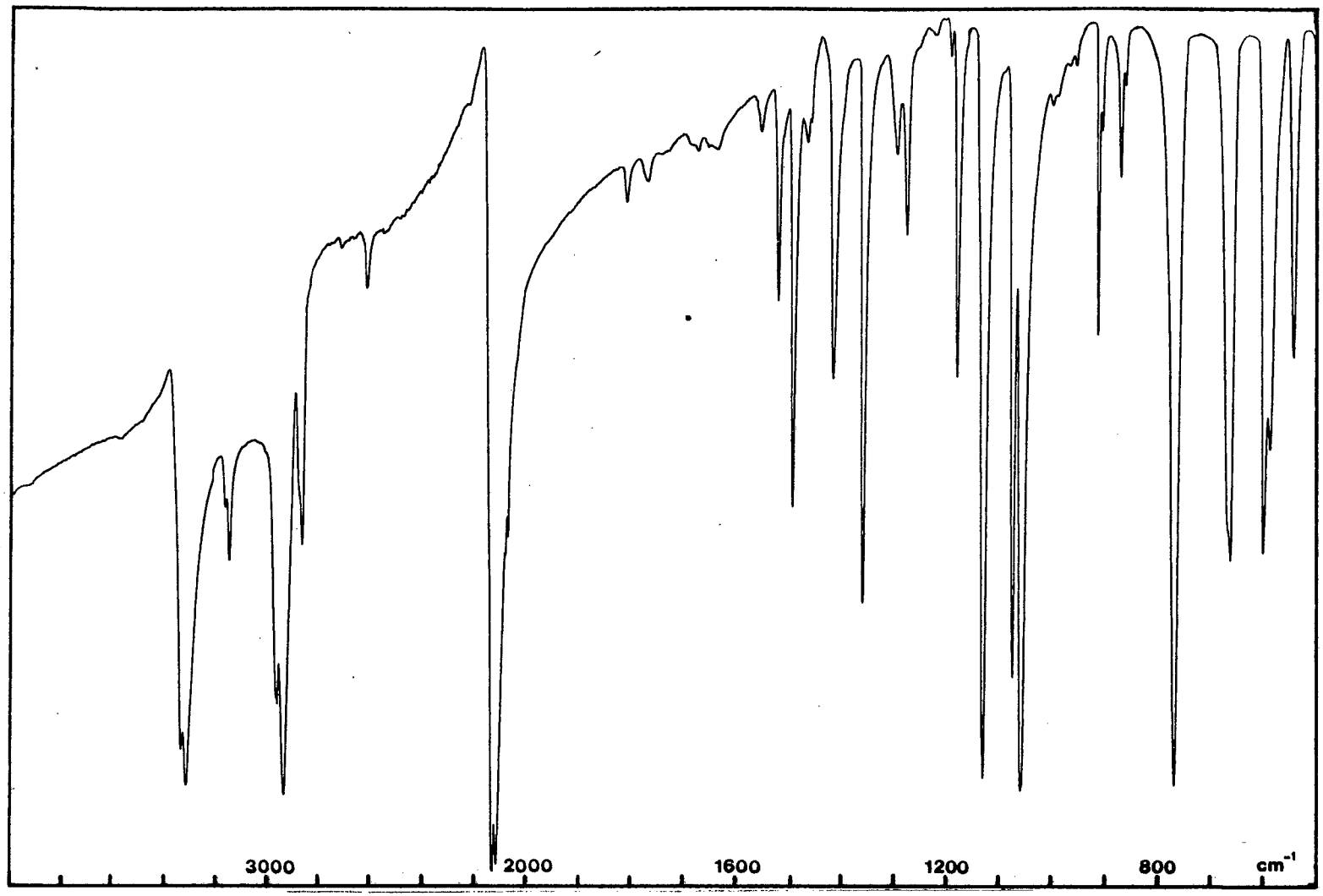

Fig. 5.5. Infrared spectrum of trans-[$PtCl_2(CO)(pyz)$]

.5 ^{1}H-NMR RESULTS

TABLE 5.5

^{1}H-NMR data for *trans*-$[PtX_2(CO)(NH_3)]$ (X=Cl,Br)[a]

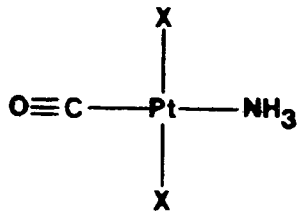

Ammonia protons	Chemical Shift (ppm)
X	
Cl	4.46 broad
Br	4.47 broad

[a] The ^{1}H-NMR spectra were run at ambient temperature on a Bruker WH-90 spectrometer using CD_3COCD_3 as the solvent and lock and TMS as a reference.

TABLE 5.6

^{1}H-NMR data for *trans*-[$PtX_2(CO)(py)$] (X=Cl,Br)[a]

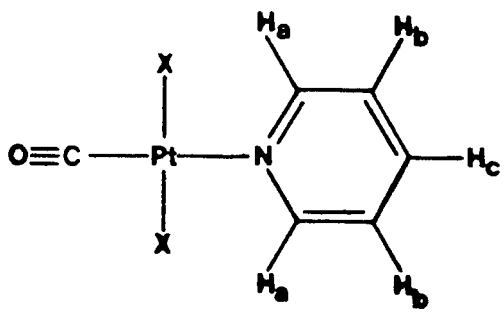

Pyridine protons		Chemical shift (ppm)		
X	J_{Pt-H_b}	H_a	H_b	H_c
Cl	30[b]	8.78	7.76	8.22
Br	29	8.78	7.72	8.18

[a] The ^{1}H-NMR spectra were run at ambient temperature on a Bruker WH-90 spectrometer using CD_3COCD_3 as the solvent and lock and TMS as a reference.

[b] Coupling observed at 270 K for the H_a proton only.

TABLE 5.7

^{1}H-NMR data for *trans*-[$PtX_2(CO)(pyO)$] (X=Cl,Br)[a]

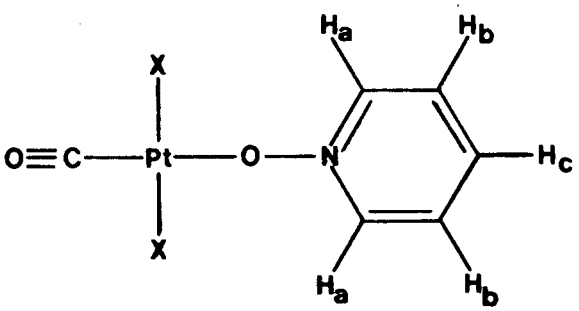

N-oxide protons	Chemical shift (ppm)		
X	H_a	H_b	H_c
Cl	8.73	7.97	8.23
Br	8.71	7.98	8.21

[a] The ^{1}H-NMR spectra were run at ambient temperature on a Bruker WH-90 spectrometer using CD_3COCD_3 as the solvent and lock and TMS as a reference.

TABLE 5.8

^{1}H-NMR data for *trans*-[$PtX_2(CO)(an)$] (X=Cl,Br)[a]

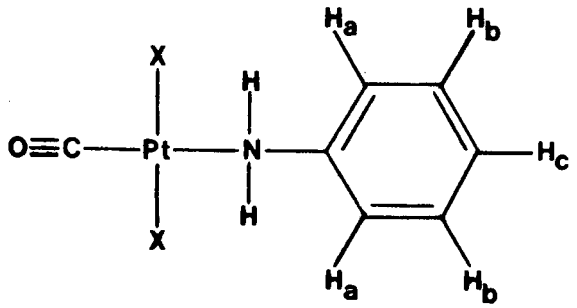

Aniline protons	Chemical shift (ppm)		
X	H_a	H_b	H_c
Cl	multiplet at		7.36
Br	multiplet at		7.42

[a] The ^{1}H-NMR spectra were run at ambient temperature on a Bruker WH-90 spectrometer using CD_3COCD_3 as the solvent and lock and TMS as a reference.

TABLE 5.9

^{1}H-NMR data for *trans*-[$PtX_2(CO)(Him)$] (X=Cl,Br)[a]

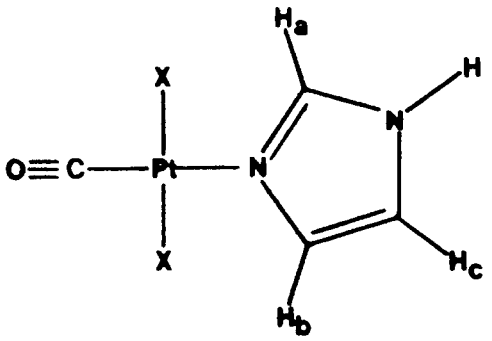

Imidazole protons				Chemical shift (ppm)		
X	J_{Pt-H_a}	J_{Pt-H_b} (Hz)		H_a	H_b	H_c
Cl	17	18		8.48	7.52	7.40
Br	18	18		8.51	7.53	7.40

[a] The ^{1}H-NMR spectra were run at ambient temperature on a Bruker WH-90 spectrometer using CD_3COCD_3 as the solvent and lock and TMS as a reference.

TABLE 5.10

^{1}H-NMR data for *trans*-[$PtX_2(CO)(pyz)$] (X = Cl,Br)[a]

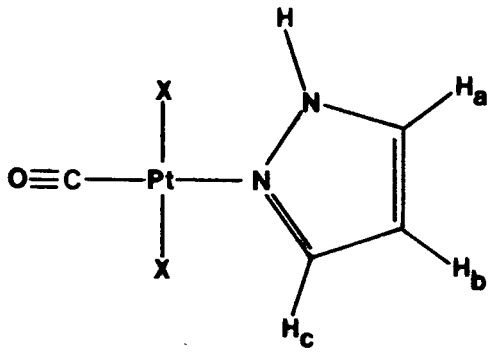

	Pyrazole protons			Chemical shift (ppm)		
X	$^JPt\text{-}H_a$	$^JPt\text{-}H_b$ (Hz)		H_a	H_b	H_c
Cl	(16)	(13)		8.48	7.52	7.40
				(8.40)	(7.79)	(6.59)
Br	(17)	(13)		8.51	7.53	7.40
				(8.37)	(7.81)	(6.58)

[a] The ^{1}H-NMR spectra were run at ambient temperature on a Bruker WH-90 spectrometer using CD_3COCD_3 as the solvent and lock and TMS as a reference.
Values in parentheses are those obtained in $CDCl_3$ solution. The coupling values were obtained at 255 K.

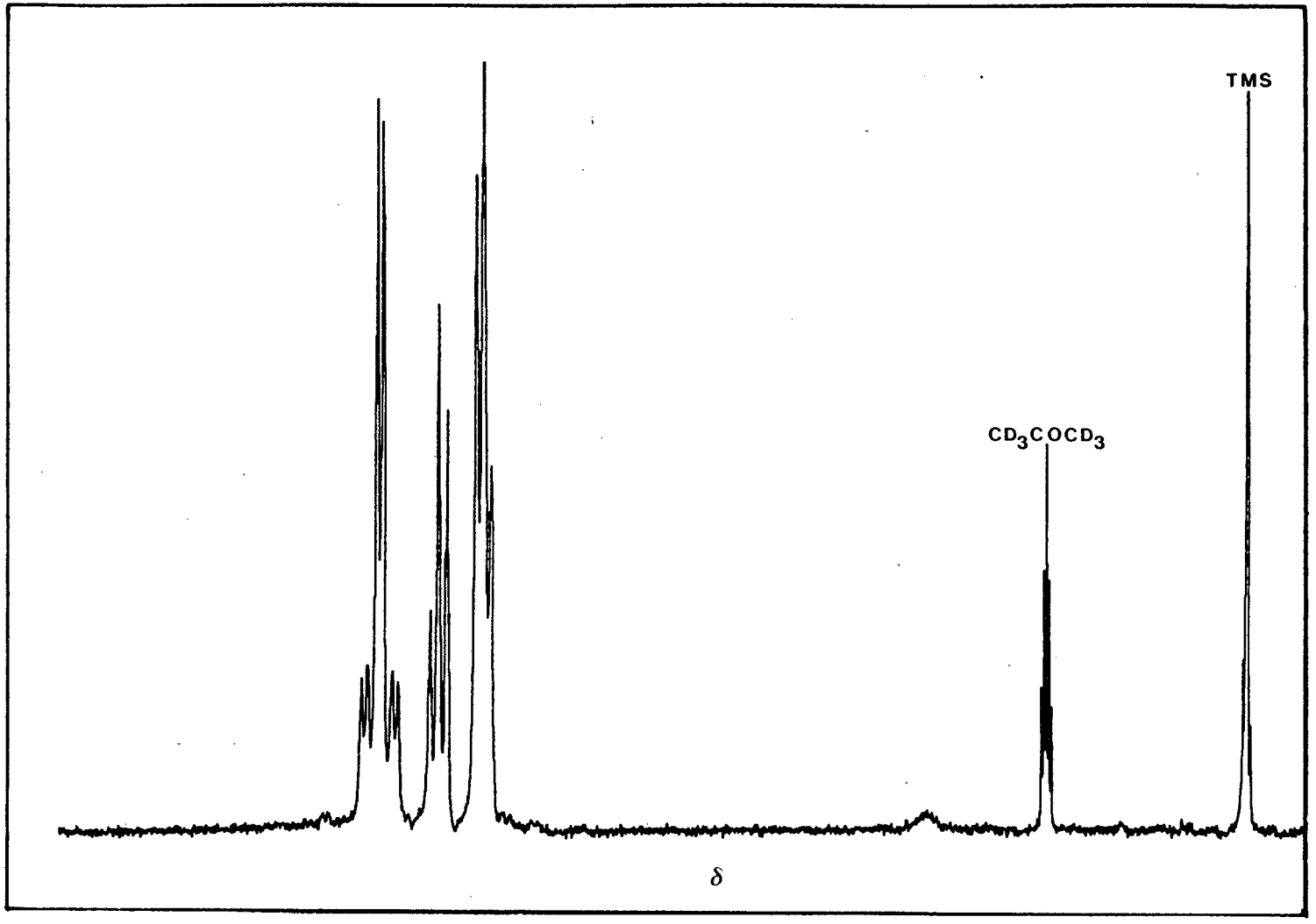

Fig. 5.6. ^{1}*H-NMR spectrum of trans-*$[PtBr_2(CO)(py)]$

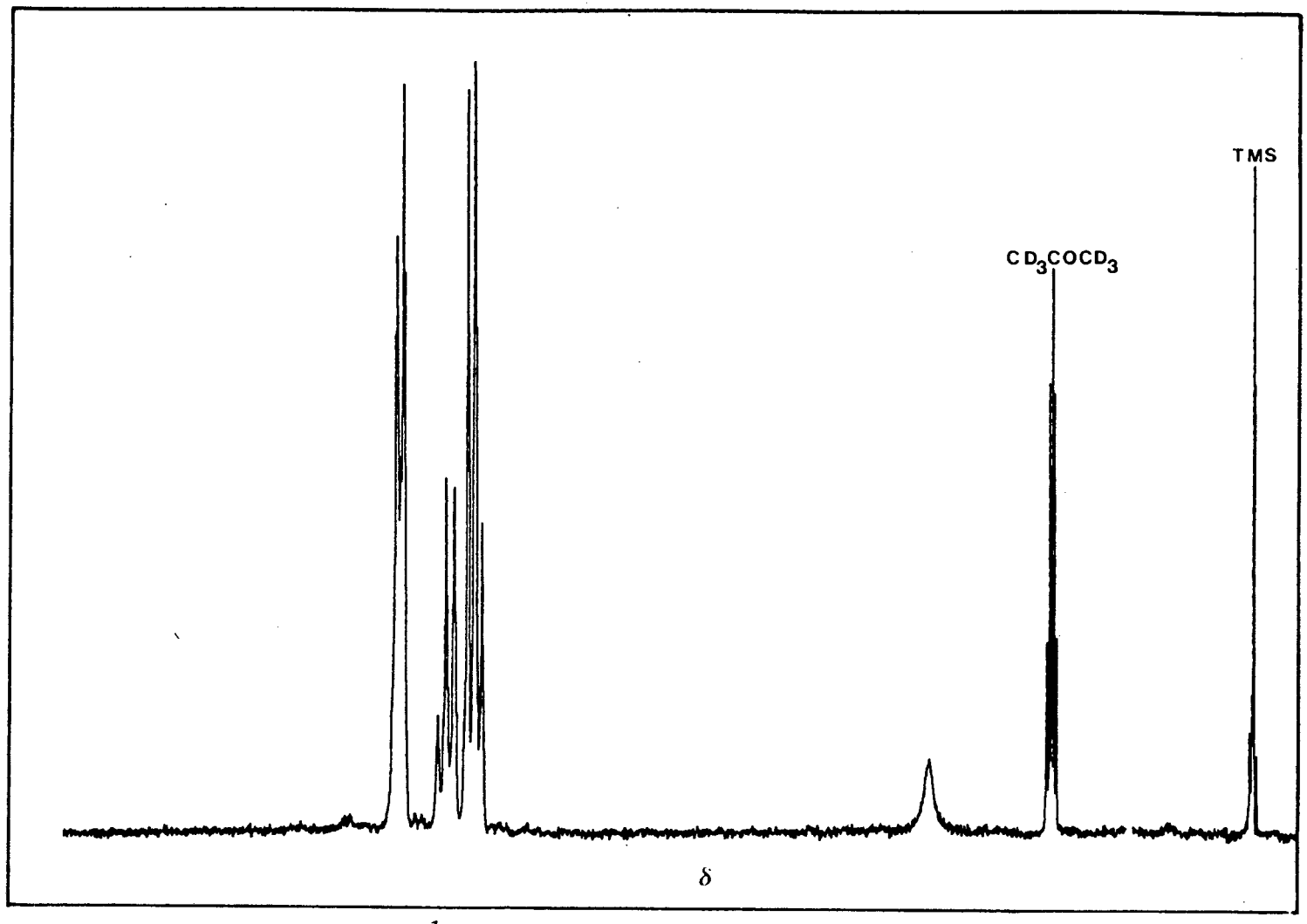

Fig. 5.7. ^{1}H-NMR spectrum of trans-[$PtCl_2(CO)(pyO)$]

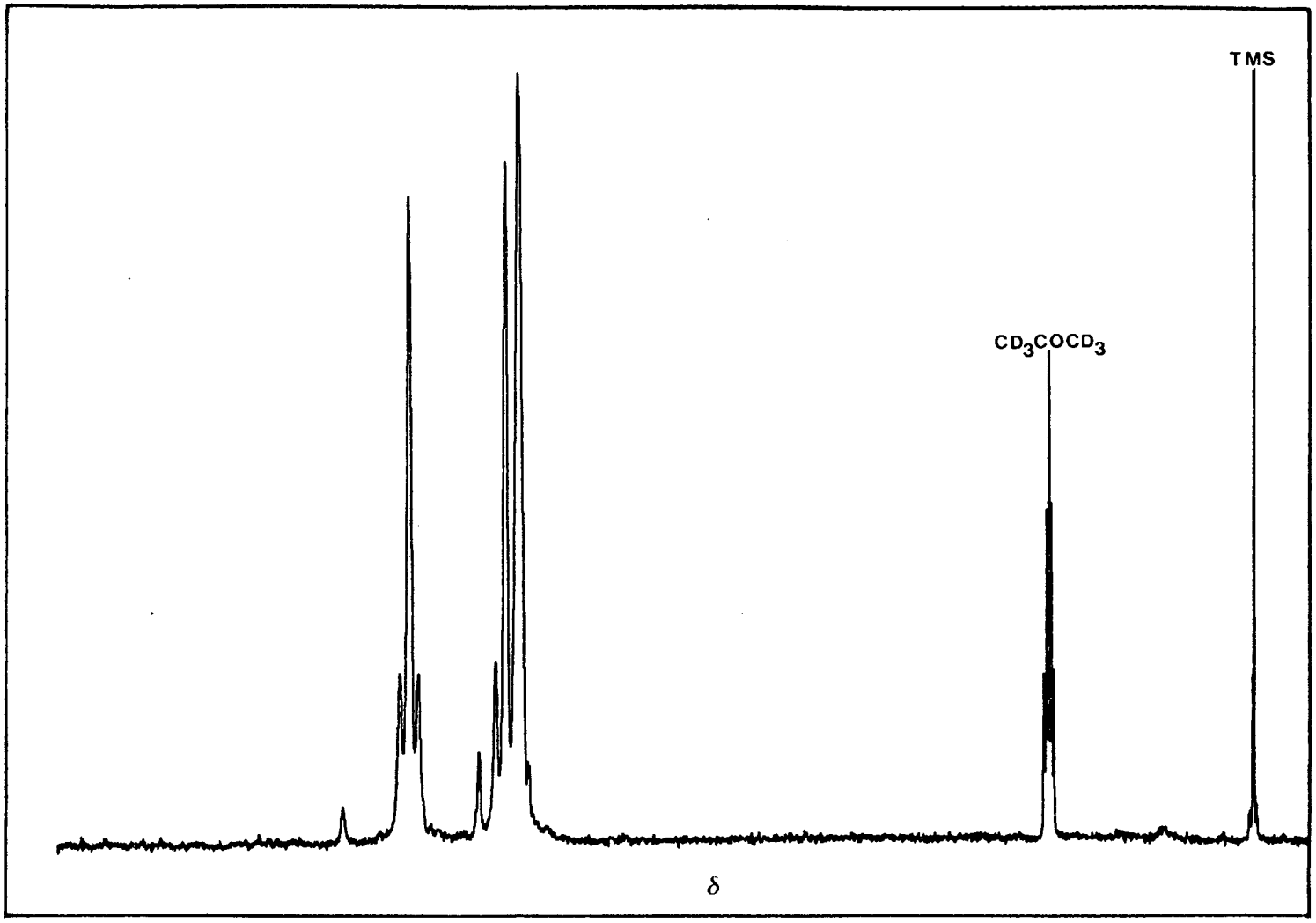

Fig. 5.8. ^{1}H-NMR spectrum of trans-[$PtBr_2(CO)(Him)$]

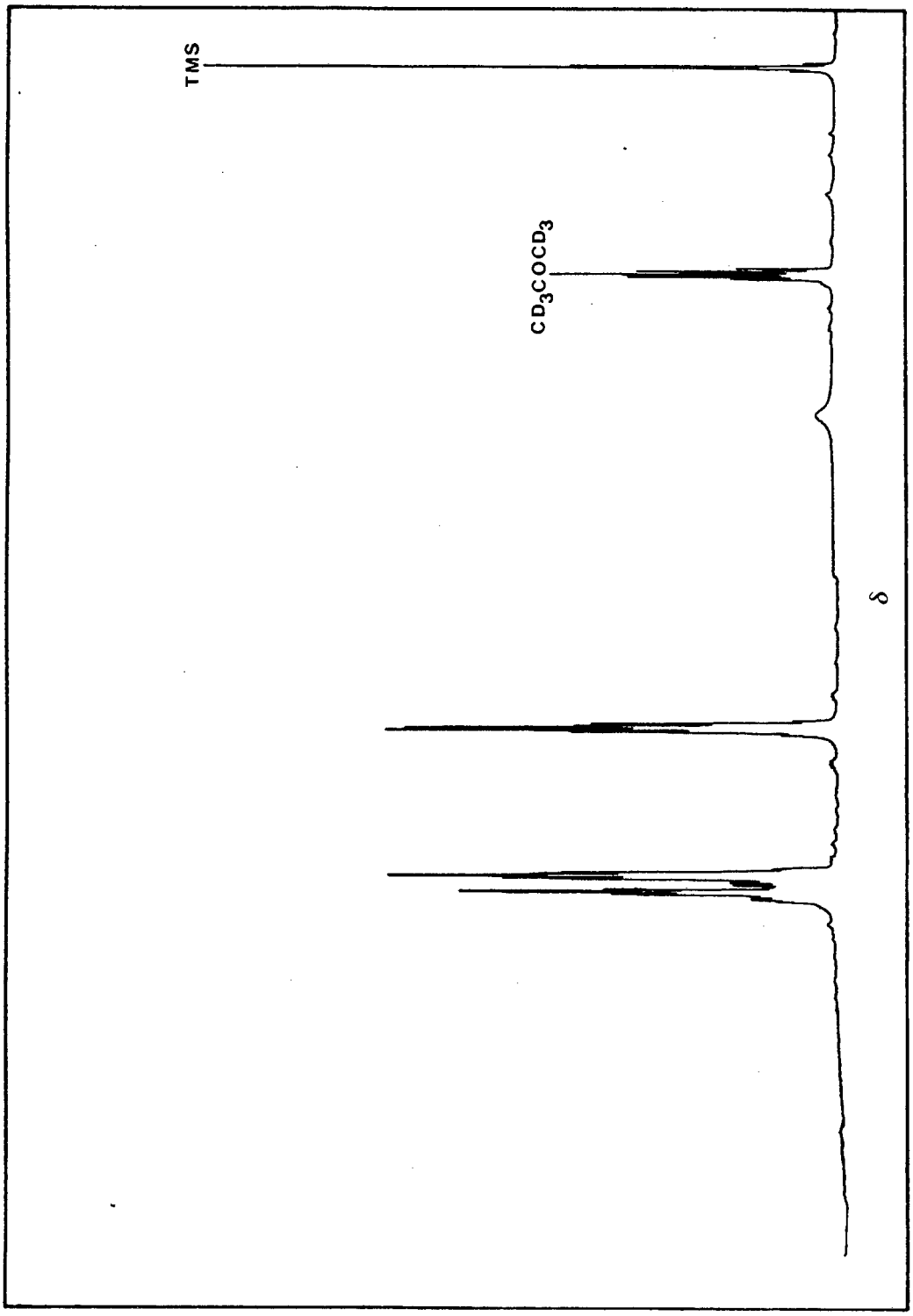

Fig. 5.9. ^1H-NMR spectrum of trans-[$PtBr_2$(CO)(py)]*

5.6 ULTRAVIOLET RESULTS

TABLE 5.11

UV data for the complexes *trans*-$[PtCl_2(CO)(L)]$[a]

L	λ_{max}(nm)	ϵ	Assignment
NH_3	200	16 605	$Cl^- \rightarrow Pt^{2+}$
	240	5 766	$\pi \rightarrow \pi^*(CO)$
	278	3 228	$5d(Pt) \rightarrow \pi^*(CO)$
py	201	14 942	$Cl^- \rightarrow Pt^{2+}$
	239	3 704	$\pi \rightarrow \pi^*(CO)$
	254	4 342	$\pi \rightarrow \pi^*(py)$
	284	894	$5d(Pt) \rightarrow \pi^*(CO), 5d(Pt) \rightarrow \pi^*(py)$
pyO	204	23 322	$Cl^- \rightarrow Pt^{2+}$
	263[b]	14 730	$\pi \rightarrow \pi^*(CO) \pi \rightarrow \pi^*(pyO), 5d(Pt) \rightarrow \pi^*(CO)$
an	201	19 233	$Cl^- \rightarrow Pt^{2+}$
	234	7 659	$\pi \rightarrow \pi^*(CO), \pi \rightarrow \pi^*(an)$
	278	2 042	$5d(Pt) \rightarrow \pi^*(CO)$
Him	201	15 748	$Cl^- \rightarrow Pt^{2+}$
	236	4 209	$\pi \rightarrow \pi^*(CO)$
	247	4 480	$\pi \rightarrow \pi^*(Him)$
	278	2 444	$5d(Pt) \rightarrow \pi^*(CO), 5d(Pt) \rightarrow \pi^*(Him)$
pyz	201	10 981	$Cl^- \rightarrow Pt^{2+}$
	225	8 592	$\pi \rightarrow \pi^*(CO)$
	265	4 660	$\pi \rightarrow \pi^*(pyz)$
	280	1 165	$5d(Pt) \rightarrow \pi^*(CO), 5d(Pt) \rightarrow \pi^*(pyz)$

[a] CH_3OH used as the solvent.

[b] Broad band.

TABLE 5.12

UV data for the complexes *trans*-$[PtBr_2(CO)(L)]$[a]

L	λ_{max}(nm)	ϵ	Assignment
NH_3	205	34 551	$Br^- \rightarrow Pt^{2+}$
	240	2 675	$\pi \rightarrow \pi^*(CO)$
	290	1 115	$5d(Pt) \rightarrow \pi^*(CO)$
py	203	29 571	$Br^- \rightarrow Pt^{2+}$
	249	4 743	$\pi \rightarrow \pi^*(CO)$
	255	4 902	$\pi \rightarrow \pi^*(py)$
	295	1 107	$5d(Pt) \rightarrow \pi^*(CO), 5d(Pt) \rightarrow \pi^*(py)$
pyO	206	38 350	$Br^- \rightarrow Pt^{2+}$
	263[b]	14 792	$\pi \rightarrow \pi^*(CO) \pi \rightarrow \pi^*(pyO), 5d(Pt) \rightarrow \pi^*(CO)$
an	202	34 273	$Br^- \rightarrow Pt^{2+}$
	238	8 047	$\pi \rightarrow \pi^*(CO), \pi \rightarrow \pi^*(CO)$
	282	2 077	$5d(Pt) \rightarrow \pi^*(CO)$
Him	206	31 187	$Br^- \rightarrow Pt^{2+}$
	242	2 859	$\pi \rightarrow \pi^*(CO)$
	255	2 079	$\pi \rightarrow \pi^*(Him)$
	290	780	$5d(Pt) \rightarrow \pi^*(CO), 5d(Pt) \rightarrow \pi^*(Him)$
pyz	205	30 968	$Br^- \rightarrow Pt^{2+}$
	245	3 908	$\pi \rightarrow \pi^*(CO)$
	256	3 006	$\pi \rightarrow \pi^*(NH_3)$
	290	902	$5d(Pt) \rightarrow \pi^*(CO), 5d(Pt) \rightarrow \pi^*(pyz)$

a CH_3OH used as the solvent.

b Broad band.

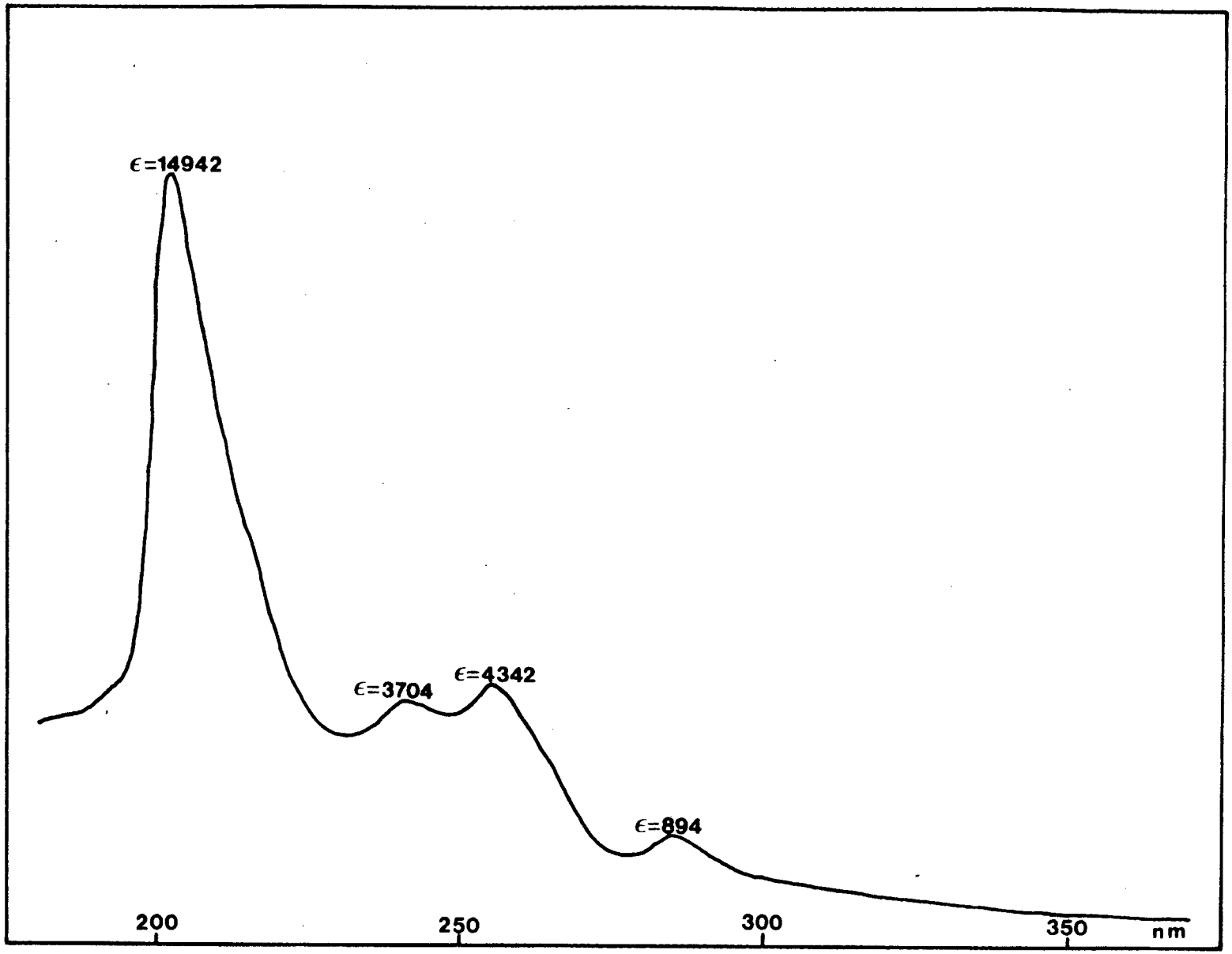

Fig. 5.10. The UV spectrum of trans-[$PtCl_2(CO)(py)$]

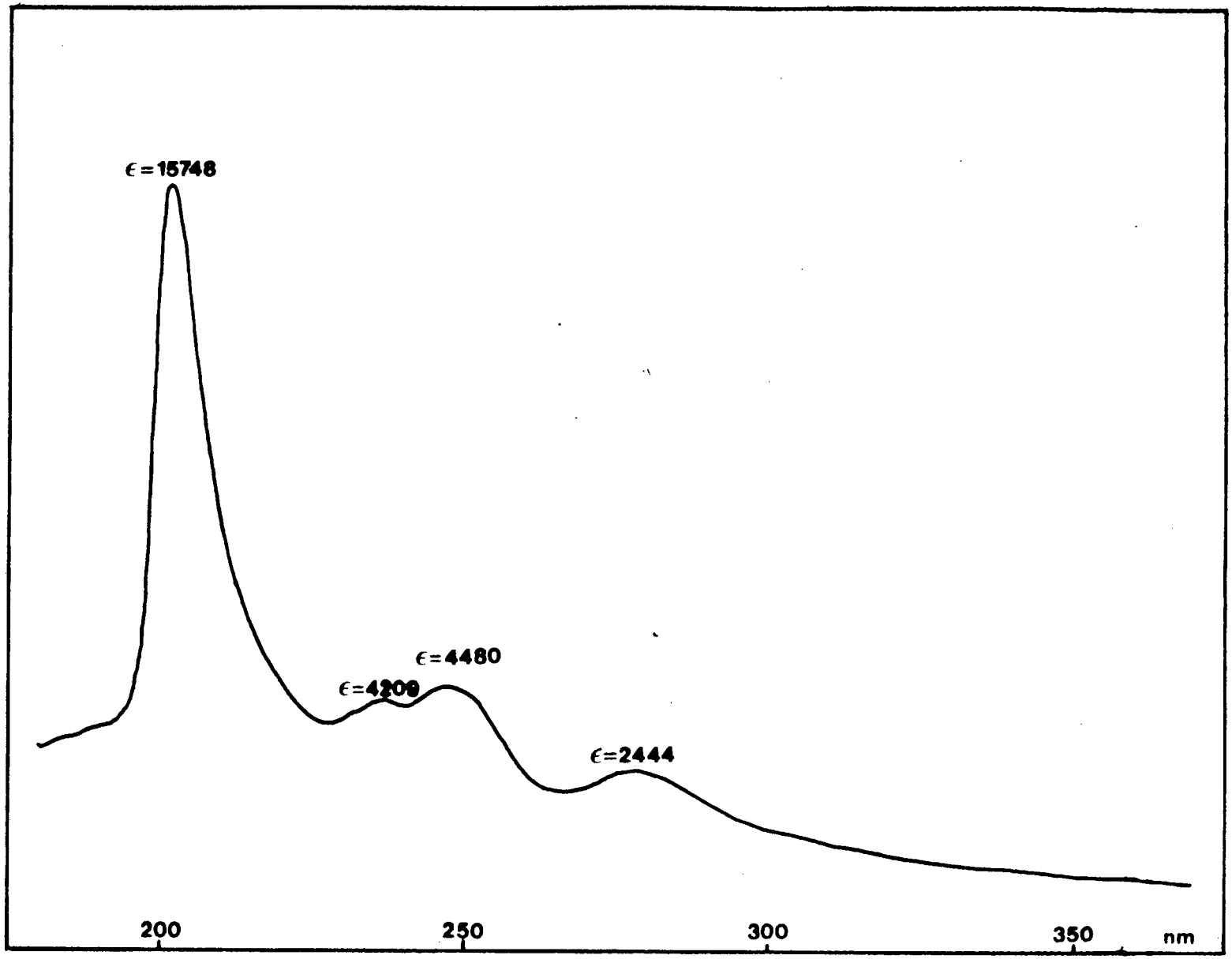

Fig. 5.11. The UV spectrum of trans-[$PtCl_2(CO)(Him)$]

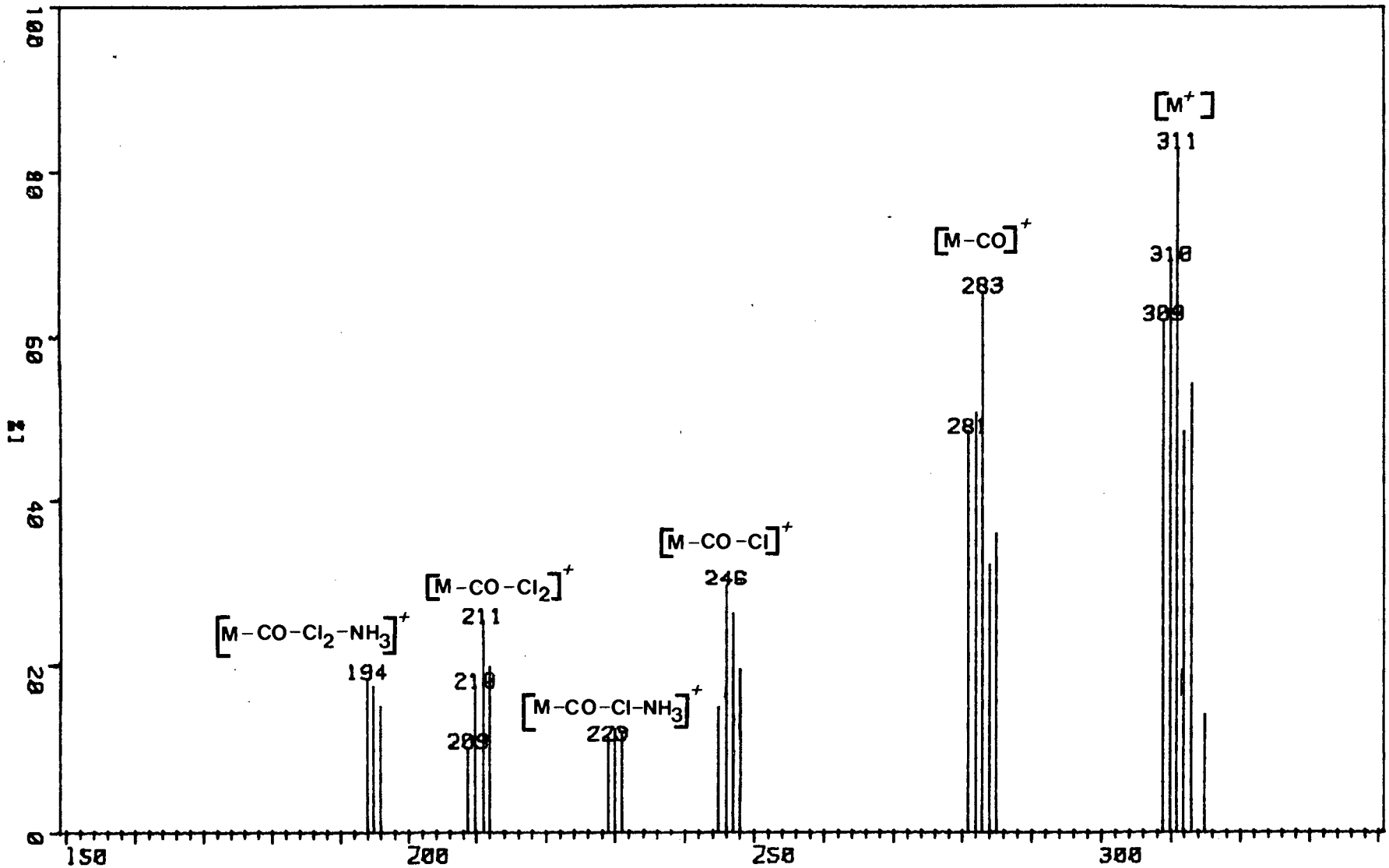

Fig. 5.12. Mass spectra of the complex trans-[$PtCl_2(CO)(NH_3)$]

5.7 RESULTS for *trans*-$[Pt_2X_4(CO)_2(pz)]$

TABLE 5.13

Internal ligand frequencies (cm^{-1}) and assignments for the complexes *trans*-$[Pt_2X_4(CO)_2(pz)]$

X=Cl		X=Br		Assignment
pz	pz-d_4	pz	pz-d_4	
3120	2331	3146	2359	
3094	2312	3115	2341	
3045	2299	3101	2323	ν(C-H)
3023	2287	3068	2297	
2993	2273	3051	2277	
2131	2131	2136	2135	
2082	2082	2089	2089	ν(C≡O)
(2134)	(2136)	(2138)	(2139)	
1490	1291	1493	1297	
1437	1172	1433	1189	ν(ring)
1422	1160	1426	1180	
1166	1136	1172	1174	
1131	884	1126	886	δ(C-H)
1122	850	1120	860	
1103	1095	1104		
1090	1060	1091	1061	ν(ring)
1013	1011			
977	976	973	987	
823	662	824	687	
		816	657	
742	724	761	723	γ(ring)
552	536	552	531	
472	452	472	441	
460				

Values in parentheses are those obtained in chloroform solution.

TABLE 5.14

Metal ligand frequencies and isotopically-induced shifts (cm^{-1}) in the infrared spectra of the complexes *trans*-$[Pt_2X_4(CO)_2(pz)]$[a]

X	δ(PtC≡O)	ν(Pt-C)	ν(Pt-N)	ν(Pt-X)	Other
Cl	510(7)	486(2)	186(1)	357(1)	151(4)
					126(2)
Br	510(6)	493(1)	174(6)	259(1)	144(2)
					100(0)
					88(0)

[a] Numbers in parentheses are the shifts (cm^{-1}) induced by ligand deuteration.

TABLE 5.15

UV data for the complexes *trans*-$[Pt_2X_4(CO)_2(pz)]$

L	λ_{max}(nm)	ϵ	Assignment
Cl	209	28012	$Cl^- \rightarrow Pt^{2+}$
	265	17336	$\pi \rightarrow \pi^*(pz), \pi \rightarrow \pi^*(CO)$
	320[b]	2930	$5d(Pt) \rightarrow \pi^*(CO), 5d(Pt) \rightarrow \pi^*(pz)$
Br	213	33005	$Br^- \rightarrow Pt^{2+}$
	263	18803	$\pi \rightarrow \pi^*(pz), \pi \rightarrow \pi^*(CO)$
	318[b]	2725	$5d(Pt) \rightarrow \pi^*(CO), 5d(Pt) \rightarrow \pi^*(pz)$

[b] Broad band.

TABLE 5.16

^{1}H-NMR data for *trans*-$[Pt_2X_4(CO)_2(pz)]$ (X = Cl,Br)[a]

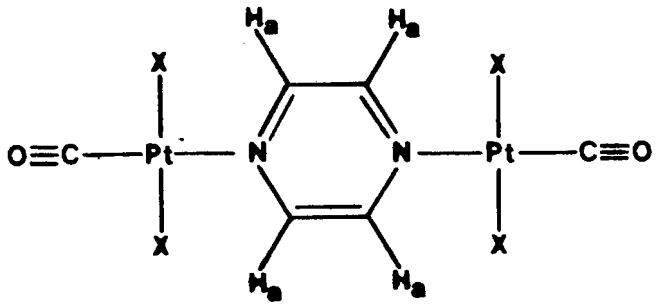

Pyrazine protons	Chemical shift (ppm)
X	H_a
Cl	9.26
Br	9.17

[a] The ^{1}H-NMR spectra were run at ambient temperature on a Bruker WH-90 spectrometer using CD_3COCD_3 as the solvent and lock and TMS as a reference.

5.8 DISCUSSION

The complexes *trans*-$[PtX_2(CO)(L)]$ (X=Cl,Br; L=aniline, pyridine *N*-oxide, pyridine, ammonia, imidazole and pyrazole).

5.8.1 *Infrared Spectra*

The vibrational spectra of Zeise's salt, $K[PtX_3(C_2H_4)]$, and its derivatives *trans*-$[PtX_2(C_2H_4)(L)]$, where L represents various oxygen and nitrogen ligands, have elicited much interest [71,79-82]. However, only recently [57,83] have firm assignments been made, by isotopic labelling studies, for the various metal-stretching modes. The great interest shown in these platinum-ethylene complexes, has been passed on to their carbonyl analogues, *trans*-$[PtX_2(CO)(L)]$. However, no isotopic labelling studies have been applied to the carbonyl complexes, hence assignments have never been complete. Using the assignments in the ethylene-complexes as a basis, as well as labelling the various ligands, band assignments for the analogous carbonyl complexes have been made.

The frequency data and assignments for the internal-ligand modes of the chloro- and bromo- complexes are recorded in Tables 5.2 and 5.3 respectively, and their far-infrared frequencies given in Table 5.4. The internal vibrations of the ligands, L, are assigned to those bands which shift

significantly on deuteration of L, and their more specific assignments made from their ν^D/ν^H ratio [32]. The assignments are straightforwardly made in relation to their ethylene analogues and earlier studies of the use of the ν^D/ν^H ratio in complexes of anilines [32], pyridine, [32] and imidazole [84]. The assignments in the pyridine *N*-oxide and pyrazole complexes follow those reported from a normal coordinate analysis of the free ligands [77,85,86].

The ν(C≡O) frequencies were also determined in chloroform solutions since this results in one single sharp band, whereas in Nujol mulls the same band occasionally displayed fine splittings. The splittings can be explained [72] by the rotational structure in the solid state.

The far-infrared assignments are in agreement with previous work [76,87,88] on similar structures, and the δ(PtC≡O) frequency is greater than the ν(Pt-C) frequency as expected in metal carbonyls [18,89]. Only one previous infrared study of the complexes has been reported. Gribov and coworkers [72] have recorded the infrared spectrum of *trans*-$[PtCl_2(CO)(NH_3)]$, and report only two bands in the skeletal region, at 532 and 477 cm^{-1}. Both were attributed to PtCO deformations, which we now attribute to the deformation and stretching of PtCO, respectively.

5.8.2. *^{1}H-NMR Spectra*

The ^{1}H-NMR data for the complexes *trans*-$[PtX_2(CO)(L)]$ (X=Cl,Br) are given in Table 5.5 (L = NH_3), 5.6 (L = py), 5.7 (L = pyO), 5.8 (L = an), 5.9 (L = Him), and 5.10 (L = pyz). An examination of the data reveals that some of the complexes show ^{195}Pt-H coupling. The coupling is readily recognized because the ^{195}Pt isotope, with a nuclear spin of 1/2, with which the protons couple, is present in 33.8% natural abundance, thus resulting in a high intensity signal which can be attributed to coupling. The observation of coupling indicates that the ligand is complexed to platinum for a sufficiently long period of time on the NMR time scale to permit the platinum and ligand protons to couple.

In both the chloro- and bromo- imidazole complexes the coupling was observed at ambient temperature. This indicates that the exchange rate of the imidazole moiety in the complex with solvent, or other imidazole ligands, is relatively slow.

In the pyridine complexes, coupling is evident in the NMR spectrum of the bromo-complex at ambient temperature, whereas in the chloro-complex, coupling is observed only at lower than ambient temperatures. This shows that the pyridine moiety is more labile in the chloro-complex than in the bromo-complex since lower temperatures were required

to slow down the exchange rate to observe the expected coupling.

In both the chloro- and bromo- pyrazole complexes, coupling could not be distinctly observed at ambient temperature. This may be due to the relatively fast exchange rate, or, because the expected region of the coupling peaks coincide where other intense peaks of the complex are present. The latter is more likely since cold temperature studies ($-20^{o}C$) only marginally improved the detectability of the coupling signals. The ^{195}Pt-H couplings were observed when the spectra were rerun in a different solvent, using chloroform rather than acetone. This was because the well-known solvent effects [90-92], fortunately, produced a large differential chemical shift on the H_a and H_b peaks which had previously been in the expected region of the coupling signal.

In the pyridine *N*-oxide complexes, no ^{195}Pt-H coupling was observed, possibly because the protons are separated by at least four bonds from the platinum atom. Although no temperature studies were performed on these complexes, four bond coupling has been observed in other platinum systems [93,94].

5.8.3. *Electronic Spectra*

The electronic spectral frequencies of *trans*-$[PtX_2(CO)(L)]$

(X=Cl,Br;L=an,pyO,py,NH_3,Him,pyz) are recorded in Tables 5.11 and 5.12. By analogy with similar complexes previously studied [53,59,60] we expect to observe the $\pi \rightarrow \pi^*(CO)$ transition as well as the $5d \rightarrow \pi^*(CO)$ inverse charge transfer and the $X^- \rightarrow Pt^{2+}$ charge transfer bands. In addition, in complexes where L is a ligand that has π-electrons present that may interact with Pt, there is the possibility of the $5d$ (Pt) $\rightarrow \pi^*$(ligand) inverse charge transfer transition. Since some of the transitions overlap with each other, resulting in broad bands, some assignments are tentative. We observe the previously reported [60] red shift in the $5d$(Pt) $\rightarrow \pi^*$ transition which results from the replacement of Cl by Br in the complexes.

5.8.4. *Mass Spectra*

A typical mass spectrum is shown in Figure 5.12. The presence of many stable isotopes, with high natural abundance, of chlorine, bromine and platinum (75.4% ^{35}Cl, 24.6% ^{37}Cl; 50.5% ^{79}Br, 49.5% ^{81}Br; 32.8% ^{194}Pt, 33.7% ^{195}Pt, 25.4% ^{196}Pt) aided unequivocal assignment of the peaks based on the clusters produced in the spectra. Substitution of pyridine by pyridine-d_5 (M.W. = 84.1) in the complex *trans*-[Pt(Br)$_2$(CO)(py)] allows for easy distinction between Br(M.W. = 79.9) fragmentation and pyridine (M.W. = 79.1) fragmentation patterns.

All the spectra of the complexes *trans*-[PtX_2(CO)(L)] show

their molecular ion peak (M^+), except for the pyridine *N*-oxide complexes which show m/e greater than their expected molecular masses. This is possibly due to the break-down of the complex, followed by recombinations to form a complex of higher molecular mass.

There is no correlation in the fragmentation pathways for chloro- and bromo- analogous complexes, and in all the spectra more than one fragmentation pathway was required to account for all the peaks. However, there appears to be very little internal fragmentation of the ligands, L, followed by recombination, since few peaks were observed which would account for this process.

5.9 DISCUSSION

The complexes *trans*-$[Pt_2X_4(CO)_2(pz)]$ (X = Cl, Br; pz = pyrizine)

It has recently been shown [83] that depending on the preparative condition employed, pyrazine reacts with Zeise's salt to form two types of complexes. In one complex the pyrazine is terminal, that is, *trans*-$[PtX_2(C_2H_4)(pz)]$, while in the other complex the pyrazine acts as a bridging ligand that is, *trans*-$[Pt_2X_4(C_2H_4)_2(pz)]$. The carbonyl analogue of the latter complex, *trans*-$[Pt_2X_4(CO)_2(pz)]$, could be prepared by the usual method. However, various attempts (see Section 5.2.4)

to prepare the carbonyl analogue of the former complex, *trans*-$[PtX_2(CO)(pz)]$, were unsuccessful.

5.9.1. *Infrared Spectra*

The infrared data are recorded in Tables 5.13 and 5.14. Using the assignments in the ethylene-analogues [83] as a basis, as well as labelling the ligand, band assignments for the carbonyl complexes have been made. As could be expected, the ν(Pt-N) frequency is substantially lower in these bridging complexes than in complexes where the ligands are terminal. The Pt-N bonding is weak as is indicated not only by the low frequency (180 cm^{-1}) of the ν(Pt-N) band, but also by its very weak intensity in the infrared spectra.

5.9.2. *^{1}H-NMR Spectra*

The bridging role of pyrazine is suggested by the single resonance of the aromatic protons indicating the equivalence of the four aromatic protons, and by its low field (deshielded) position in relation to similar complexes not having a briding ligand.

5.9.3. *Electronic Spectra*

The UV data are recorded in Table 5.15. Assignments are made in relation to their ethylene analogues [83]. Two

bands of high intensity occur within the range 200-300 nm. The band of higher energy is assigned to a charge transfer $X \rightarrow Pt^{2+}$ transition, while the band at lower energy is attributed to a combination of the $\pi \rightarrow \pi^*$ transition of both carbon monoxide and pyrazine. However, assignments are tentative due to the very broad nature of the bands.

CHAPTER 6

CHAPTER 6

6 SPIN DYNAMIC STUDIES

6.1. INTRODUCTION

Inorganic and organometallic chemistry is unindated by a large number of stereochemically nonrigid molecules. This situation was not recognized until the 1960's, when NMR studies uncovered for many molecules spectral features explicable only in terms of rapid molecular rearrangements [95,96,97]. By the late 1960's, NMR studies of stereochemically nonrigid molecules became quite common. Since then, an impressive array of computer programmes for generating theoretical spectra from a set of chemical shifts and coupling constants have been developed. Hence, computer aided NMR studies have been used extensively in the study of rapid equilibria. From these studies, activation parameters for the experimental system can be determined. The generally used method for obtaining activation parameters is therefore to carry out a complete band shape study of the kinetics over as wide a temperature range as possible, and then to obtain the Arrhenius activation parameters from a plot of $\ln K$ against $1/T$, which would provide the parameters of interest from the slopes and intercepts.

This has been applied by various workers [98,99,100] to

platinum(II) olefin complexes. These platinum complexes are particularly amenable to ^{1}H-NMR studies because the spectra are characterized by the appearance of relatively intense ^{195}Pt-H spin coupling to both olefin and the ligand.

The present work was undertaken to extend the recently reported [101] NMR exchange studies of the complexes *trans* $[PtX_2(C_2H_4)(Him)]$ (X = Cl,Br; Him = imidazole). Variable temperature studies of the ^{1}H-NMR spectra of the above complexes in a known concentration of free ligand, imidazole, were determined and with the aid of the computer programme DNMR5 (see Chapter 1.6), activation parameters for the exchange of imidazole in the complexes were obtained.

The effect of varying solvents on the above complexes were also examined. Further, exchange studies on the complex *trans*-$[PtX_2(C_2H_4)(pyz)]$ (X = Cl,Br; pyz = pyrazole) have also been determined and their results are still to be analyzed.

6.2. EXPERIMENTAL

The complexes *trans*-$[PtX_2(C_2H_4)(Him)]$ were prepared as previously described, see Chapter 5.2.1. They were further recrystallized from chloroform to remove traces of free ligand. Known solution concentrations of complex and free

ligand, imidazole were prepared in acetone-d_6 to give final complex and free imidazole molarities of approximately 0.2M and 0.001M respectively.

The ^{1}H-NMR spectra of the above solutions were each obtained at 90 MHz on a Bruker WH-90 D/S Fourier transform spectrometer in the region 7ppm to 9ppm, using appropriate expansions, in the temperature range +30° to -80°C.

It was necessary to modify the computer programme DNMR5 to accommodate our experimental system. This was made possible by considering our experimental system to be divided into two parts. The two parts considered were i) the two complexes with Pt(I=1/2) and free imidazole itself, that is, a four nuclei three nuclear configuration process, and, ii) the two complexes with Pt(I=0) and free imidazole itself, that is, a three nuclei three nuclear configuration process.

After obtaining computed spectra for each part, independently, these were appropriately scaled and added together to give the final computed spectra.

The computed and experimental spectra were compared, and whenever the spectra bore an adequate resemblance to each other, then the kinetic parameters of the experimental spectra were considered to be equal to those of the

computed spectra. Plots of $\ln K$ against $1/T$ were obtained by the computer which took into account the error analysis factor on $\ln K$.

6.3 RESULTS

TABLE 6.1

The ^{1}H-NMR spectrum of *trans*-$[PtCl_2(C_2H_4)(imidazole)]$[a]

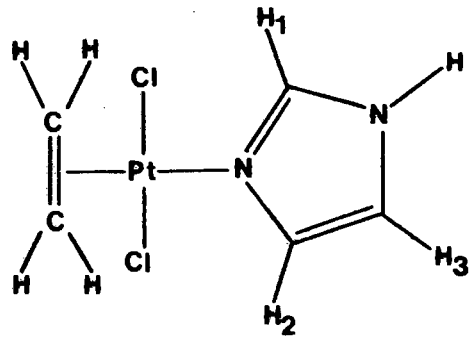

Chemical shift (ppm)					
Olefin protons		Imidazole protons			
H		H_1	H_2	H_3	
4.56		8.55	7.66	7.38	
Coupling constants (H_z)					
Olefin protons		Imidazole protons			
^JPt-H		$^JPt-H_1$	$^JPt-H_2$	$^JPt-H_3$	
60.0		19.0	20.0	b	

[a] The ^{1}H-NMR spectrum was run at 205 K on a Bruker WH-90 spectrometer using CD_3COCD_3 as the solvent and lock and TMS as a reference.

[b] Coupling constant not observed, and was assumed to be $7H_z$ in the computer simulation based on previous work [102].

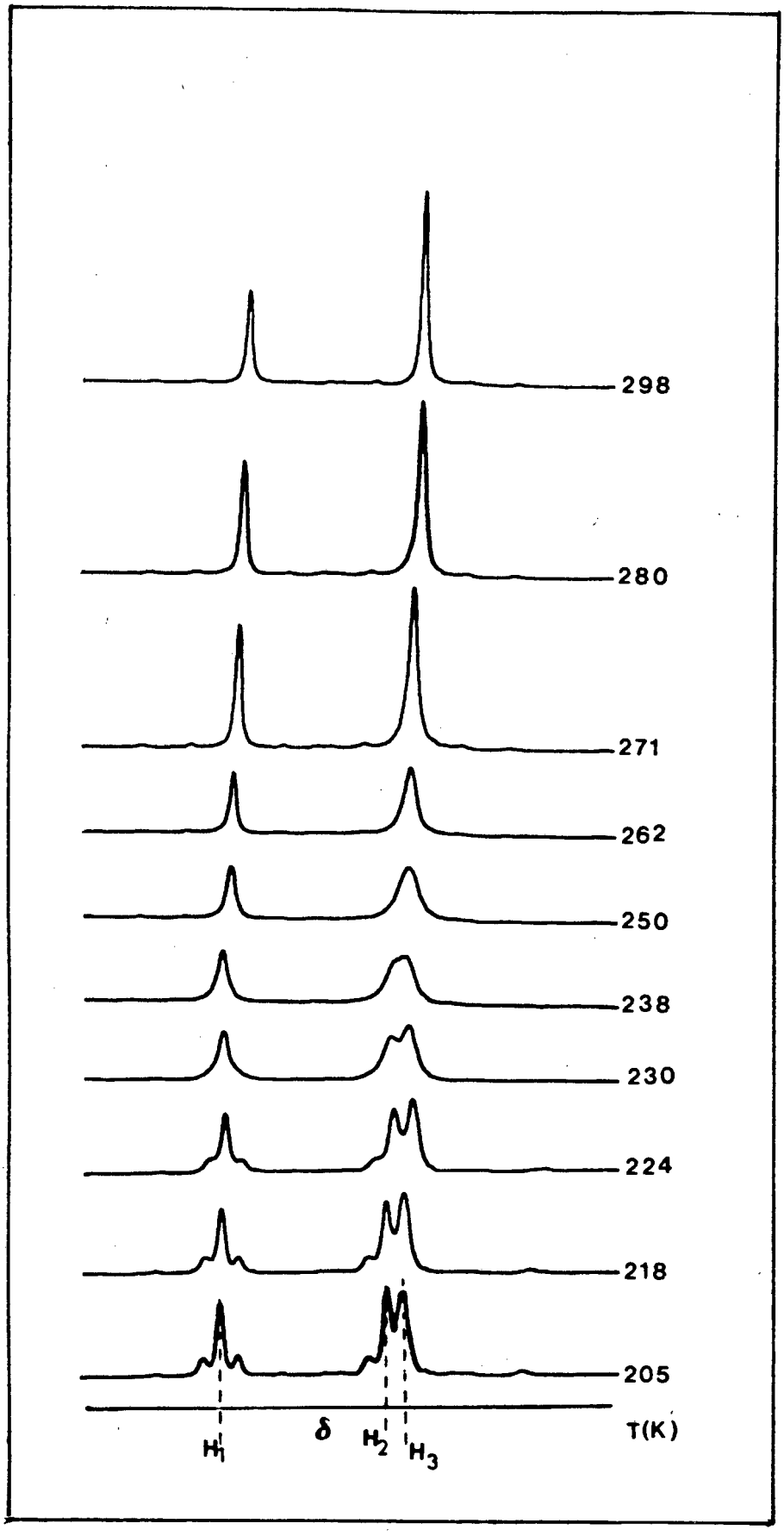

Fig. 6.1. ^{1}*H-NMR temperature dependent spectrum of trans-* $[PtCl_2(C_2H_4)(Him)]$

TABLE 6.2

Activation parameters for *trans*-$[PtCl_2(C_2H_4)(imidazole)]$ derived by band shape analysis of the H_2 and H_3 resonances assuming intermolecular exchange.

T(K)	K (s^{-1})	ln$K$	error analysis factor of ln$K$	$^1/_T$ x 10^3
205	0.9 ± 0.3	-0.105 ± 0.33	0.069	4.88
218	6.0 ± 1.0	1.792 ± 0.17	0.138	4.59
224	12.0 ± 1.0	2.485 ± 0.08	0.275	4.46
230	22.0 ± 2.0	3.091 ± 0.09	0.252	4.35
238	58.0 ± 5.0	4.060 ± 0.08	0.266	4.20

Parameters used in the above simulation were those experimentally found for the system.

T_2 = 0.15 s and 0.10 s for the complex and the ligand imidazole, respectively.

Internal imidazole coupling obtained as previously reported [103,104] on similar structures.

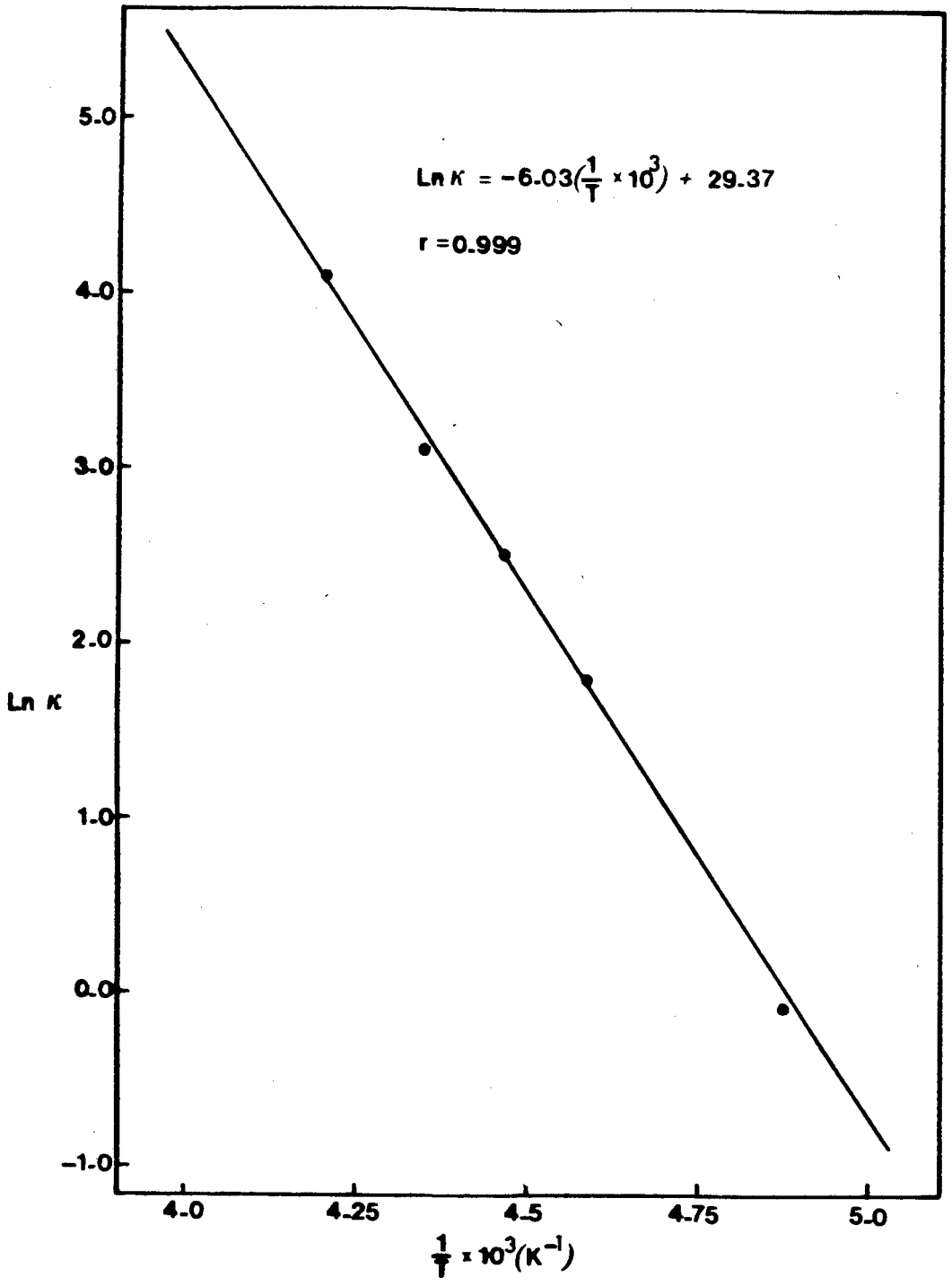

Fig. 6.2. Plot of lnK vs 1/T for trans-[$PtCl_2(C_2H_4)(Him)$]

TABLE 6.3

The ^{1}H-NMR spectrum of *trans*-$[PtBr_2(C_2H_4)(imidazole)]$[a]

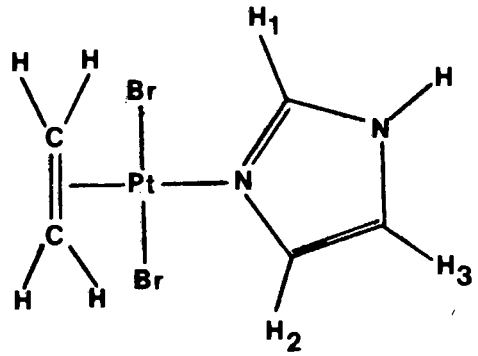

Chemical shift (ppm)

Olefin protons	Imidazole protons		
H	H_1	H_2	H_3
4.76	8.62	7.63	7.51

Coupling constants (Hz)

Olefin protons	Imidazole protons		
J_{Pt-H}	J_{Pt-H_1}	J_{Pt-H_2}	J_{Pt-H_3}
60.0	18.0	20.0	b

[a] The ^{1}H-NMR spectrum was run at 220 K on a Bruker WH-90 spectrometer using CD_3COCD_3 as the solvent and lock and TMS as a reference.

[b] Coupling constant not observed, and was assumed to be 7 Hz in the computer simulation based on previous work [102].

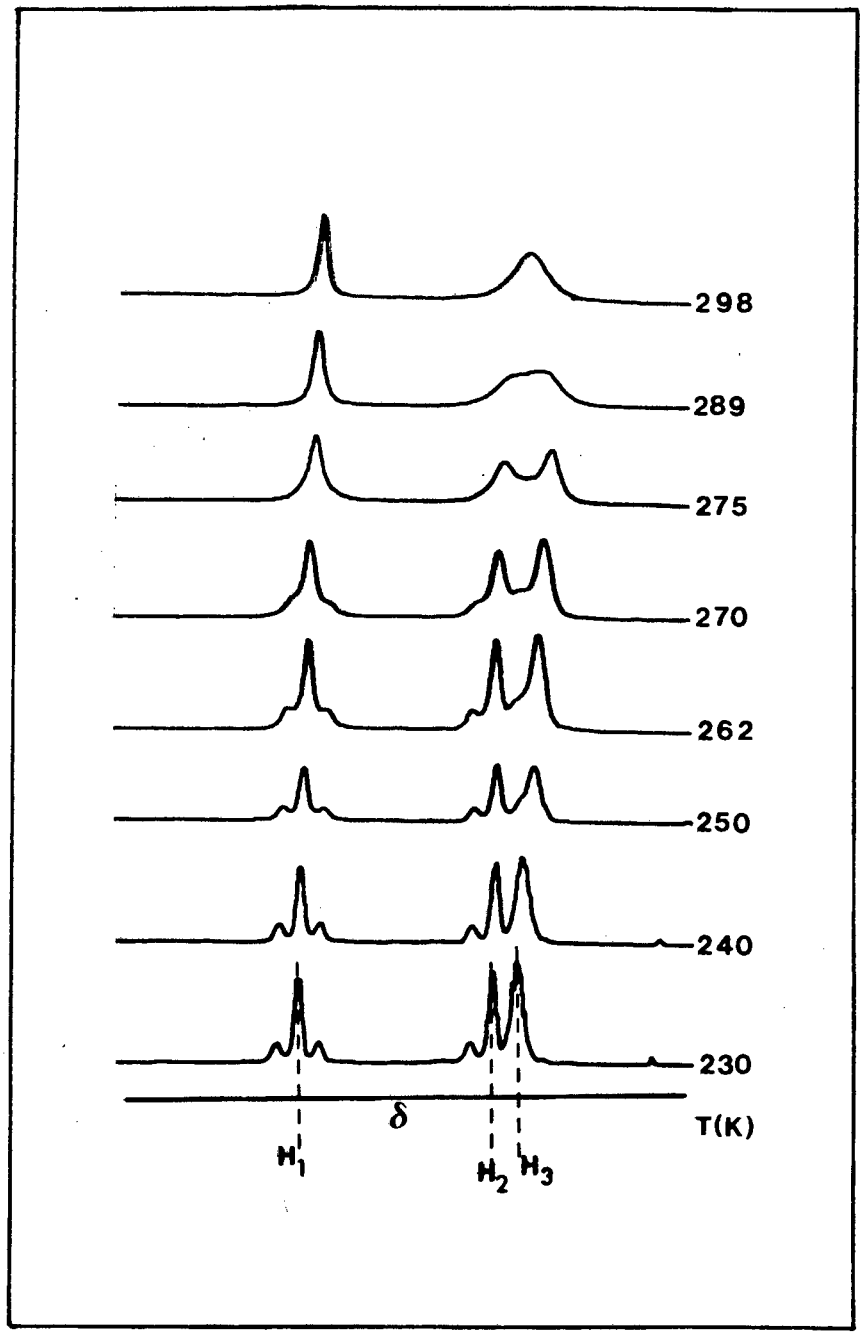

Fig. 6.3. ^{1}H*-NMR temperature dependent spectrum of trans-*
$[PtBr_2(C_2H_4)(Him)]$

TABLE 6.4

Activation parameters for *trans*-[$PtBr_2(C_2H_4)$(imidazole)] derived by band shape analysis of the H_2 and H_3 resonances assuming intermolecular exchange.

T(K)	$K(s^{-1})$	$\ln K$	Error analysis Factor for $\ln K$	$1/T \times 10^3$
230	0.8 ± 0.2	-0.223 ± 0.25	0.076	4.35
240	2.0 ± 0.5	0.693 ± 0.25	0.076	4.17
250	5.0 ± 0.5	1.609 ± 0.10	0.189	4.00
262	18.0 ± 1.5	2.890 ± 0.08	0.228	3.82
270	35.0 ± 3.0	3.555 ± 0.09	0.222	3.70
275	55.0 ± 5.0	4.007 ± 0.09	0.209	3.64

Parameters used in the above simulation where those experimentally found for the system.
T_2 = 0.15 s and 0.10 s for the complex and the ligand, imidazole, respectively. Internal imidazole coupling obtained as previously reported [103,104].

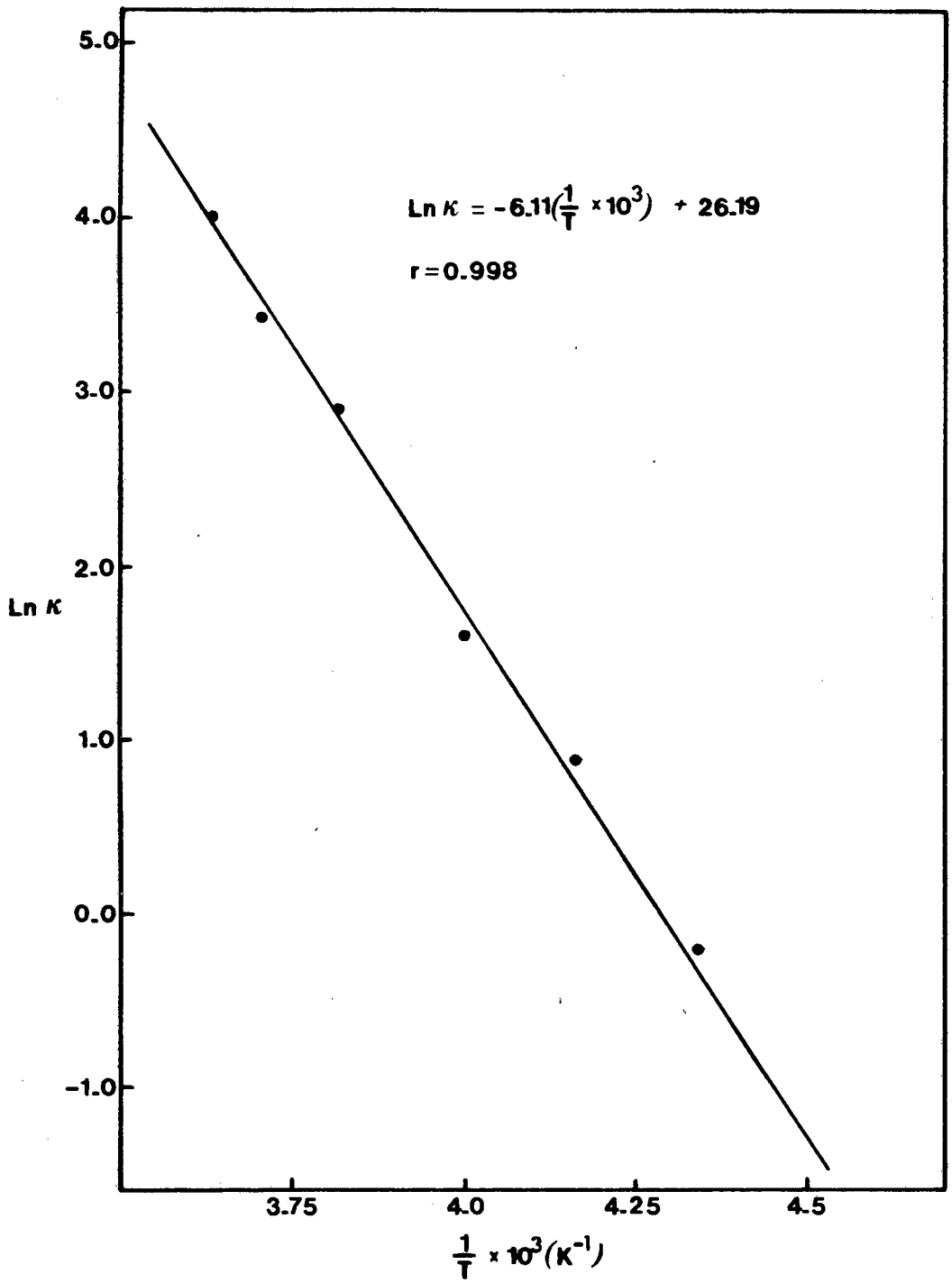

Fig. 6.4. Plot of lnK vs 1/T for trans-[$PtBr_2(C_2H_4)(Him)$]

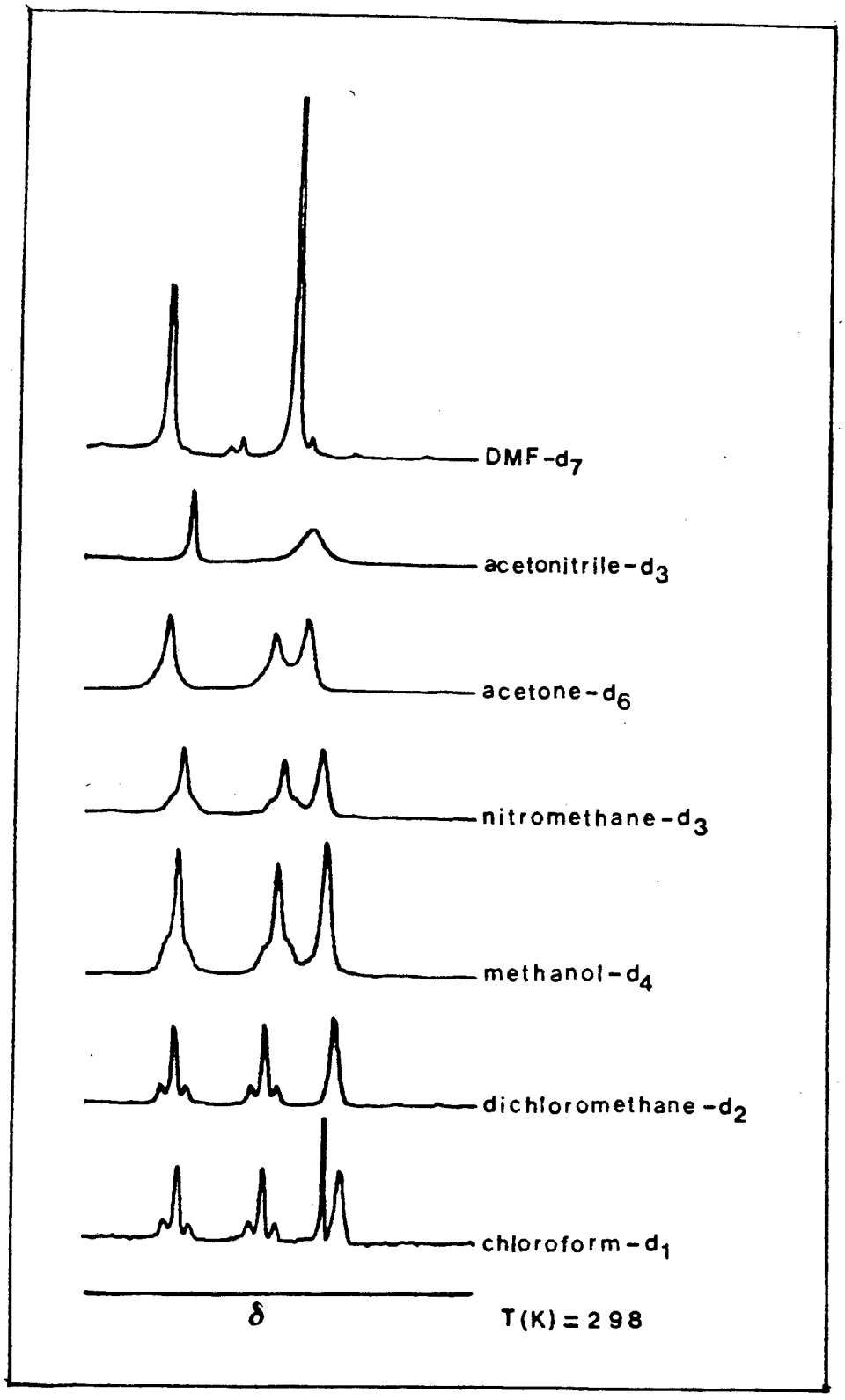

Fig. 6.5. ^{1}*H-NMR solvent dependent spectrum of trans-*
$[PtCl_2(C_2H_4)(Him)]$

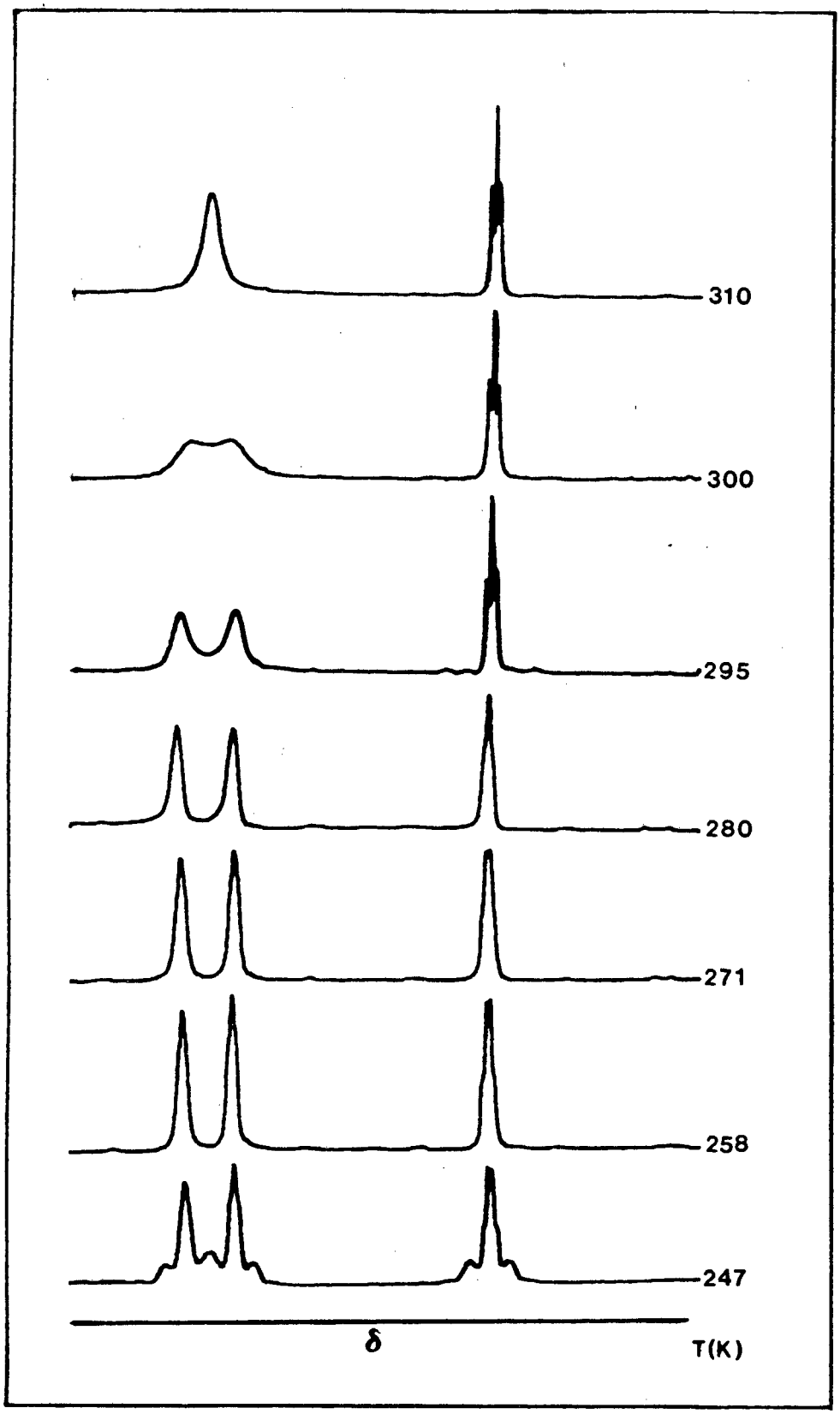

Fig. 6.6. ^{1}H-NMR temperature dependent spectrum of trans-$[PtCl_2(C_2H_4)(pyz)]$

6.4. DISCUSSION

With the presence of free imidazole in a solution of the complexes *trans*-$[PtX_2(C_2H_4)(Him)]$, there can occur five possible nuclear configurations; two with Pt having a nuclear spin number, I, equal to 0, and two where $I = 1/2$, the fifth configuration being imidazole itself. These configurations are shown in Figure 6.7.

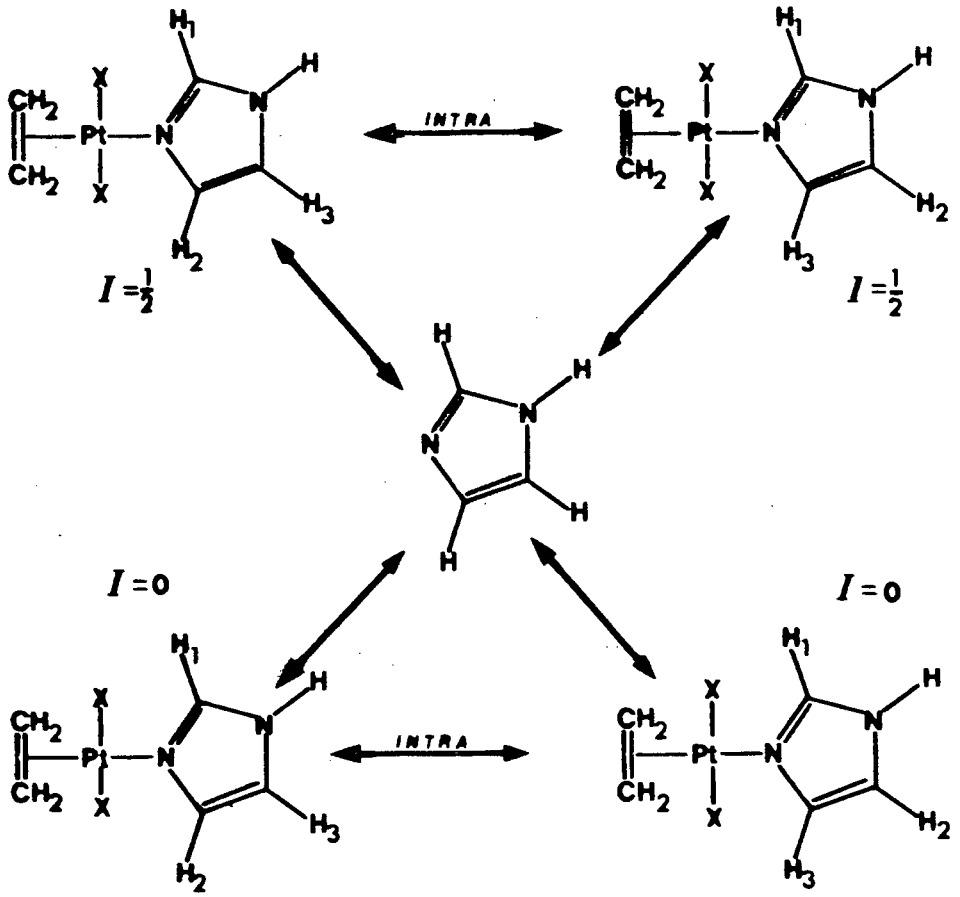

FIGURE 6.7

Considering the above, there are two types of exchanges involving the imidazole ligand on the complex which can occur, namely intramolecular and intermolecular.

In intramolecular exchange processes, nuclear positions in a molecule are permutable without bond-breaking, hence spin-spin coupling will be maintained between the nuclei involved. In intermolecular exchange processes, there are bond-breaking and bond-formation steps. Bond scissions necessarily leads to loss of spin-spin coupling between nuclei in the two fragments generated in the scission process. This loss of spin correlation is the most definitive NMR test of an intermolecular exchange process and is extremely sensitive [105].

6.4.1. The complex *trans*-[$PtCl_2(C_2H_4)$(imidazole)]

The NMR results for the complex are listed in Table 6.1 and the temperature-dependent spectra shown in Figure 6.1. The data reveal that at room temperature there are only two signals for the H_1, H_2 and H_3 protons of imidazole. The lower field signal is assigned to H_1 while the other signal is assigned to H_2 and H_3, which are equivalent if exchange is occurring. The previously reported [101] changes in the spectra are observed lowering the temperature. That is, i) the single resonance of H_2 and H_3 collapses into two separate resonances, and ii) the coupling between Pt(I = 1/2) and H_1 and H_2 become clearly visible. Further, the data shows that at ambient temperature there is no ^{195}Pt-H coupling, and bearing in mind the previous paragraph, the exchange process is necessarily intermolecular and not intramolecular. Further evidence

for an intermolecular process is the observation that the slow exchange limit is characterized by a multiplet, the transition region by a broadening of the multiplet, and the fast exchange limit by a single resonance.

Hence, in the simulation studies, intramolecular exchange was assumed to be zero, and the rate constants determined by intermolecular exchange only. This is contrary to the above-mentioned paper in which intramoleular exchange was assumed to be the process occurring , and this assumption employed in those simulation studies. The spin dynamics were fed into our modified DNMR5 [37], an iterative simulation programme, assuming intermolecular exchange. By means of band shape analysis, the rate constants for the exchange process were determined and are listed in Table 6.2. A plot of $\ln K$ against $1/T$ was made (Figure 6.2) using error analysis which has been shown to be the only valid means of determining the slope and intercept accurately since measurements near the coalescence temperature are most accurate [40]. The plot results in a straight line, the slope of which yields $\Delta H^{\ddagger}$, the enthalpy of activation, directly, and an intercept from which $\Delta S^{\ddagger}$, the entropy of activation may be determined, since

$$\ln K = \ln A - \Delta H^{\ddagger}/RT$$

and

$$\ln A = \ln(kT/h) + \Delta S^{\ddagger}/R$$

where K is the rate constant in s^{-1}, T is the temperature

in Kelvin, K is the Boltzmann constant and h is Planck's constant. The results obtained were

$$\Delta H^{\ddagger} = 50.12 \pm 1.36 \text{ kJ mol}^{-1}$$

$$\Delta S^{\ddagger} = -0.72 \pm 1.72 \text{ kJ mol}^{-1}\text{K}^{-1}$$

The enthalpy of the exchange process is similar to that compared for substitution reactions at a square-planar platinum centre [106]. The small value of $\Delta S^{\ddagger}$ indicates that solvent has little effect on the exchange process. This is somewhat surprising since changing the solvent had a marked effect on the rate of the exchange process, as shown in Figure 6.5.

However, it should be noted that in the various solvent runs, no extra added ligand was present, whereas in the above case extra added ligand was present. Hence, possibly, the excess ligand has a more dominant role in the exchange process when it is present, and this would result in a small value of $\Delta S^{\ddagger}$ being obtained.

6.4.2. *The complex trans-[PtBr$_2$(C$_2$H$_4$)(imidazole)]*

The NMR results for the complex are listed in Table 6.3 and the temperature dependent spectra shown in Figure 6.3. As observed in the chloro-complex, there are only two signals for the H_1, H_2 and H_3 protons of imidazole. Lowering the temperature caused the same phenomena to occur as in the corresponding chloro-complex except that the

coalescence temperature is higher. Hence the exchange rate is slower in the case of the bromo-complex. This was also the result obtained (see Chapter 5.8.2.) for the analogous chloro- and bromo-pyridine complexes.

As observed in the chloro-complexes, the evidence obtained was once again favour of an intermolecular exchange process occurring. The spin dynamics were fed into the modified DNMR5 programme and the activation parameters were determined assuming intermolecular exchange, as previously described. The results obtained (from Figure 6.4) were

$$\Delta H^{\ddagger} = 50.83 \pm 1.49 \text{ kJ mol}^{-1}$$

$$\Delta S^{\ddagger} = -27.11 \pm 1.90 \text{ kJ mol}^{-1} \text{ K}^{-1}$$

Studies on the effect of solvent are being pursued, and it is hoped that an understanding of the role of the solvent in the exchange process will become apparent. Further, studies on the complex *trans*-$[PtX_2(C_2H_4)(\text{pyrazole})]$ have been undertaken (see Fig. 6.6) and the results are presently being analyzed with a view to comparing the effect of altering only the position between the two available coordination sites on the ligand.

APPENDIX A

APPENDIX A

```
*****************************************************************

    THIS PROGRAM HAS BEEN CHANGED TO WORK IN FREE FORMAT
    AND DO SIMULATION ONLY
    IT HAS ALSO BEEN ENLARGED TO TAKE MORE COMPLEX SYSTEMS

*****************************************************************

  PROGRAM DNMR5(BAND,INPUT,OUTPUT,PUNCH,ZZZG67,TAPE11=BAND,
 1TAPE5=INPUT,TAPE6=OUTPUT,TAPE7=PUNCH,TAPE67=ZZZG67)

  PROGRAM FOR ITERATIVE ANALYSIS OF EXCHANGE BROADENED NMR SPECTRA

  DAVID S. STEPHENSON AND GERHARD BINSCH              MUENCHEN 1978

  COMMON/CB10/IN,IO,IOP,INT
  DATA IN,IO,IOP,INT/5,6,9,11/
1 CALL INITAL(IFILEP)
  CALL DNMR3
  CALL SPECT(IFILEP)
  GO TO 1
  INPUT IS AS FOLLOWS
  1.   TEXT
       PROBLEM NAME, IF FIRST FIELD BLANK THEN END OF RUN
  2.   N,NE,MU,NMES,NSYM,IFILEP
       N=NUMBER OF NUCLEI
       NE=NUMBER OF NUCLEAR CONFIGURATIONS
       MU=1 FOR MUTUAL EXCHANGE,=0 OTHERWISE
       NMES=NUMBER OF SETS OF MAGNETICALLY EQUIVALENT NUCLEI,
       NMES MUST INCLUDE ALL SETS OF MAGNETICALLY EQUIVALENT
       NUCLEI EVEN THE TRIVIAL SETS CONTAINING ONLY ONE NUCLEUS
       THUS IF THE OPTION IS NOT TO BE USED THEN NMES=N
       NSYM=NUMBER OF SYMMETRY PAIRS. A SYMMETRY PAIR IS DEFINE
       AS TWO NUCLEI RELATED BY PERMUTATION SYMMETRY.
       NSYM=0 IF NO SYMMETRY
       NOTE.  THE SYMMETRY AND MAGNETIC EQUIVALENCE OPTIONS
       CANNOT BE USED SIMULTANEOUSLY
       IFILEP = 1  IF SPECTRUM TO BE WRITEN TO FILE 12 OTHERWISE = 0
  3.   NO,SCAL,HEIGHT,SF(1),SF(NO)
       NO=NUMBER OF SPECTRAL POINTS IN SIMULATION
       SCAL=PLOT SCALING FACTOR IN HZ/MM
       HEIGHT IS THE MAXIMUM SPECTRUM HEIGHT IN MM. FOR CARD
       SF(1)=FREQUENCY OF FIRST POINT IN SIMULATED SPECTRUM
       SF(NO)=FREQUENCY OF LAST POINT IN SIMULATED SPECTRUM
  4.   NNMES(I),I=1,NMES
       NUMBER OF NUCLEI IN MAGNETICALLY EQUIVALENT SET I
       OMIT IF NMES=N
```

APPENDIX A Continued/

```
5.   W(I,J),J=1,NMES
      CHEMICAL SHIFTS IN HZ FOR NUCLEAR CONFIGURATION I,
      IF NSYM.NE.0 THE LABELING MUST BE CHOSEN SO THAT ALL
      SYMMETRY PAIRS PRECEDE THOSE SPINS NOT RELATED BY SYMMETRY
6.    NEXT SET OF CARDS INPUT COUPLING CONSTANTS (HZ) FOR
      NUCLEAR CONFIGURATION I
     AJ(I,J,K),....
      FIRST CARD AJ(I,1,2),AJ(I,1,3),......AJ(I,1,NMES)
      SECOND CARD AJ(I,2,3),AJ(I,2,4),......AJ(I,2,NMES)
      ETC.
      LAST CARD AJ(I,NMES-1,NMES)
      SKIP 7 IF NMES=1
7.    IF MU=0 REPEAT 6 AND 7 FOR ALL NUCLEAR CONFIGURATIONS I
8.    IF MU=1 READ IN EXCHANGE VECTORS FOR MUTUAL EXCHANGE
      ONE VECTOR PER CARD
     IE(I,K),K=1,NMES
      FIRST CARD - SECOND EXCHANGE VECTOR
      SECOND CARD - THIRD EXCHANGE VECTOR
      ETC.
      THE INTEGER ELEMENTS OF THE NTH EXCHANGE VECTOR REPRESENT
      THE LABELING OF THE NUCLEI (OR THE LABELING OF THE SETS IF
      EQUIVALENCE IS USED) IN THE NTH CONFIGURATION IN TERMS OF
      THE CONSECUTIVE LABELING IN THE FIRST CONFIGURATION
9 .   IF MU=0 READ IN POPULATIONS OF NUCLEAR CONFIGURATIONS
     POP(I),I=1,NE
10.  T2(I),I=1,NE
      THE RELAXATION TIMES OF THE INDIVIDUAL NUCLEAR CONFIGS.
11.  RC(I,J)
      RATE CONSTANTS IN 1/SEC ONE PER CARD
      CARD SEQUENCE IS RC(1,2),RC(1,3),...RC(1,NE),RC(2,3),..
      IF MU=1 THIS SET CONSISTS OF SINGLE CARD RC(1,2) ONLY
      SKIP IF NE.EQ.1
12.   RETURN TO 1
DEBUG SUBCHK
END
```

PROGNOSIS

PROGNOSIS

Although the present thesis is, at the most, only an introducton to the chemistry of square-planar platinum(II) complexes, it may be fruitful to comment briefly on possible areas for future work.

Firstly, infrared and Raman studies using ^{13}C-carbonyl species could be carried-out for a complete vibrational study of the complexes, *trans*-$[PtX_2(CO)(L)]$. The added advantage of having these specifically labelled complexes is that ^{13}C-NMR studies could be performed. Platinum is an ideal metal for ^{13}C-NMR studies, since ^{195}Pt (33% natural abundance) complexes strongly with directly bonded nuclei, resulting in considerable fine structure. Further, these ^{13}C-NMR spectra are more sensitive to changes in bonding than the ^{1}H-NMR spectra [107]. This has been applied by a few workers [60,107-109], and their studies show some useful correlations with their infrared data.

Secondly, the ligand, CO, could readily be replaced by other ligands with have not yet been extensively studied, such as acetylene. The various spectroscopic techniques could then be reapplied to these complexes. The results

obtained could be compared with those of the extensively studies carbonyl and ethylene analogues in relation to their different bonding properties.

Thirdly, further ^{1}H-NMR/Computer studies could be applied to the other fluxional complexes encountered in this research. The accumulative data should lead to a more meaningful rationalization of the possible exchange processes occurring.

Lastly, X-ray crystal determinations on the carbonyl analogues of Zeise's salt, $K[Pt(CO)Cl_3]$ would positively reinforce the expected behaviour resulting from the *trans*-effect of the CO ligand.

Considering the above, it would appear that further studies in this field are potentially extensive. Hence it is apt to quote *Pliny the Elder*[*]:

"From the end spring new beginnings".

[*] *Historia Naturalis, Bk. ix, sec.65.*

REFERENCES

REFERENCES

1. F.A. Cotton & G. Wilkinson, **Advanced Inorganic Chemistry,** Wiley (Inerscience), New York, 4th ed., (1980) 901.

2. W.C. Zeise, **Mag. Pharm.,** 35 (1830) 105.

3. H.W. Quinn & J.H. Tsai, **Adv. Inorg. and Radiochem.,** 12 (1269) 217.

4. J.H. Nelson & H.B. Jonassen, **Coord. Chem. Rev.,** 6 (1971) 27.

5. R.G. Guy & B.L. Shaw, **Adv. Inorg. and Radiochem.,** 4 (1962) 77.

6. F.R. Hartley, **Chem. Rev.,** 69 (1969) 799.

7. R. Jones, **Chem. Rev.,** 68 (1968) 785.

8. U. Belluco, B. Crociani, R. Pietropaolo & P. Uguagliati, **Inorg. Chem. Acta Rev,** 3 (1969) 19.

9. F.R. Hartley, **The Chemistry of Platinum and Palladium,** Applied Science Publishers, London, (1973).

10. S.E. Livingstone in **Comprehensive Inorganic Chemistry,** Pergamon Press, Oxford, (1973) Vol. 3, Ch.43.

11. H. Irving & R.J.P. Williams, **Nature,** 162, (1948) 746; **J. Chem. Soc.,** (1953) 3192.

12. S. Ahrland, J. Chatt & N.R. Davies, **Quart. Rev,** 12 (1958) 265.

13. R.G. Pearson, **J. Amer. Chem. Soc.,** 85 (1963) 3533.

14. B.N. Figgs, **Introduction to Ligand Fields,** Wiley (Interscience), New York, (1966).

15. A. Streitwieser & C.H. Heathcock, **Introduction to Organic Chemistry,** Collier Macmillan Publishers, London, (1976) Ch. 10.

16. J.R. Ferraro, **Low-Frequency Vibrations Of Inorganic and Coordination Compounds,** Plenum Press, New York, (1971).

17. D.M. Adams, **J. Chem. Soc.,** (1964) 1771.

18. K. Nakamoto, **Infrared Spectra Of Inorganic and Coordination Compounds,** Wiley, New York, (1963).

19. G.A. Foulds, P.S. Hall, D.A. Thornton, J. Mol. Struct., (in press).

20. L.G. Hulett & D.A. Thornton, **Spectrochim. Acta,** 27A (1971) 2089.

21. G.S. Shephard & D.A. Thornton, **Helv. Chim. Acta**, 54 (1971) 2212.

22. G.T. Behinke & K. Nakamoto, **Inorg. Chem.**, 6 (1967) 433.

23. S. Pinchas & I. Laulicht, **Infrared Spectra of Labelled Compounds**, Academic Press, London, (1971).

24. K. Nakamoto, **Angew, Chem. Internat, Ed.**, 11 (1972) 666.

25. G.C. Percy & H.S. Stenton, **J. Chem. Soc. Dalton**, (1976) 1466,2429.

26. F.A. Cotton, **Chemical Application of Group Theory**, Wiley (Interscience), New York, 2nd ed., (1971).

27. M. Orchin & H.H. Jaffe, **J. Chem. Ed.**, 47 (1970) 246, 372, 510.

28. R.S. Halford, **J. Chem. Phys.**, 14 (1946) 8.

29. D.M. Adams & D.C. Newton, **Tables for Factor Group and Point Group Analysis**, Beckman-RIIC Ltd., Croydon, (1970).

30. L.P. Bicelli, **Ann. Chim. Rome**, 48 (1958) 749.

31. A.T. Hutton & D.A. Thornton, **Spectrochim. Acta**, 34A (1978) 645.

32. G.A. Foulds, J.B. Hodgson, A.T. Hutton, G.C. Percy, P.E. Rutherford & D.A. Thornton, **Spectroscopy Letters**, 12(1) (1979) 25.

33. A.Allerhand, H.S. Gutowsky, J.Jonas & R.A. Meinzer, **J. Amer. Chem. Soc.**, 88 (1966) 3185.

34. E.F. Mooney, **Ann, Rev. NMR Spectroscopy**, 1 (1968).

35. J.D. Swalen, **Prog. NMR Spectroscopy**, 1 (1966) 205.

36. C.W. Haigh, **Ann. Rep. NMR Spectroscopy**, 4 (1971) 311.

37. D.S. Stephenson & G. Binsch, **QCPE Program No. 365**, Chemistry Department, Indiana University.

38. D.S. Stephenson & G. Binsch, **J. Mag. Res.**, 32 (1978) 145.

39. R.R. Shaup, E.D. Becker & M.L. McNeel, **J. Phys. Chem.**, 76 (1972) 71.

40. A. Allerhand & E. Thiele, **J. Chem. Phys.**, 45 (1966) 902.

41. J. Chatt, **J. Chem. Soc.**, (1949) 3340.

42. J. Chatt & A.A. Williams, **J. Chem. Soc.** (1951) 3061.

43. J.A. Wunderlich & D.P. Mellor, **Acta Cryst.**, 7 (1954) 130; 8 (1955) 57.

44. J.A. Jarvis, B.T. Kilbourn & P.G. Owston, **Acta Cryst**, B26 (1970) 876.

45. M.J.S. Dewar, **Bull. Soc. Chim. Fr.**, 18 (1951) C79.

46. J. Chatt & L.A. Duncanson, **J. Chem. Soc.**, (1953) 2939.

47. J.S. Anderson, **J. Chem. Soc.**, (1936) 1042.

48. C.H. Langford & H.B. Grey, **Ligand Substitution Processes**, W.A. Benjamin, New York, (1965).

49. G.B. Bokii & G.A. Kukina, **Kristallografiya**, 2 (1957) 400; **Chem. Abs.**, 52 (1958) 3455h.

50. Reference 9, p. 381.

51. H. Isci & W.R. Mason. **Inorg. Chem.**, 14 (1975) 905, 913.

52. R. Brady, B.R. Flynn, G.L. Geoffroy, H.B. Grey, J. Peone & L. Vaska, **Inorg. Chem.**, 15 (1976) 1485.

53. D. Sutton, **Electronic Spectra of Transition Metal Complexes**, McGraw Hill, Great Britain, (1968).

54. J. Chatt & M. Searle, **Inorganic Syntheses**, 5 (1957) 210.

55. R.D. Cramer, E.L. Jenner, R.V. Lindsey & U.G. Stolberg, **J. Amer. Chem. Soc.**, 85 (1963) 1691.

56. R. Cramer, Inorg. Chem., 4 (1965) 445.

57. Reference 54, notes added by submitters.

58. T.P.E. Auf der Heyde, G.A. Foulds, D.A. Thornton, H.O. Desseyn & B.J. van der Veken, **J. Mol Struct.**, 98 (1893) 11.

59. G.A. Foulds & D.A. Thornton, **J. Mol. Struct.**, 98 (1983) 309.

60. M.A.M. Meesters, D.J. Stufkens & K. Vriese, **Inorg. Chim. Acta**, 14 (1975) 25.

61. P. Schutzenberger, **J. Chem. Soc.**, (1871) 1008.

62. L. Mond, C. Langer & F. Quincke, **J. Chem. Soc.**, (1890) 749.

63. J.S. Anderson, **J. Chem. Soc.**, (1934) 971.

64. E.W. Abel, **Quart, Rev.**, 17 (1963) 133.

65. E.W. Abel & F.G.A. Stone, **Quart. Rev.**, 23 (1969) 325.

66. J.E. Huheey, **Inorganic Chemistry**, Harper & Row, New York, 2nd ed., (1978) 404.

67. R.J. Irving & E.A. Magnusson, **J. Chem. Soc.**, (1956) 1860, (1957) 2018, (1958) 2283.

68. W.H. Clement & M. Orchin, **J. Organomet. Chem.**, 3 (1965) 98.

69. D.P. Mellor, **Chem. Rev.**, 33 (1943) 137.

70. F. Basolo & R.G. Pearson, **Mechanisms of Inorganic Reactions**, Wiley, New York, 2nd ed., (1967) 376.

71. M. Orchin & P.J. Schmidt, **Inorg. Chim. Acta Rev.**, 1 (1968) 123.

72. L.A. Gribov, A.D. Gel'man, F.A. Zakharova & M.M. Orlova, **Russ. J. Inorg. Chem.**, 5 (1960) 473.

73. G.A. Foulds & D.A. Thornton, **Spectrochima Acta**, 37A (1981) 917.

74. Reference 67, first paper.

75. Mylius & Foester, **Ber.**, 24 (1891) 2424.

76. J. Browning, P.L. Goggin, R.J. Goodfellow, M.G. Norton, A.J.M. Rattray, B.F. Taylor & J. Mink, **J. Chem. Soc. Dalton**, (1977) 2061.

77. A. Gambi & S. Ghersetti, **Spectrosc. Lett.**, 8 (1977) 627.

78. C.H. Kline & J. Turkevich, **J. Chem. Phys.**, 12 (1944) 300.

79. M. Orchin & P.J. Schmidt, **Coord. Chem. Rev.**, 3 (1968) 345.

80. J. Hiraishi, **Spectrochim. Acta**, 25A (1969) 749.

81. S.I. Shupack & M. Orchin, **J. Amer. Chem. Soc.**, 85 (1963) 902.

82. S.I. Shupack & M. Orchin, **Inorg. Chem**, 3 (1964) 374.

83. G.A. Foulds, D.A. Thornton & J. Yates, **J. Mol. Struct.**, 98 (1983) 315.

84. J.B. Hodgson, G.C. Percy & D.A. Thornton, **J. Mol. Struct.**, 66 (1980) 75.

85. V. Tabaick, V. Pellegrin & Hs. H. Gunthard, **Spectrochimica Acta**, 35A (1079) 1055.

86. M. Cordes & J.L. Walter, **Spectrochimica Acta**, 24A (1968) 237.

87. M.J. Cleare & W.P. Griffith, **J. Chem. Soc.** (1969) 372.

88. P.L. Goggin & R.J. Goodfellow, **J. Chem. Soc. Dalton**, (1973) 2355.

89. F. Carderazzo, R. Ercoli & G. Natta in **Organic Syntheses via Metal Carbonyls**, Wiley (Interscience), New York, 1 (1968).

90. G.R. Bedford, **Ann. Rep. NMR Spectroscopy**, 4 (1971) 36.

91. R.J. Abraham, **The Analysis of High Resolution NMR Spectra**, Elsevier Publishers, Amsterdam, (1971) 265.

92. J.W. Akitt, **NMR and Chemistry**, Chapman & Hall, London, (1973) 105.

93. A.R. Brause, F.Kaplan & M. Orchin, **J. Amer. Chem. Soc.** 89 (1967) 2661.

94. P.J. McCarthy & A.E. Martell, **Inorg. Chem.**, 6 (1967) 781.

95. E.L. Mutterties, W. Mahler & R. Schmutzler, **Inorg. Chem.**, 2 (1963) 613.

96. E.L. Mutterties, W. Mahler, K.J. Packer & R. Schmutzler, **Inorg. Chem.**, 3 (1964) 1298.

97. J.P. Fackler, J.A. Fetchin, J. Mayhew, W.C. Seidel, T.J. Swift & M. Weeks, **J. Amer. Chem. Soc.**, 91 (1969) 1941.

98. H. Boucher & B. Bosnich, **Inorg. Chem.**, 16 (1977) 717.

99. S. Miya & K. Saito, **Inorg. Chem.**, 20 (1981) 287.

100. J. Ashley-Smith, Z. Douek, B.F.G. Johnson & J. Lewis, **J. Chem. Soc. Dalton**, (1974) 128.

101. G.A. Foulds, G.E. Jackson & D.A. Thornton, **J. Mol. Struct.**, 98 (1983) 323.

102. M.H. Chrisholm & H.C. Clark, **Inorg. Chem.**, 12 (1973) 991.

103. G.V. Fazakerley & K.R. Koch, **Inorg. Chim. Acta.**, 36 (1979) 13.

104. M. Alei, L.O. Morgan, W.E. Wageman & T.W. Whaley, **J. Amer. Chem. Soc.**, 102 (1980) 2881.

105. L.M. Jackman & F. Cotton, Eds., **Dynamic Nuclear Magnetic Resonance Spectrosopy**, Academic Press, New York, (1975) 299.

106. U. Belluco, M. Grazini & P. Rigo, **Inorg. Chem.**, 5 (1966) 1123.

107. M.A.M. Meesters, D.J. Stufkens & K. Vriese, **Inorg. Chim. Acta**, 15 (1975) 137.

108. D.G. Cooper & J. Powell, **Inorg. Chem.**, 16 (1977) 142.

109. T. Iwayangi & Y. Saito, **Inorg. Nucl. Chem. Letters**, 11 (1975) 459.